UC Berkeley
Earlier Faculty Research

Title
Real-time Vehicle Reidentification System for Freeway Performance Measurements

Permalink
https://escholarship.org/uc/item/2fh092zk

Author
Jeng, Shin-Ting

Publication Date
2007

UNIVERSITY OF CALIFORNIA,

IRVINE

Real-time Vehicle Reidentification System for Freeway Performance Measurements

DISSERTATION

submitted in partial satisfaction of the requirements

for the degree of

DOCTOR OF PHILOSOPHY

in Civil Engineering

by

Shin-Ting Jeng

Dissertation Committee:

Professor Stephen G. Ritchie, Chair

Professor Wilfred W. Recker

Professor Amelia C. Regan

2007

© 2007 Shin-Ting Jeng

The dissertation of Shin-Ting Jeng

is approved and is acceptable in quality

and form for publication on microfilm and digital formats:

_____

_____

_____

Committee Chair

University of California, Irvine

2007

DEDICATION

To my family

TABLE OF CONTENTS

LIST OF FIGURES

LIST OF TABLES

APPENDICES

ACKNOWLEDGEMENTS

I would like to gratefully appreciate the complete support and invaluable advice that I received from Professor Stephen G. Ritchie, my advisor, throughout my Ph.D. study at the University of California, Irvine. Without his academic guidance, sincere encouragement, and financial support, this dissertation would not have been possible.

Appreciation is also extended to Professor Wilfred W. Recker and Professor Amelia C. Regan, my committee members, for their precious comments. I also would like to thank Professor Michael G. McNally, and Professor R. Jayakrishnan for their teaching and encouragement.

I am deeply indebted to Professor Ritchie's research team, including Dr. Cheol Oh, Dr. Seri Park, Andre, and Wendy, for their great help in both research works and my life at UCI. I am grateful to Mr. Duncan Phillips for his productive co-works and kindness. I also thank Ms. Lyn Long, Ms. Ziggy Bates, Ms. Anne Marie DeFeo, and Ms Kathy Riley, for their friendship and kind assistance. I also wish to thank all other ITS members here.

I warmly thank the assistance of John Slonaker at California Department of Transportation's Division of Research and Innovation and Steve Hilliard of Inductive Signature Technologies, Inc., in conducting this dissertation research.

My special thanks go to my beloved friends, E. L., Sonja, Sandra, Jennifer and Yieh-hue, whose affection, encouragement, tolerance and blessing have made me overcome the difficulties and complete this dissertation. A special note of thankfulness is also expressed to others who have helped me in one way or another.

Last but not least, I am grateful to acknowledge my mother, aunts, and sisters, for their true love, endless support and understanding during the past four years.

CURRICULUM VITAE

Shin-Ting Jeng

EDUCATION

2007   Ph.D. in Civil Engineering (Transportation System Engineering)
University of California, Irvine

2003   M.Eng. in Civil Engineering (Transportation Engineering)
National University of Singapore, Singapore

1996   B.B.A. in Transportation and Communication Management Science
National Cheng Kung University, Taiwan

HONORS, FELLOWSHIPS, AND GRANTS

2005-2006   Ph.D. Dissertation Grants, University of California Transportation Center
(UCTC)

2005   Helen M. Overly Scholarship, Woman's Transportation Seminar (WTS)

2003-2007   Graduate Research Scholarship, University of California, Irvine

2000-2002   Graduate Research Scholarship, National University of Singapore

PUBLICATIONS

Jeng, S.-T., Ritchie, S. G., and Tok, A. (2007). "A New Inductive Signature Data Compression and Transformation Method for On-Line Vehicle." In *Proceedings of the 86th Annual Meeting of the Transportation Research Board (CD-ROM)*, Washington, D.C.

Tok, A., Ritchie, S. G., and **Jeng, S.-T.** (2007). "Understanding Commercial Vehicle Travel through New High Fidelity Inductive Sensors." In *Proceedings of the 86th Annual Meeting of the Transportation Research Board (CD-ROM)*, Washington, D.C.

Jeng, S.-T., and Ritchie, S. G. (2006). "A New Inductive Signature Data Compression and Transformation Method for On-Line Vehicle." In *Proceedings of the 85th Annual Meeting of the Transportation Research Board (CD-ROM)*, Washington, D.C.

Jeng, S.-T., and Ritchie, S. G. (2005). "A New Inductive Signature Method for Vehicle Reidentification." In *Proceedings of the 84th Annual Meeting of the Transportation Research Board (CD-ROM)*, Washington, D.C.

Ritchie, S. G., Park, S., Oh, C., **Jeng S.-T.**, Tok, A. (2005). "Anonymous Vehicle Tracking for Real-time Freeway and Arterial Street Performance Measurement." *UCB-ITS-PRR-2005-9*, California PATH Research Report.

Ritchie, S. G., Park, S., Oh, C., **Jeng S.-T.**, Tok, A. (2005). "Field Investigation of Advanced Vehicle Reidentification Techniques and Detector Technologies—Phase 2." *UCB-ITS-PRR-2005-8*, California PATH Research Report.

Lee, D.-H., **Jeng, S.-T.**, and Chandrasekar, P. (2004). "Applying Data Mining Techniques for Traffic Incident Analysis." *Journal of the Institution of Engineers, Singapore,* Vol. 44, No. 2, pp. 90-102.

Lee, D.-H., and **Jeng, S.-T.** (2004). "Integrated Freeway Incident Management—Using Data Mining and Expert Systems." In *Proceedings of the 83rd Annual Meeting of the Transportation Research Board (CD-ROM)*, Washington, D.C.

Oh, C., Ritchie, S. G., and **Jeng, S.-T.** (2004). "Anonymous Vehicle Reidentification with Heterogeneous Detection Systems." In *Proceedings of the 83rd Annual Meeting of the Transportation Research Board (CD-ROM)*, Washington, D.C.

Lee, D.-H., **Jeng, S.-T.**, and Ng, M. H. (2003). "Defining the Incident Impact Area for Traffic Diversions: Knowledge Discovery via a Data Mining Approach." In *Proceedings of the 82nd Annual Meeting of the Transportation Research Board (CD-ROM)*, Washington, D.C.

Lee, D.-H., **Jeng, S.-T.**, and Chandrasekar, P. (2002). "Applying Data-Mining Technique to Traffic Diversion." In *Proceedings of the 9th World Congress on Intelligent Transport Systems (CD-ROM)*, ITS World Congress, Chicago, IL.

Lee, D.-H., **Jeng, S.-T.**, and Chandrasekar, P. (2002). "Investigating an Incident Situation using Data Mining." In *Proceedings of the 81st Annual Meeting of the Transportation Research Board (CD-ROM)*, Washington, D.C.

PRESENTATIONS

Jeng, S.-T., Ritchie, S. G., and Tok, A. (2007). "A New Inductive Signature Data Compression and Transformation Method for On-Line Vehicle." Presented at the 86th Annual Meeting of the Transportation Research Board, Washington, D.C.

Tok, A., Ritchie, S. G., and **Jeng, S.-T.** (2007). "Understanding Commercial Vehicle Travel through New High Fidelity Inductive Sensors." Presented at the 86th Annual Meeting of the Transportation Research Board, Washington, D.C.

Jeng, S.-T., and Ritchie, S. G. (2006). "A New Inductive Signature Data Compression and Transformation Method for On-Line Vehicle." Presented at the 85th Annual Meeting of the Transportation Research Board, Washington, D.C.

Jeng, S.-T., and Ritchie, S. G. (2005). "A New Inductive Signature Method for Vehicle Reidentification." Presented at the 84th Annual Meeting of the Transportation Research Board, Washington, D.C.

Park, S., **Jeng, S.-T.**, and Yang, C.-H. (2005). "Simulated Network Evaluation based on Vehicle Reidentification." Presented at the 12th World Congress on Intelligent Transportation Systems, San Francisco, CA.

Lee, D.-H., and **Jeng, S.-T.** (2004). "Integrated Freeway Incident Management—Using Data Mining and Expert Systems." Presented at the 83rd Annual Meeting of the Transportation Research Board, Washington, D.C.

Oh, C., Ritchie, S. G., and **Jeng, S.-T.** (2004). "Anonymous Vehicle Reidentification with Heterogeneous Detection Systems." Presented at the 83rd Annual Meeting of the Transportation Research Board, Washington, D.C.

Lee, D.-H., **Jeng, S.-T.**, and Ng, M. H. (2003). "Defining the Incident Impact Area for Traffic Diversions: Knowledge Discovery via a Data Mining Approach." Presented at the 82nd Annual Meeting of the Transportation Research Board, Washington, D.C.

Lee, D.-H., **Jeng, S.-T.**, and Chandrasekar, P. (2002). "Investigating an Incident Situation using Data Mining." Presented at the 81st Annual Meeting of the Transportation Research Board, Washington, D.C.

TEACHING AND RESEARCH EXPERIENCE

01/03-03/07   <u>Graduate Student Researcher</u> for Dr. Stephen G. Ritchie

Institute of Transportation Studies (ITS)
University of California, Irvine

12/00-08/02   <u>Research Assistant</u> for Dr. Der-Hong Lee
Intelligent Transportation & Vehicle Systems (ITVS) Lab
National University of Singapore, Singapore

05/01-06/01   <u>Teaching Assistant</u> for final year project and practical training
08/01-06/02   Department of Civil Engineering
National University of Singapore, Singapore

09/97-06/98   <u>Research Assistant</u> for Dr. Jui-Hsien Ling
Department of Transportation and Communication Management Science
National Cheng Kung University, Taiwan

07/96-01/97   <u>Research Assistant</u> for Dr. Chun-Yi Chen
Department of Transportation and Communication Management Science
National Cheng Kung University, Taiwan

PROFESSIONAL SERVICE

2003 to Present   Member, Transportation Research Board (TRB)

2003 to Present   Member, Institute of Transportation Engineers (ITE)

FOREIGN LANGUAGES

Mandarin (native fluency), Japanese (fluency in reading and listening)

ABSTRACT OF THE DISSERTATION

Real-time Vehicle Reidentification System for Freeway Performance Measurements

By

Shin-Ting Jeng

Doctor of Philosophy in Civil Engineering

University of California, Irvine, 2007

Professor Stephen G. Ritchie, Chair

Computational resources in the traffic operation field as well as the bandwidth of field communication links, are often quite limited. Accordingly, for real-time implementation of Advanced Transportation Management and Information Systems (ATMIS) strategies, such as vehicle reidentification, there is strong interest in development of field-based techniques and models that can perform satisfactorily while minimizing computational and communication requirements in the field. The ILD (Inductive Loop Detector)-based Vehicle ReIDentification system (ILD-VReID) is an example of a currently applied approach. Although ILDs are not without limitations as a traffic sensor, they are widely used for historical reasons and the sunken investment in the large installed base makes their use in this research highly cost-effective. Therefore, this dissertation develops a

new vehicle reidentification algorithm, RTREID-2, for real-time implementation by adopting a PSR (Piecewise Slope Rate) approach that extracts features from raw vehicle signature data. The results of cases studies indicate that RTREID-2 is capable of accurately providing individual vehicle tracking information and performance measurements such as travel time and speed. The potential contributions of RTREID-2 are: application to square and round single loop configurations, and reduced computational requirements because re-estimation or transferability of the speed models used in the previously developed approach is not necessary. As a consequence, RTREID-2 is free of site-specific calibration and transferability issues. A freeway corridor study also demonstrates that RTREID-2 has the potential to be implemented successfully in a congested freeway corridor, utilizing data obtained from both homogenous and heterogeneous loop detection systems. A real-time vehicle classification model, which is based on the PSR approach, was also developed on the part of RTREID-2. The classification model can successfully classify vehicles into 15 classes using single loop detector data without any explicit axle information. The initial results also suggest the potential for transferability of the vehicle classification approach and are very encouraging. To investigate real-time freeway performance measurement in a real-world setting, the design of a RTPMS (Real-time Traffic Performance Measurement System) that is based on RTREID-2 is also presented in this dissertation. A simulation of RTPMS is conducted to evaluate its feasibility. The simulation results demonstrate the potential of implementing RTPMS in real world applications.

CHAPTER 1 INTRODUCTION

1.1 BACKGROUND

Vehicle reidentification has emerged due to its substantial potential for effective implementation of ATMIS (Advanced Transportation Management and Information Systems). In the studies of vehicle reidentification, the main stress falls on travel information, travel time estimation, and origin-destination (OD) estimation. According to the technologies applied, the vehicle reidentification systems can be categorized as the vehicle signature based system (signatures are obtained from the traffic detectors such as inductive loop detector and radar detector), the VIP (video image processing) based system, the AVI (automatic vehicle identification) based system, the GPS (global positioning systems) based system, and the CP (cellular phone)-based system. Among all of the aforementioned systems, however, the ILD (inductive loop detector) based systems are cost-effective because the ILDs are largely installed in the field.

ILD-based vehicle ReIDentification (ILD-VReID) systems track vehicles via vehicle signature reidentification algorithms. Starting from Böhnke and Pfannerstill (1986), numerous studies have been made on ILD-VReID systems since 1980's. The research field initially focused on freeways (Kühne and Immes, 1993; Sun et al., 1999; Ritchie et al., 2001) and was extended into arterials (Oh and Ritchie, 2003) utilizing homogeneous detection systems. Moreover, Oh, Ritchie, and Jeng (2004) proposed a

new analysis to expand the capabilities of ILD-VReID, which attempted to reidentify vehicles via heterogeneous detectors.

Although a great deal of effort has been made on ILD-VReID systems over the past decades, and the outcomes of the previous studies are valuable, little is known about reidentifying vehicles along a corridor, and real-time implementation. What seems to be lacking is a real-time ILD-VReID system, which can provide performance for a freeway corridor. In addition, the current ILD-VReID algorithms are limited in several ways. For example, the speed estimation procedure of the ILD-VReID algorithms may become an obstacle to systems equipped with single loop detectors.

Therefore, this dissertation research presents a new ILD-VReID system for real-time implementation by utilizing vehicle signature data obtained from single loop detectors. The proposed system is capable of providing individual vehicle tracking and vehicle class information, and performance such as travel time along a freeway corridor.

1.2 RESEARCH OBJECTIVE

The purpose of this dissertation is to develop an algorithm for vehicle reidentification to be implemented in real-time, and to provide traffic performance measurements. This dissertation focuses on an ILD-VReID system and evaluating the feasibility of implementing the proposed vehicle reidentification algorithm in a freeway corridor. The objectives of this dissertation can be categorized as follows:

- Develop an ILD-VReID algorithm that is readily applied:

The existing ILD-VReID algorithms involve speed estimation processes and are less flexible while implementing in real-time and applying to a single loop detection system. A new approach using an interpolation method (REID-2), which is straightforward, adopts no speed estimation models, and is readily applied to both single and double loop detectors, is proposed in this dissertation.

- Improve the proposed vehicle reidentification algorithm (REID-2) for real-time implementation:

Computational resources in the traffic operations field as well as the bandwidth of field communication links are often quite limited. Accordingly, for real-time implementation of vehicle reidentification, there is strong interest in development of field-based techniques and models that can perform satisfactorily while minimizing field computational and communication requirements. Therefore, this dissertation investigates a relatively simple data compression and transformation technique that could be applied successfully to real-time vehicle reidentification (RTREID-2). A Piecewise Slope Rate (PSR) approach is developed to compress and transform the raw vehicle signatures.

- Perform RTREID-2 along a freeway corridor:

Section-related or link-based data can arguably provide reliable and accurate inputs for traffic surveillance and performance measurement systems. To obtain section-related data, vehicle reidentification plays an important role since section performance measurements can be generated easily via a vehicle reidentification system. This dissertation evaluates the performance of the proposed algorithm, RTREID-2, based on a 6.2-mile freeway corridor on northbound I-405 under congested morning peak-period conditions. The corridor consists mostly of round inductive loop detectors with some square loops, providing an opportunity to assess the applicability and transferability of the proposed algorithm for homogenous and heterogeneous loop detection systems.

- Apply the proposed Piecewise Slope Rate (PSR) approach to vehicle classification:

Vehicle class is an important characteristic of traffic measurement. It is helpful to monitor heavy vehicle traffic for road maintenance and safety, have insight into traffic composition for modeling traffic flow, and to obtain performance measurements based on each vehicle class for traffic surveillance. In this dissertation, a heuristic method combined with a decision tree and K-means clustering approach is proposed to develop a vehicle classification model. The features used in the proposed model are extracted from PSR values.

- Design a Real-time Traffic Performance Measurement System (RTPMS) scheme based on an ILD-VReID system

A real-time performance measurement system is discussed in this dissertation. The overall system can be divided into two sub-systems: field data preprocessing system and performance measurement system. The field data preprocessing system extracts PSR features, while the performance measurement system generates vehicle tracking and vehicle class information, and presents real-time performance measurements. A simulation of this system is also conducted to access its feasibility.

1.3 RESEARCH OUTLINE

The overall dissertation framework is described in Figure 1-1:
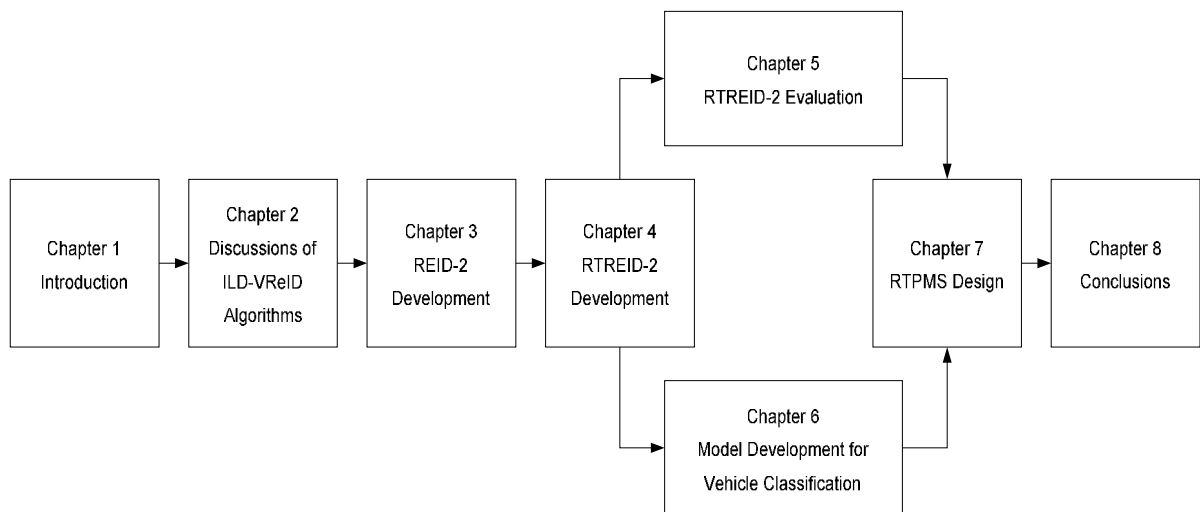
Figure 1-1 Dissertation framework.

This dissertation consists of eight chapters as follows:

Chapter 1 introduces the background and objectives of this dissertation, and Chapter 2 gives reviews of ILD-VReID algorithms and applications.

In Chapter 3, methodologies that are adopted to develop the proposed ILD-VReID algorithm (REID-2) are described and discussed. A case study utilizing REID-2 is demonstrated, and travel time estimation is performed to evaluate the performance of the proposed algorithm. Furthermore, REID-2 is compared with REID-1, which is a lexicographic optimization method for vehicle reidentification developed by Sun et al. (1999).

Chapter 4 provides a description of the proposed vehicle signature compression and transformation approach (PSR approach), which is applied to the proposed real-time vehicle reidentification algorithm (i.e., RTREID-2). The procedure of RTREID-2 is presented. Analyses of sensitivity and computational performance are conducted to investigate the performance of RTREID-2. Travel time estimation based on vehicle reidentification with RTREID-2 is undertaken to evaluate the performance of RTREID-2. RTREID-2 is also compared with REID-2 and REID-1.

In Chapter 5, a freeway corridor analysis is performed. The study sites and datasets used in this study are discussed first. A single-section freeway analysis is performed to investigate the performance of RTREID-2 given three cases including

square-to-square loops, round-to-round loops, and square-to-round loops cases. A freeway corridor analysis is then presented, where travel time and speed measures from RTREID-2 are compared with GPS data obtained from control vehicles.

In Chapter 6, a vehicle classification model, which is an application of the PSR approach, is introduced. The features used in the proposed model are extracted from PSR values, and a heuristic method combined with decision tree and K-means clustering methods is suggested to perform the vehicle classification tasks.

Chapter 7 demonstrates the framework of RTPMS. The sub-systems of RTPMS are detailed, and modules adopted in RTPMS are described. In addition, a simulation is performed to assess the proposed RTPMS framework.

Chapter 8 summarizes remarks and findings of this dissertation along with directions and recommendations for future research.

CHAPTER 2 REVIEWS OF ILD-VReID VEHICLE REIDENTIFICATION

Several technologies have been studied for vehicle reidentification in the last three decades such as the AVI based system, the GPS based system, the CP based system, the VIP based system, and the ILD-based system. For AVI based system, an in-vehicle tag is used to provide individual vehicle information including location, unique ID, and speed for roadside tag reader. The information is then sent back to control center for vehicle reidentification purpose. The GPS based system utilizes GPS-equipped vehicles and geographical information system (GIS) to locate a vehicle and its traveling information including latitude and longitude information and timestamp. As indicated in its name, the CP based system obtains vehicle travel information via cell phones. The wireless cell phone tower picks up the emitting signals from drivers' cell phones and sends them back to a control center.

The three systems described above can be categorized as "Intrusive detection systems" which employ vehicles as a sensor. Although intrusive detection systems could provide more accurate vehicle tracking results, the limitations involved due to market penetration problems and privacy concerns are major obstacles to deploy intrusive sensors in a wide-area traffic surveillance system (Oh, 2003).

The VIP based system and the ILD-based system are considered "non-intrusive detection systems" which utilize sensors installed within the road or at the roadside. The

VIP based system uses video or cameras to catch images of each passing vehicle, and extracts individual vehicle information including vehicle length, width, color, and sometimes, license plate. The extracted vehicle features from both upstream and downstream detection stations are then compared with each other to find the best matches. For the ILD-based system, an advanced high-speed scanning loop detector card captures inductance changes that are different from a traditional detector card. While the outputs obtained from the traditional detector card are usually binary to indicate the presence of a vehicle, more features that represent unique characteristics of individual vehicles can be extracted from the outputs of the advanced detector card.

As opposites of intrusive detection systems, non-intrusive detection systems are almost free from privacy concerns and market penetration problem. Among the non-intrusive detection systems ILDs, although not without limitations as a traffic sensor, are widely used for historical reasons and the sunken investment in the large installed base makes their use in this dissertation highly cost-effective. Moreover, the ILD-based systems have proven their capability for anonymous vehicle tracking in previous studies, and could be potentially applied to reidentify individual vehicles across multiple detection stations. Therefore, the ILD-based system is chosen in this dissertation to investigate its capabilities for real-time implementation and freeway corridor deployment.

In this chapter, ILDs-VReID algorithms are reviewed. In addition, the applications of ILD-VReID are demonstrated and discussed. Details of vehicle detection technologies utilized in other vehicle reidentification systems can be found elsewhere

(ITE, 1990; Mimbela et al., 2000; Jet Propulsion Laboratory, 1997; Knee et al., 2004). The operating principles of ILDs can be found in the Traffic Detector Handbook (ITE, 1990).

2.1 ILDs-VReID ALGORITHMS

An ILD-VReID system aims to reidentify vehicles by utilizing inductive vehicle signatures. The resulting change in inductance due to the passage of a vehicle over a loop detector makes it possible to measure an inductive vehicle signature, which ideally is unique to that vehicle. Advantages of employing an ILD-based system include tracing vehicles individually across multiple detection stations without privacy concerns, relatively inexpensive deployment, reproducible vehicle signatures, less complexity of analysis, and fewer market penetration problems.

The initial investigation of ILD-VReID system was carried out in 1980's. Böhnke and Pfannerstill (Böhnke and Pfannerstil, 1986; Pfannerstil, 1989) first noticed that section-related traffic data could be obtained via reidentifying platoons of vehicles passing through a section of a road. The inductive vehicle signatures were treated as the input of a pattern recognition system developed by this research, and the system was intended to reidentify a platoon of vehicles.

Kühne and Immes (1993) proposed an approach, which can reidentify a platoon of vehicles via finding the correlation of vehicle feature series at downstream and

created using
BCL easyPDF
Printer Driver
Click here to purchase a license to remove this image

upstream sites. However, the algorithm aimed to identify vehicle types rather than reidentifying each individual vehicle. Later on, Kühne et al. (1997) suggested a more sophisticated method, which can identify single vehicles (vehicle types) and vehicle platoons.

The improved algorithm first normalized vehicle signatures in order to eliminate the system sensitivity and detector-specific effects. The features thus obtained were processed for feature comparison. The authors suggested that reidentifying a single vehicle with absolute accuracy was not necessary for accurate section-related measures and ten percent of the traffic population was able to generate significant results. Furthermore, they also suggest that, "The most promising approach is a mixture of single vehicle and vehicle platoon reidentification which use weighting functions… (Kühne et al., 1997)."

Sun et al. (Sun, 1998; Sun et al., 1999) suggested an approach, which provided a solution to reidentify single vehicles via lexicographic optimization method for freeways. In this algorithm, the vehicle reidentification problem was defined as: given a downstream vehicle signature, find the corresponding vehicle signature within a candidate vehicle set obtained from an immediately upstream station. Accordingly, five levels were defined in this lexicographic optimization problem including time window determination, vehicle classification, vehicle length restriction, vehicle features differences minimization and vehicle matching. The reidentification rates of passenger vehicle and non-passenger vehicle were 75% and 78% respectively.

Furthermore, Tabib and Abdulhai (Tabib, 2001; Tabib and Abdulhai, 2002) attempted to improve the fourth level of Sun et al.'s model using different distance measurements. It was found that adopting "waveform shift" could bring in more consistent and reliable reidentification results due to its insensitivity to congestion level.

Following Sun et al.'s framework, Oh and Ritchie (Oh and Ritchie, 2002; Oh, 2003) extended the vehicle reidentification techniques from freeway to a single signalization intersection. To address the turning movement characteristic at intersection, a turning filtering optimization level was added to the original model. The turning filtering algorithm mainly depended on travel time estimation for each turning movement (left turn, through, and right turn movements). The reidentification rates under congested and non-congested traffic condition for through movement vehicles were 72.1% and 80.9% respectively.

A decision tree for ILD-VReID was suggested by Tawfik et al. (2004). Their model integrated distances measurements (Abdulhai and Tabib, 2002) into the decision tree developed by their previous study (Tawfik et al., 2002). The authors pointed out that although the results demonstrated significant improvement of reidentification rate (90%), this method was recommended as a post-processing method for system performance evaluation.

Although the aforementioned studies obtained improved results, some potential limitations and disadvantages exist. For instance, speed estimation processes are involved to extract vehicle length information, challenging implementation under single loop detection system. Discussion of these potential limitations is detailed in Section 2.3.

To address this issue, an inductive loop signature-based method for vehicle reidentification, named REID-2 was proposed by the author (Jeng and Ritchie, 2005). REID-2 used an interpolation method, involved no speed estimation models, and was straightforward and readily applied to both single and double loop detectors. The results showed that REID-2 was comparable with the lexicographic vehicle reidentification method (REID-1) previously developed and used at UCI (Park and Ritchie, 2004; Sun et al., 1999), and was even superior when applied to the single loop case. The details of REID-2 are discussed in Chapter 3.

Kwon and Parsekar (2005) presented a deconvolution method of processing inductance waveforms for vehicle reidentification. The research goal was to restore the lost features of vehicle signatures caused by a relatively large detection zone via applying a deconvolution process. The results showed that about 89% reidentification accuracy could be achieved by moving the deconvolved signature over likely matches and finding the minimum difference. The performance summary also indicated that the computation time was 6.8 seconds with 562 vehicles given deconvolved signatures. The concept of restoring "the details of vehicle signatures that were lost in the raw ILD outputs (Kwon

13

and Parsekar, 2005)" demonstrates a new way to pre-process raw vehicle signature for an ILD-VReID system.

2.2 APPLICATIONS OF ILD-VREID

Although individual detection stations can provide essential traffic information, section-related data is seen to provide more reliable and accurate inputs for traffic surveillance and performance measurement systems (Böhnke and Pfannerstill, 1986; Kühne et al., 1997; Sun et al., 1999; Oh and Ritchie, 2002; Oh and Ritchie, 2003; Park and Ritchie, 2004; Oh, Tok and Ritchie, 2004). The development of traffic surveillance and performance measurement systems can benefit from utilizing ILD-VReID since section-related data can be easily generated using the results of ILD-VReID.

Kühne et al. (1997) pointed out that a traffic control system using section-related data was more sensitive for congestion detection and delay estimation than using local data in their case study. The results of Sun et al. (1999) also indicated that estimated section travel times and section densities for both congested and moderate flow data had trivial error (less than 4%). Furthermore, Park and Ritchie (2004) demonstrated the capability of ILD-VReID in vehicle classification, speed variance analysis and driver's lane changing behavior analysis. The results of this case study show that section speed variability was highly influenced by lane change behaviors and long vehicles.

14

In addition, ILD-VReID can be applied to real-time level-of service (LOS) criteria development. Oh and Ritchie (2002) suggested that the real-time LOS criteria for signalized intersections are useful for real-time performance evaluation and travel information. More recently, Oh, Tok, and Ritchie (2004) extended their original work to freeway LOS. It is worth noting that the real-time LOS criteria for both intersections and freeway surveillance systems are readily transferable to other similarly equipped systems.

OD Estimation is one further application of ILD-VReID. OD information can be obtained via utilizing the outputs of ILD-VReID. Oh (2003) set up a procedure of time-variant OD estimation for a signalized network using a Monte Carlo simulation method. The inputs of the procedure, i.e. the estimated flow, were obtained from the results of ILD-VReID. Path travel time (Oh and Ritchie, 2003) can also be obtained through the OD estimation procedure; however, the accuracy of the estimated path travel time may not be effective if a low reidentification rate is represented along the path.

2.3 DISCUSSIONS OF ILD-VREID

Following the assumption that each vehicle possesses distinct features, the procedure of up-to-date ILD-VReID algorithms (Sun et al., 1999; Oh and Ritchie, 2003; Oh and Ritchie, 2002) can be illustrated in Figure 2-1. In Figure 2-1, raw vehicle signatures are normalized based on estimated speed (Sun and Ritchie, 1999; Oh, Ritchie, and Oh, 2002; Oh, Ritchie, and Park, 2002), and then, the salient features are extracted for the use of matching vehicle signatures. Furthermore, to reduce the size of feasible search space

before matching vehicle features, a spatial search space reduction and a temporal search space reduction are performed.

```
                        ┌─────────────────────┐
                        │ Raw Vehicle Signatures │
                        │      Processing       │
                        └─────────────────────┘
                                   │
                                   ▼
┌─────────────────────┐   ┌─────────────────────┐
│  Speed Estimation   │──▶│  Vehicle Signatures │
│                     │   │    Normalization    │
└─────────────────────┘   └─────────────────────┘
                                   │
                                   ▼
                          ┌─────────────────────┐
                          │  Vehicle Signatures │
                          │  Features Extraction │
                          └─────────────────────┘
                                   │
                                   ▼
┌─────────────────────┐   ┌─────────────────────┐
│  Turning Movement   │──▶│  Spatial Search Space │
│   Classification    │   │      Reduction      │
└─────────────────────┘   └─────────────────────┘
                                   │
                                   ▼
┌─────────────────────┐   ┌─────────────────────┐
│    Travel Time      │──▶│ Temporal Search Space │
│    Estimation       │   │      Reduction      │
└─────────────────────┘   └─────────────────────┘
                                   │
                                   ▼
                          ┌─────────────────────┐
                          │  Vehicle Signatures │
                          │   Reidentificaiton  │
                          └─────────────────────┘
```
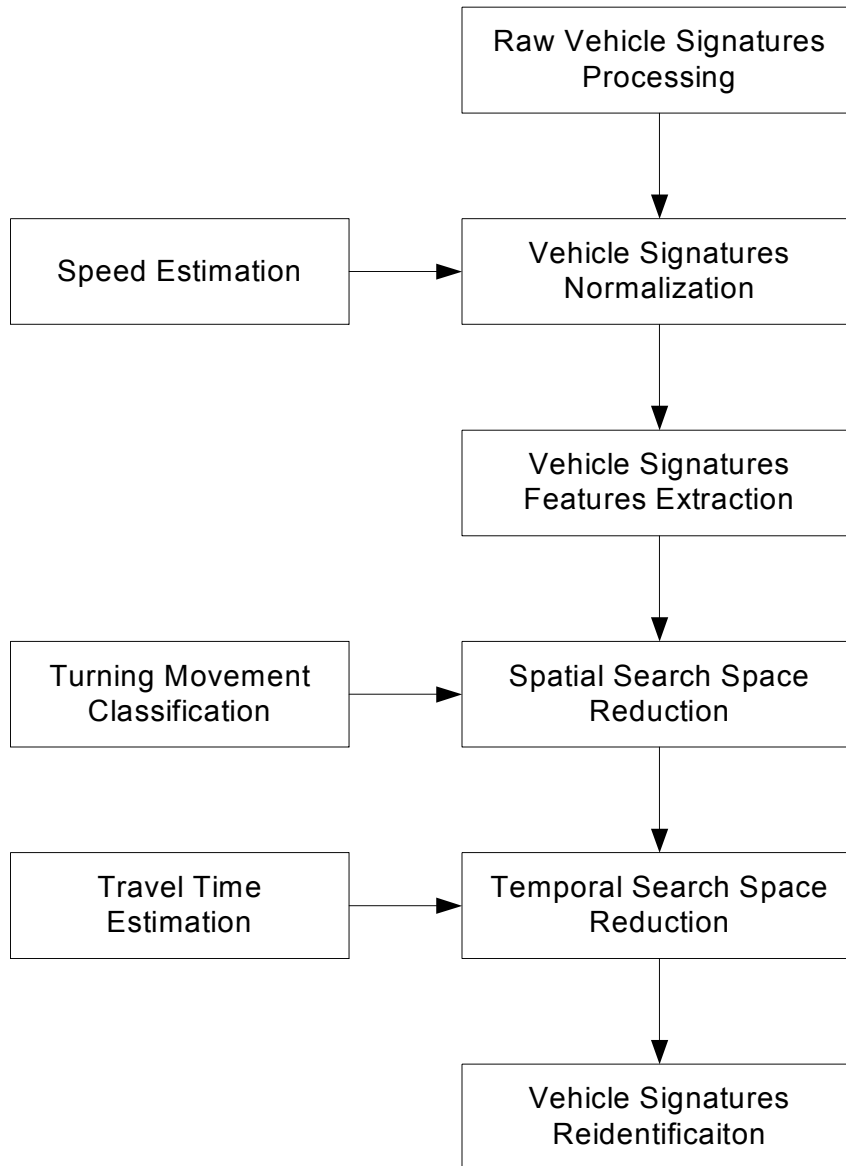
Figure 2-1 The procedure of ILD-VReID algorithm.

The task of spatial search space reduction is to identify the upstream origin of each vehicle and a turning movement classification is implemented. There are two cases

16

for spatial search space reduction: freeway and arterial. For the freeway case, the upstream origin can be mainline detection stations and/or ramp detection stations. The arterial case is considered more challenging than the freeway case since the traffic flow on the arterials are interrupted by signal control. Given a downstream detection station, there are three possible upstream origins if the downstream intersection has four approaches. The details of finding upstream origins for the arterial case are described elsewhere (Oh, 2003; Oh, Ritchie, and Park, 2002).

For temporal search space reduction, a time window restriction is applied. The aim of temporal search space reduction is to determine a feasible and reasonable time period so that the correct vehicle can be included in the candidate vehicle set. Besides, the computational efficiency should be satisfied at the same time. Therefore, the estimated travel time is utilized to set up the lower and the upper bounds of the desired time window. Additionally, signal control (e.g. ramp metering and signalized intersection), detected speed, and posted speed limit are the key factors that affect travel time estimation. A candidate vehicle set can then be found after spatial and temporal search space reduction processes. Finally, each vehicle is reidentified via vehicle features matching among its corresponding candidate vehicle set.

Although the aforementioned algorithm can bring out up to 80% correct matching rate, several potential disadvantages exist. First, there are estimation processes involved in the procedure of the algorithm including speed estimation, searching upstream origin, and travel time estimation. The accuracy of the estimation processes may deteriorate the

later vehicle signature mapping to a certain extent, especially when the system is equipped with single loops. This is because speed information is essential to extract electronic vehicle length feature, which is an important feature for the lexicographic optimization method (as described below). Since single loop speed estimation is required for the single loop case, the accuracy of the estimated speed will affect the results of electronic vehicle length feature extraction.

Secondly, vehicle feature extraction aims to differentiate vehicles sufficiently. It is desirable to maintain a minimum number of vehicle features to deal with the computational complexity; however, the selected vehicle features used in the ILD-VReID algorithm may not be adequate to represent a vehicle.

Thirdly, for the previously developed ILD-VReID algorithms (Sun et al., 1999; Oh and Ritchie, 2003; Oh, Ritchie, and Park, 2002), the lexicographic optimization method is adopted. As mentioned above, five levels are defined in the optimization process (Sun et al., 1999):

- First level: Construct a time window to define a set of feasible upstream candidate vehicles.

- Second level: Discard vehicles that are not from the same vehicle class as the downstream vehicle from the candidate vehicle set obtained in the first level via setting a percentage tolerance for maximum inductance magnitude.

- Third level: Reduce the size of the candidate vehicle set by setting a percentage tolerance for electronic vehicle lengths.

- Fourth level: Minimize the difference between upstream and downstream vehicle features including shape, magnitude, lane position, and speed features (via computing distance measures). The objective function is formulated as a linear function using weighted averaging.

- Fifth level: Choose a suitable distance measure that is best given the distance measures used in the fourth level.

For the first level, the time window can be deterministically or dynamically defined using historical travel times for off-line analysis, and latest maximum and minimum travel times or current local speeds for real-time implementation. However, when there are single loop detectors placed in the network, a single loop speed estimation algorithm is necessary (Sun and Ritchie, 1999; Oh, Ritchie, and Oh, 2002) in order to construct the time window; but our experience to date is that use of such algorithms causes vehicle reidentification performance to decline.

In addition, the speed estimation algorithms for single loop detector may vary for different types of detectors (e.g. square loops or round loops) and a calibration is necessary prior to the implementation. Furthermore, for the objective function in the

fourth level, the weights are determined using historical data, and the optimal distance measure is selected in the fifth level using an historical/calibration dataset (Sun et al., 1999). Although these procedures can be performed in real-time, the task of defining a training set used for fourth and fifth levels, and the optimization procedure will complicate the ILD-VReID problem.

Finally, the estimated travel times are obtained using a subset of vehicles with higher match probability, and discriminant thresholds are used for this purpose. However, since the size of the subset is a function of the discriminant threshold, it should be chosen carefully (Sun et al., 1999).

To address those difficulties, a new approach utilizing an interpolation method, which is straightforward and readily applied to both single and double loop detectors, is proposed in Chapter 3.

CHAPTER 3 INTERPOLATION METHOD FOR VEHICLE REIDENTIFICATION

3.1 BACKGROUND STUDY OF REID-2

As discussed in Chapter 2, the previously developed ILD-VReID algorithms possess a number of limitations. Therefore, a new approach utilizing an interpolation method is proposed to address those difficulties. Assume there are two vehicle signatures to be matched as shown in Figure 3-1. The x-axis and y-axis denote number of samples and inductance magnitude respectively.
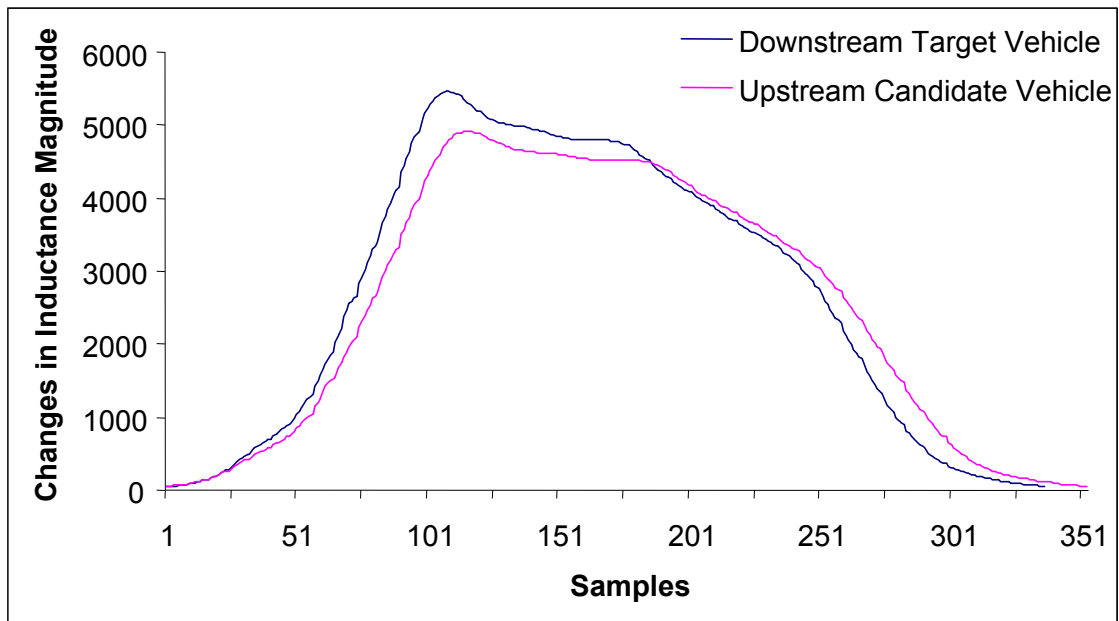
Figure 3-1 Vehicle signatures obtained from ILD.

The vertical differences between two signatures are due to the different detectors and external environmental factors while the horizontal differences between two signatures are caused by different speeds. Those differences can be eliminated using normalization techniques, which avoid unnecessary estimation processes.

For example, the y-axis can be normalized using the maximum magnitude for each vehicle signature; however, another issue has to be addressed after data normalization process. The size of the datasets of each vehicle signature may not be the same because the durations that the ILD are activated may vary, i.e. the same vehicle may travel at different speeds at upstream and downstream detection stations.

For instance, if the vehicle is traveling at a relatively higher speed, the duration that the ILD is activated is shorter and fewer data points are generated. Similarly, the duration that the ILD is activated is longer and more data points are generated if the speed of the vehicle is lower. To address this issue, an interpolation method is suggested. Based on an assumption that a vehicle maintains a constant speed when it traverses an ILD, the speed can be treated as a scalar on the x-axis. Hence, an equidistance interpolation is capable of rescaling the vehicle signatures along the x-axis and calculating the magnitudes corresponding to the interpolated data points. The key point is to match vehicle signatures via computing the vertical differences, i.e. the differences of magnitudes for each data point (see Figure 3-1).

However, while the same vehicle will generate exactly the same vehicle signature every time it passes by an ILD in an ideal detection system (Ritchie and Sun, 1998), there are some common scenarios that cause detection errors and those detection errors may result in a "no match" case:

- Tailgating: If a vehicle is following another vehicle too closely, the lead vehicle and the tailgating vehicle may generate one combined signature instead of two distinct signatures.

- Lane changing: If a vehicle is changing lanes, it may hit the ILD partially. This will not keep vehicle signatures intact, and the traffic characteristic such as the occupancy and the speed will be affected.

- External factors: Variations in ILD and adjacent environment conditions will bring in disturbances.

It is important to notice that the proposed method is based on the hypothesis that the vehicle signatures can be seen as the fingerprint of each individual vehicle and all the ILDs are identical. In other words, a vehicle will possess the same normalized signatures when it passes by all the detection stations (Ritchie and Sun, 1998).

To formulate the vehicle reidentification problem via the interpolation approach, assume the functions of the downstream target vehicle signature (DS Target) and the

upstream candidate vehicle signature (US Candidate) can be expressed as $f(x_{A_i})$ and $f(x_{B_j})$ respectively, where:

$$f(x_{A_i}) \in \text{DS Target}, \ i = 1, 2, \ldots, m$$

$$f(x_{B_j}) \in \text{US Candidate}, \ j = 1, 2, \ldots, n$$

where the function values are the changes in magnitude, and x_{A_i} and x_{B_i} denote the time intervals.

All the data are at equidistant time intervals. The objective is to find the most alike vehicle signature among all upstream candidate vehicle signatures given a downstream target vehicle signature. If $m = n$, the problem can be formulated as shown in Equations 3.1 and 3.2:

$$\max \quad \mu \tag{3.1}$$

$$s.t. \quad \mu \leq f_k(x_{A_i}, x_{B_i}) = \sum_{i=1}^{m} \left| f_k(x_{A_i}) - f_k(x_{B_i}) \right| \tag{3.2}$$

$$\mu \geq 0$$
$$k = 1, \ldots, l$$

where l is the number of upstream candidate vehicle.

For the case that the number of data points of the upstream candidate vehicle signature varies from that of the downstream target vehicle signature ($m \neq n$), the sizes of the given data sets have to be equalized, which means to set $m = n$ and to estimate the function values of the added data points. However, there are only data points instead of an analytic expression, and the functions of the two vehicle signatures are unknown. Approximation algorithms may provide a way to build a function that can approximate vehicle signatures, but it is computationally expensive to find an approximation function for each individual vehicle and this method will not promise pass through all known data points. Therefore, interpolation algorithms are suggested in this dissertation.

After implementing interpolation process, the Equation 3.2 can be rewritten as:

$$
\begin{aligned}
s.t. \quad & \mu \leq f_k(x_{A_i}, x_{B_i}) = \sum_{i=1}^{n} \left| f_k(xI_{A_i}) - f_k(x_{B_i}) \right| \quad && if \quad m < n \\
& \mu \leq f_k(x_{A_i}, x_{B_i}) = \sum_{i=1}^{m} \left| f_k(x_{A_i}) - f_k(xI_{B_i}) \right| \quad && if \quad n < m
\end{aligned}
\tag{3.3}
$$

where xI_{A_i} and xI_{B_i} is the new data set with interpolated points.

In general, interpolation algorithms can be categorized as follows:

created using
BCL easyPDF
Printer Driver
Click here to purchase a license to remove this image

- Linear interpolation: Assume the function values are changing at a constant rate.

- Polynomial interpolation: It is a process that fitting a polynomial to a given data set and is often applied when the data points are not linearly correlated.

- Rational interpolation: This method is for finding interpolation function using quotients of polynomials and is applied to functions with poles.

- Trigonometric interpolation: It is a combination of the cosine and sine functions and is superior in finding interpolation functions that are periodic of a known period.

- Cubic spline interpolation: It is a kind of piecewise curve fitting method. This method utilizes piecewise functions (these pieces may overlap) and calculates an intermediate function value between bounding values.

For the ILD-VReID problem, it is known that the data are equidistance distributed, and it can be observed from Figure 3-1 that interpolated function values will not be singularity points or lie in the proximity of a pole. In addition, the data points are neither linearly nor periodically scattered. Therefore, polynomial interpolation and spline interpolation methods are viable for this dissertation research, and will be further discussed.

3.2 REVIEWS OF INTERPOLATION ALGORITHMS

3.2.1 Polynomial Interpolation

Newton Interpolation

In Newton interpolation, it is not necessary that the function values are given at equal intervals and the function is defined by:

$$P_n(x) = a_0 + (x - x_0)a_1 + (x - x_0)(x - x_1)a_2 + \cdots (x - x_0)(x - x_1) \cdots (x - x_{n-1})a_n \qquad (3.4)$$

where $a_n = f[x_0, \ldots, x_n] = \dfrac{f[x_1, x_2, \ldots, x_n] - f[x_0, x_1, \ldots, x_{n-1}]}{x_n - x_0}$

if the x values are equidistance data, Newton-Gregory forward or backward interpolation can simplify the computation process.

Newton-Gregory Forward Interpolation

In Newton-Gregory forward interpolation, the function is defined by:

$$P_n(x) = f_0 + \binom{s}{1}\Delta f_0 + \binom{s}{2}\Delta^2 f_0 + \binom{s}{3}\Delta^3 f_0 + \binom{s}{4}\Delta^4 f_0 + \cdots + \binom{s}{n}\Delta^n f_0 \qquad (3.5)$$

27

where,

$$\Delta f_j = f_{j+1} - f_j$$
$$\Delta^2 f_j = \Delta\left[\Delta f_j\right] = \Delta f_{j+1} - \Delta f_j$$
$$\Delta^3 f_j = \Delta\left[\Delta^2 f_j\right] = \Delta^2 f_{j+1} - \Delta^2 f_j$$
$$\vdots$$
$$\Delta^n f_j = \Delta^{n-1} f_{j+1} - \Delta^{n-1} f_j$$

$$s = \frac{x - x_0}{h}$$

$$\binom{s+j}{k} = \frac{(s+j)(s+j-1)(s+j-2)\cdots(s+j-k+1)}{k!}$$

$$h = x_i - x_{i-1}, \qquad i = 1,\ldots,n$$

It is obvious that h is a constant since the data are equispaced.

Newton-Gregory Backward Interpolation

In Newton-Gregory backward interpolation, the function values are fitted at x_{-n} to x_0, and the function is defined by:

$$P_n(x) = f_0 + \binom{s}{1}\Delta f_{-1} + \binom{s+1}{2}\Delta^2 f_{-2} + \binom{s+2}{3}\Delta^3 f_{-3} + \binom{s+3}{4}\Delta^4 f_{-4} + \cdots + \binom{s+n-1}{n}\Delta^n f_n$$

$$(3.6)$$

where s and h are the same as defined in Newton-Gregory forward interpolation

Hermite Interpolation

In Hermite interpolation, the function is given by n points (x_i, f_i) and by m derivatives $f_i^{(k)}$ at each point. The function is defined by:

$$Q(t) = \sum_{l=0}^{p-1} (c_{2l} + c_{2l+1}t)[t(t-1)]^l$$

(3.7)

where

$$t = (x - x_k)/h \qquad (h = x_{k+1} - x_k)$$

$$c_{2l} = Q(t_{p-l-1}, t_{p-l}, \ldots, t_{p+l-1})$$

$$c_{2l+1} = Q(t_{p-l-1}, t_{p-l}, \ldots, t_{p+l})$$

Lagrange Interpolation

In Lagrange interpolation, the function is given by n points (x_i, f_i) and the function is defined by:

$$P(x) = \sum_{k=0}^{n} f(x_k) \left\{ \prod_{\substack{i=0 \\ i \neq k}}^{n} \frac{(x - x_i)}{x_k - x_i} \right\}$$

(3.8)

where

$$l_k(x) = \prod_{\substack{j=0 \\ j \neq k}}^{n} \frac{(x - x_j)}{x_k - x_j}$$

$$l_k(x_k) = 1$$

$$l_k(x_i) = 0, \quad i \neq k$$

Inverse Interpolation

Inverse interpolation is an approach that finds the x values corresponding to given function values. The function is defined by:

$$x = \frac{f(x) - f[x_i] - f[x_i, x_{i+1}, x_{i+2}](x - x_i)(x - x_{i+1}) - \cdots}{f[x_i, x_{i+1}]} + x_i \tag{3.9}$$

Gauss Forward Interpolation

Gauss forward interpolation fits data at $x_{-[[n/2]]}$ to $x_{[[n+1/2]]}$, and the function is defined by:

$$P_n(x) = f_0 + \binom{s}{1}\Delta f_0 + \binom{s}{2}\Delta^2 f_{-1} + \binom{s+1}{3}\Delta^3 f_{-1} + \binom{s+1}{4}\Delta^4 f_{-2} + \cdots$$
$$+ \binom{s + [[(n-1)/2]]}{n}\Delta^n f_{-[[n/2]]} \tag{3.10}$$

where $\left[\left[\dfrac{m}{2}\right]\right]$ is greatest integer in $\dfrac{m}{2}$.

Gauss Backward Interpolation

Gauss backward interpolation fits data at $x_{-[[n+1/2]]}$ to $x_{[[n/2]]}$, and the function is defined by:

$$P_n(x) = f_0 + \binom{s}{1}\Delta f_{-1} + \binom{s+1}{2}\Delta^2 f_{-1} + \binom{s+1}{3}\Delta^3 f_{-2} + \binom{s+2}{4}\Delta^4 f_{-2} + \cdots$$
$$+ \binom{s+[[n/2]]}{n}\Delta^n f_{-[[(n+1)/2]]}$$

(3.11)

Stirling Interpolation

Stirling interpolation is based on a diagonal difference table and the data are fitted at $x_{-[[n/2]]}$ to $x_{[[n/2]]}$ (if n is even). The function is defined as:

$$P_n(x) = f_0 + \binom{s}{1}\frac{\Delta f_{-1} + \Delta f_0}{2} + \frac{\binom{s+1}{2} + \binom{s}{2}}{2}\Delta^2 f_{-1} + \binom{s+1}{3}\frac{\Delta^3 f_{-2} + \Delta^3 f_{-1}}{2}$$
$$+ \frac{\binom{s+2}{4} + \binom{s+1}{4}}{2}\Delta^4 f_{-2} + \cdots$$
$$+ \begin{cases} \dfrac{\binom{s+[[n/2]]}{n} + \binom{s+[[(n-1)/2]]}{n}}{2}\Delta^n f_{-[[n/2]]} & \textit{if } n \text{ is even} \\[2ex] \binom{s+[[(n-1)/2]]}{n}\dfrac{\Delta^n f_{-[[(n+1)/2]]} + \Delta^n f_{-[[n/2]]}}{2} & \textit{if } n \text{ is odd} \end{cases}$$

(3.12)

Bessel Interpolation

Bessel interpolation utilizes diagonal difference table that is similar to Stirling interpolation. The data are fitted at $x_{-[[n/2]]}$ to $x_{[[n+1/2]]}$ (if n is odd). The function is defined as:

$$P_n(x) = \frac{f_0 + f_1}{2} + \frac{\binom{s-1}{1} + \binom{s}{1}}{2} \Delta f_0 + \binom{s}{2} \frac{\Delta^2 f_0 + \Delta^2 f_{-1}}{2} + \frac{\binom{s}{3} + \binom{s+1}{3}}{2} \Delta^3 f_{-1}$$

$$+ \binom{s+1}{4} \frac{\Delta^4 f_{-1} + \Delta^4 f_{-2}}{2} + \cdots$$

$$+ \begin{cases} \binom{s+[[(n-2)/2]]}{n} \dfrac{\Delta^n f_{-[[(n-2)/2]]} + \Delta^n f_{-[[n/2]]}}{2} & \text{if } n \text{ is even} \\[4ex] \dfrac{\binom{s+[[(n-2)/2]]}{n} + \binom{s+[[n/2]]}{n}}{2} \Delta^n f_{-[[n/2]]} & \text{if } n \text{ is odd} \end{cases}$$

(3.13)

3.2.2 Cubic Spline Interpolation

This is a method that passes "a set of cubics through the points, using a new cubic in each interval" (Gerald and Wheatley, 1989). In other words, cubic spline interpolation algorithm is a kind of piecewise curve fitting method. For the case with equal interval, given *ith* interval, the cubic function connecting points (x_i, f_i) and (x_{i+1}, f_{i+1}) is defined by:

$$f = a_i(x - x_i)^3 + b_i(x - x_i)^2 + c_i(x - x_i) + d_i$$

(3.14)

where

$$a_i = \frac{\Delta^2 f_{i+1} - \Delta^2 f_i}{6h}$$

$$b_i = \frac{\Delta^2 f_i}{2}$$

$$c_i = \frac{f_{i+1} - f_i}{h} - \frac{2h\Delta^2 f_i + h\Delta^2 f_{i+1}}{6}$$

$$d_i = f_i$$

Moreover, $\Delta^2 f_0$ and $\Delta^2 f_n$ are commonly set to be zero at the endpoints in order to construct a boundary condition. This is called a natural spline interpolation.

3.2.3 Comparison of selected Interpolation Algorithms

For polynomial interpolation algorithms described in Section 3.2.1, all of them are the variation of divided differences methods except Lagrange interpolation. For Lagrange interpolation, it is advantageous to build a polynomial interpolation function for unevenly spaced data. However, this method produces relatively larger error due to oscillation when the data points are close together (Gerald and Wheatley, 1989).

Among the divided difference methods, inverse interpolation is to find the x's, which is not considered in the proposed method, and Hermite interpolation is applicable when there exists an analytical expression and the derivatives up to a certain order are

known. Furthermore, Newton-Gregory forward and backward interpolations, Gauss forward and backward interpolations, Stirling interpolation, and Bessel interpolation are suitable to be applied to equidistance data and will generate identical polynomial when going through the same data points.

For cubic spline interpolation, since it is a piecewise curve fitting method, this function represents smooth curves through the data points. Hence, despite the drawback of lower computational efficiency, cubic spline interpolation yields fewer oscillations that other interpolation formula may create (Gerald, 1989; Recktenwald, 2000). Therefore, cubic spline interpolation is preferable in practice and is chosen for implementing the proposed method.

After implementing the interpolation process, the vehicle reidentification problem can be rewritten as Equations 3.15 and 3.16. Given a downstream target vehicle signature, the objective is to find the most alike vehicle signature among all upstream candidate vehicle signatures.

created using
BCL easyPDF
Printer Driver
Click here to purchase a license to remove this image

$$\text{max} \quad \mu \tag{3.15}$$

$$s.t. \quad \mu \le f_k(x_{A_i}, x_{B_i}) = \sum_{i=1}^{m} \left| f_k(x_{A_i}) - f_k(x_{B_i}) \right|$$

$$\mu \le f_k(x_{A_i}, x_{B_i}) = \sum_{i=1}^{n} \left| f_k(xI_{A_i}) - f_k(x_{B_i}) \right| \quad if \quad m < n$$

$$\mu \le f_k(x_{A_i}, x_{B_i}) = \sum_{i=1}^{m} \left| f_k(x_{A_i}) - f_k(xI_{B_i}) \right| \quad if \quad n < m \tag{3.16}$$

$$\mu \ge 0, \quad k = 1,\dots,l$$

$$f(x_{A_i}) \in \text{DS Target}, \ i = 1,2,\dots,m$$

$$f(x_{B_j}) \in \text{US Candidate}, \ j = 1,2,\dots,n$$

where, the function values of $f(\cdot)$ and $f(\cdot)$ are the reductions in magnitude, and x_{A_i} and x_{B_i} denote the time intervals and:

l : The number of upstream candidate vehicles

$f(x_{A_i})$: The function of the downstream target vehicle signature (DS Target)

$f(x_{B_j})$: The function of the upstream candidate vehicle signature (US Candidate)

xI_{A_i} and xI_{B_i} : The new data set with interpolated points

3.3 PROCEDURE OF REID-2

Based on an assumption that a vehicle will possess the same normalized signature when it passes by detection stations (Ritchie and Sun, 1998), the key idea of REID-2 is to match vehicle signatures by computing and summing the difference in magnitudes for each interpolated data point. Vehicle matches are identified based on search methods applied to the summed magnitude differences, within appropriate time windows. The procedure of REID-2 is illustrated in Figure 3-2.

As shown in Figure 3-2, the inputs are the raw vehicle signature data for a target vehicle and all other vehicles that passed by its corresponding upstream detection station(s). The magnitude of each individual vehicle will be normalized using its range and the normalized magnitudes distribute from zero to one. Only a subset of each vehicle signatures that the normalized magnitudes are within the range from 0.2 to 1.0 will be selected in order to eliminate variations between different detection stations caused by the external environment factors.

To define a feasible candidate vehicle set, temporal search space reduction that establishes a feasible time period for searching possibly matched vehicles at upstream detection stations (Sun et al., 1999; Oh and Ritchie, 2003; Oh, 2003) is performed. Since the aim of temporal search space reduction is to include correct vehicles in the candidate vehicle set, estimated travel times are utilized to set up the lower and the upper bounds of the desired time window.
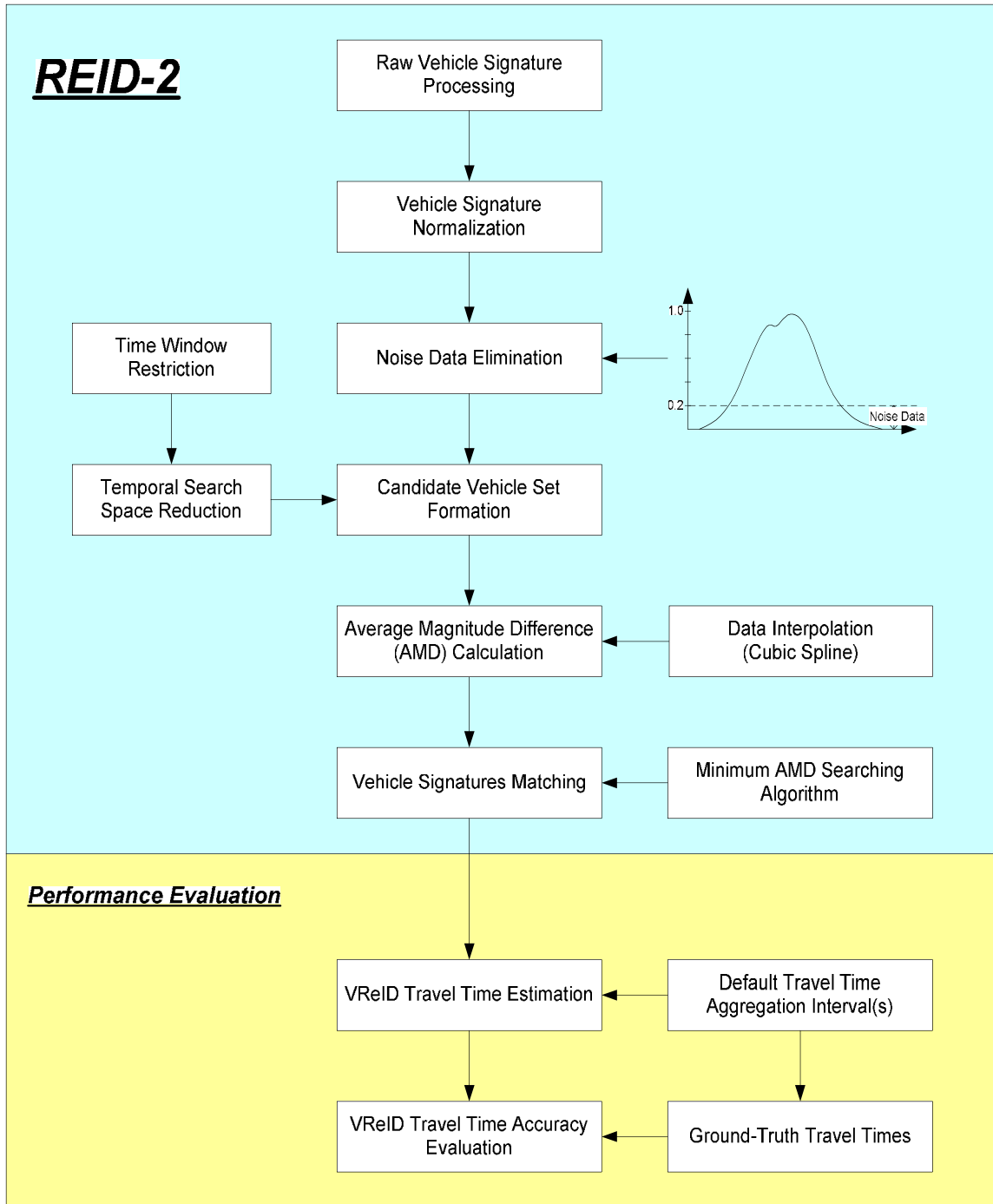
Figure 3-2 The procedure of REID-2 algorithm.

After a candidate vehicle set is found, the operation of REID-2 can be summarized in five steps:

Step 1: Given a downstream target vehicle signature and an upstream candidate vehicle signature, compare the number of data points

Step 2: Stretch the vehicle signature with fewer data points to make both downstream and upstream vehicle signatures have same number of data points using cubic spline interpolation method

Step 3: Compute and sum up the differences of normalized magnitudes between a downstream target vehicle and an upstream candidate vehicle

Step 4: Find the average of the total magnitudes differences (AMD)

Step 5: Perform minimum AMD searching approach

The minimum AMD searching approach aims to maximum the amount of matched vehicles. Thus, the approach firstly defines an upstream candidate vehicle set for a downstream vehicle within a time window. In addition, a reverse time window is applied to each upstream candidate vehicle to find its corresponding candidate vehicle set at its downstream. Both upstream and downstream candidate vehicle sets are sorted in ascending order according to the magnitude differences. Starting from looking into the

created using
BCL easyPDF
Printer Driver
Click here to purchase a license to remove this image

first feasible upstream candidate vehicle (i.e. with the minimum AMD), for example, US_3, given the downstream vehicle (DS_1), the results of vehicle signatures matching can be categorized into two groups:

- System correct match: if the first feasible downstream candidate vehicle for US_3 is DS_1, the proposed algorithm will treat DS_1 as "system correct match case," and DS_1 and US_3 will be crossed out from the candidate vehicle sets. Otherwise, the approach will look into the next feasible upstream candidate vehicle for DS_1. The searching procedure is repeated and will be terminated when there is no feasible upstream candidate vehicle exists for DS_1. When the searching procedure is terminated, the minimum AMD searching approach will re-search the upstream candidate vehicle list, and the first feasible upstream candidate vehicle will be chosen as the matched vehicle at upstream.

- System no match: If there is no feasible upstream candidate vehicle after performing the searching procedure described above, the proposed algorithm will treat DS_1 as "system no match" case.

The process is implemented for all downstream vehicles first, and then the process is implemented for all upstream vehicles. "Iteration" thus consists of one search for downstream vehicles and one search for upstream vehicles. The iterations end when all downstream vehicles are assigned to the aforementioned groups. This minimum AMD

searching approach ensures that vehicles can only be matched once, and decreases the number of system no match cases. It must be noted that for the system correct match case, a vehicle may be mismatched, and it can be examined via ground-truthed data.

Five performance indices (Oh, 2003) including total matching rate (TMR), correct matching rate (CMR), mismatching rate (MR), reliability rate (RR), and mean absolute percentage error (MAPE) of estimated travel times are selected for the performance evaluation:

$$TMR = \frac{\text{total number of matched vehicles}}{\text{total number of vehicles}} \tag{3.17}$$

$$CMR = \frac{\text{total number of correct matched vehicles}}{\text{total number of vehicles}} \tag{3.18}$$

$$MR = \frac{\text{total number of mismatched vehicles}}{\text{total number of vehicles}} \tag{3.19}$$

$$RR = \frac{CMR}{TMR} \tag{3.20}$$

$$MAPE = \frac{\sum_{n=1}^{N} \left[\left| \frac{TTime_{obs,n} - TTime_{est,n}}{TTime_{obs,n}} \right| \times 100 \right]}{N} \tag{3.21}$$

where,

$TTime_{obs,n}$: Observed average travel time at time step n (ground-truthed)

$TTime_{est,n}$: Estimated average travel time at time step n (reidentification

algorithm)

N : Total number of time steps

3.4 CASE STUDY

3.4.1 Data Description

A dataset including twenty minutes of vehicle signature and video ground-truthed data for case study was obtained from the northbound I-405 freeway on July 23rd, 2002, between 15:00 and 15:20. The study site was about 0.63-mile in length, and there were two contiguous detection stations at Laguna Canyon (LC; upstream) and Sand Canyon (SC; downstream). Both detection stations were equipped with square double loop detectors in each lane. In this dissertation, results from the first loop of each double loop pair were used in order to replicate single loop operations. This dataset was collected under moderate flow traffic (1,300 VPHPL (vehicles-per-hour-per-lane)), and consisted of 2,533 vehicle signatures for each detection station. The same dataset has been utilized for other research purposes and the research outcomes can be found elsewhere (e.g. Park and Ritchie, 2004; Oh, Tok and Ritchie, 2004).

To evaluate the performance of REID-2, the lexicographic optimization method (REID-1) previously developed at UCI (Park and Ritchie, 2004; Sun et al., 1999) was also implemented. The approach of REID-1 is discussed in Chapter 2. The size of the time window for REID-2 was the same for all vehicles and was calculated based on the speed distribution at Laguna Canyon, where the minimum was 50mph and the maximum was 90mph. The lower bound and upper bound of the time window were set to be 28.0 seconds (i.e., 90mph) and 48.0 seconds (i.e., 50mph), respectively. For the time window setting applied to REID-1, vehicle types and lane types were considered in addition to speed. The size of the time window for REID-1 is described as follows:

If (HOV (**H**igh **O**ccupancy **V**ehicle) lane)

{

    lower bound = 28.0 sec;

    upper bound = 37.0 sec;

}

else

{

    if (vehicle type = long trailer)

    {

        lower bound = 35.0 sec;

        upper bound = 48.0 sec;

    }

    else

```
    {
        lower bound = 29.0 sec;

        upper bound = 43.0 sec;

    }

}
```

In addition, vehicle signatures obtained from the front loop of the double loop detectors were selected to emulate single loop detectors. REID-1 was also implemented for single loop and double loop cases, and the results were then compared with the results obtained from REID-2.

Furthermore, for the case with double loop, both front and rear loops' signatures at downstream and upstream detection stations can be utilized to increase the probability of obtaining good vehicle signatures for REID-2. For instance, a vehicle, DS_1, can produce two vehicle signatures at downstream detection station (say d1 and d2) and its corresponding candidate vehicle, US_1, can produce two vehicle signatures at upstream detection station (say u1 and u2).

These four vehicle signatures are grouped as (d1, u1), (d1, u2), (d2, u1), and (d2, u2). The process of finding magnitude difference (MD) is performed for all four groups, and the group with minimum MD is chosen as the final MD for DS_1 and US_1. This method is significant when only one of the vehicle signature obtained from a double loop detector is clean.

It was observed that the total number of iterations to perform the AMD searching approach for the double loop case was 41 in contrast to 52 for the single loop case. The performance indices for both double and single loop cases are plotted in Figure 3-3, and the results of the first 10 iterations are detailed in Table 3-1.
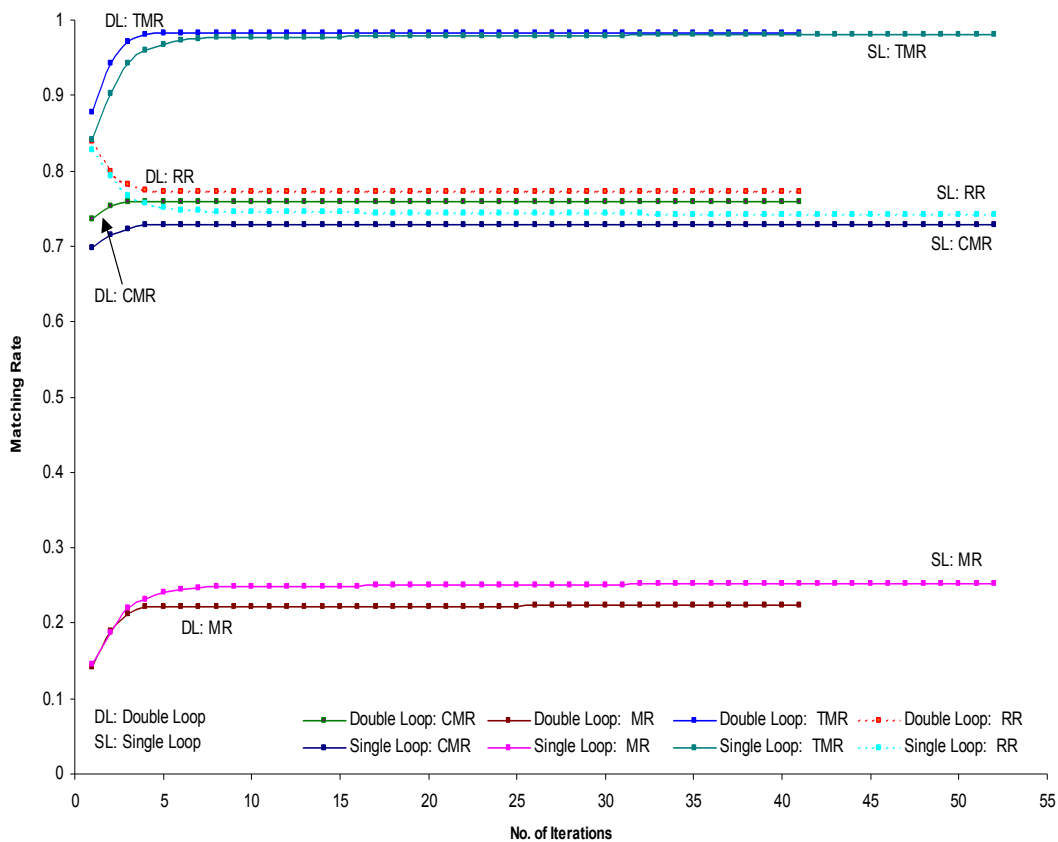
Figure 3-3 Performance evaluation of REID-2.

As shown in Figure 3-3, there is an immediate sharp increase in the TMRs, and at the same time, there is a rapid drop in the RRs, at the beginning of the minimum AMD searching iterations. After approximately five iterations, all of the performance indices remain stable. The declines in the RRs indicate that although the matching possibility is increased via REID-2, the longer iterations result in more mismatched cases and fewer correctly matched cases.

Since the system performance was evaluated via the RRs, the results obtained from the first iteration for both double and single loop cases, which generate the best RR, were selected for further analyses as discussed in the following sections. It must be noticed that although the RRs thus obtained were improved, the CMRs were decreased as a trade-off for both cases.

Table 3-1 The Results of the Performance Indices for REID-2 (10 iterations)

No. of Iterations	1		2		3		4		5	
	Double Loop	Single Loop	Double Loop	Single Loop	Double Loop	Single Loop	Double Loop	Single Loop	Double Loop	Single Loop
Correct Matched Volume	**1864**	**1767**	1907	1812	1922	1832	1924	1843	1924	1844
Mismatched Volume	**358**	**366**	479	474	537	555	560	588	564	608
No Matched Volume	**311**	**400**	147	247	74	146	49	102	45	81
Total Matched Volume	**2222**	**2133**	2386	2286	2459	2387	2484	2431	2488	2452
Total Volume	**2533**	**2533**	2533	2533	2533	2533	2533	2533	2533	2533
Matching Rate	--									
CMR	**73.59%**	**69.76%**	75.29%	71.54%	75.88%	72.33%	75.96%	72.76%	75.96%	72.80%
MR	**14.13%**	**14.45%**	18.91%	18.71%	21.20%	21.91%	22.11%	23.21%	22.27%	24.00%
No Matched Rate (NMR)	**12.28%**	**15.79%**	5.80%	9.75%	2.92%	5.76%	1.93%	4.03%	1.78%	3.20%
TMR	**87.72%**	**84.21%**	94.20%	90.25%	97.08%	94.24%	98.07%	95.97%	98.22%	96.80%
RR	**83.89%**	**82.84%**	79.92%	79.27%	78.16%	76.75%	77.46%	75.81%	77.33%	75.20%

No. of Iterations	6		7		8		9		10	
	Double Loop	Single Loop	Double Loop	Single Loop	Double Loop	Single Loop	Double Loop	Single Loop	Double Loop	Single Loop
Correct Matched Volume	1924	1845	1924	1845	1924	1845	1924	1845	1924	1845
Mismatched Volume	564	620	564	626	564	628	564	628	564	628
No Matched Volume	45	68	45	62	45	60	45	60	45	60
Total Matched Volume	2488	2465	2488	2471	2488	2473	2488	2473	2488	2473
Total Volume	2533	2533	2533	2533	2533	2533	2533	2533	2533	2533
Matching Rate	--									
CMR	75.96%	72.84%	75.96%	72.84%	75.96%	72.84%	75.96%	72.84%	75.96%	72.84%
MR	22.27%	24.48%	22.27%	24.71%	22.27%	24.79%	22.27%	24.79%	22.27%	24.79%
NMR	1.78%	2.68%	1.78%	2.45%	1.78%	2.37%	1.78%	2.37%	1.78%	2.37%
TMR	98.22%	97.32%	98.22%	97.55%	98.22%	97.63%	98.22%	97.63%	98.22%	97.63%
RR	77.33%	74.85%	77.33%	74.67%	77.33%	74.61%	77.33%	74.61%	77.33%	74.61%

3.4.2 Reidentification Performance

The comparisons between REID-1 and REID-2 are tabulated in Table 3-2. It can be seen from Table 3-2 that, for the double loop case, the CMR of REID-2 is 73.59%, while the CMR of REID-1 is 72.13%. For the single loop case, the CMR of REID-2 is 69.76%, while the CMR of REID-1 is only 58.07%.

In addition, although the TMR of REID-2 (87.72%) is greater than that of REID-1 (80.77%), the RR is 83.89%, which is less than the RR of REID-1 (89.30%) for the double loop case. The more important findings are observed from the single loop case. Not only the TMR of REID-2 (84.21%) is greater than that of REID-1 (72.52%), but also the RR (82.84%) is higher than the RR of REID-1 (80.08%). The effects on the different levels of the reliability rate can be examined via the accuracy of the estimated travel times and that will be discussed in the next section.

In spite of the lower RR of REID-2 for the double loop case, the results are quite encouraging since the CMR of REID-2 for double and single loop cases is superior to that of REID-1. Moreover, for the single loop case, the higher RR implies that REID-2 is more reliable than REID-1.

**Table 3-2 Comparisons between REID-1 and REID-2**

Methods for Vehicle Reidentification	REID-2		REID-1	
			Speed Configuration	
	Double Loop	Single Loop	Double Loop	Single Loop
Correct Matched Volume	1864	1767	1827	1471
Mismatched Volume	358	366	219	366
No Matched Volume	311	400	487	696
Total Matched Volume	2222	2133	2046	1837
Total Volume	2533	2533	2533	2533
Matching Rate	--			
CMR	73.59%	69.76%	72.13%	58.07%
MR	14.13%	14.45%	8.65%	14.45%
NMR	12.28%	15.79%	19.23%	27.48%
TMR	87.72%	84.21%	80.77%	72.52%
RR	83.89%	82.84%	89.30%	80.08%

It is worth reiterating that a major potential contribution of REID-2 is application to single loop vehicle reidentification and performance measurement. This is due to elimination of the speed estimation procedure for the single loop case. In addition, REID-2 for vehicle reidentification may be potentially applied to square and round single loops without speed model re-estimation, or suffering the degradation without speed re-estimation.

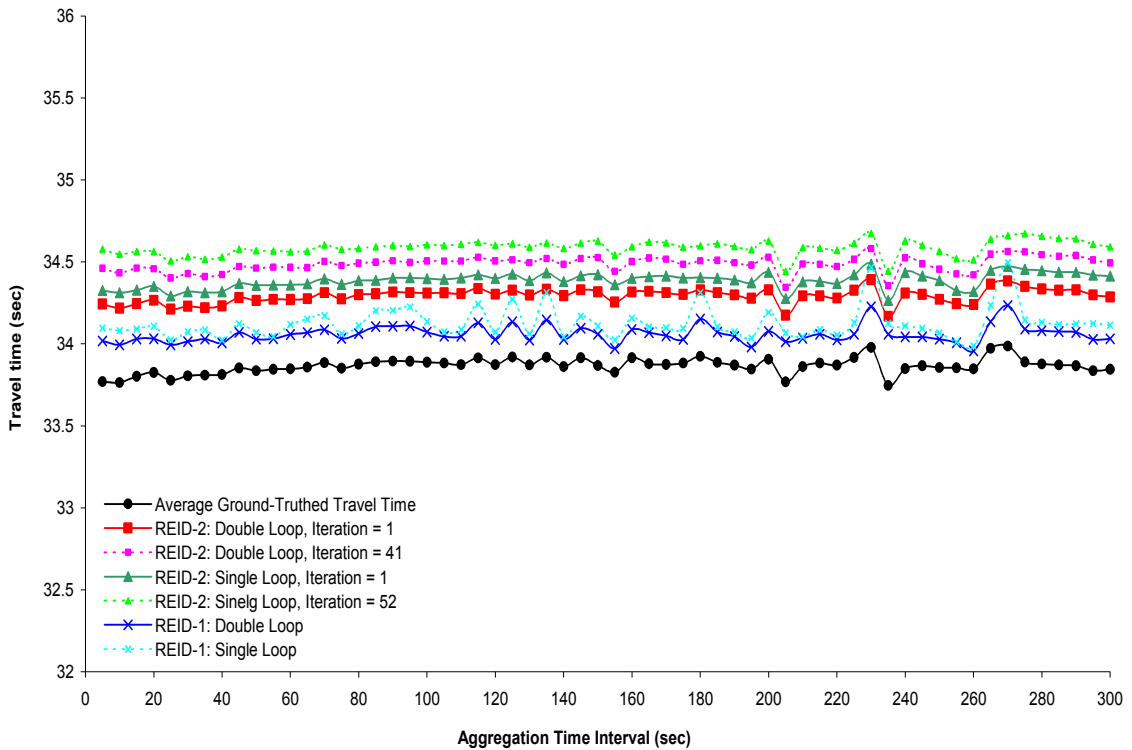### 3.4.3 Travel Time Accuracy Evaluation

The results of travel time accuracy evaluation are shown in Figures 3-4 to 3-7. It can be expected that the double loop case will perform better than the single loop dose, since the double loop case possesses higher RR. Figure 3-4 depicts the average MAPEs for each

aggregation time interval. There are 60 aggregation periods ranging from 5-seconds to 300-seconds in this study. Overall, the average MAPEs are about within the range of 1.00% to 2.50% for REID-2. In addition, it was observed that the double loop case results brought out less MAPEs (about 21.97% lower on the whole) than the single loop case did for REID-2. It is because the double loop case has higher possibility to produce and to find "good" vehicle signatures.
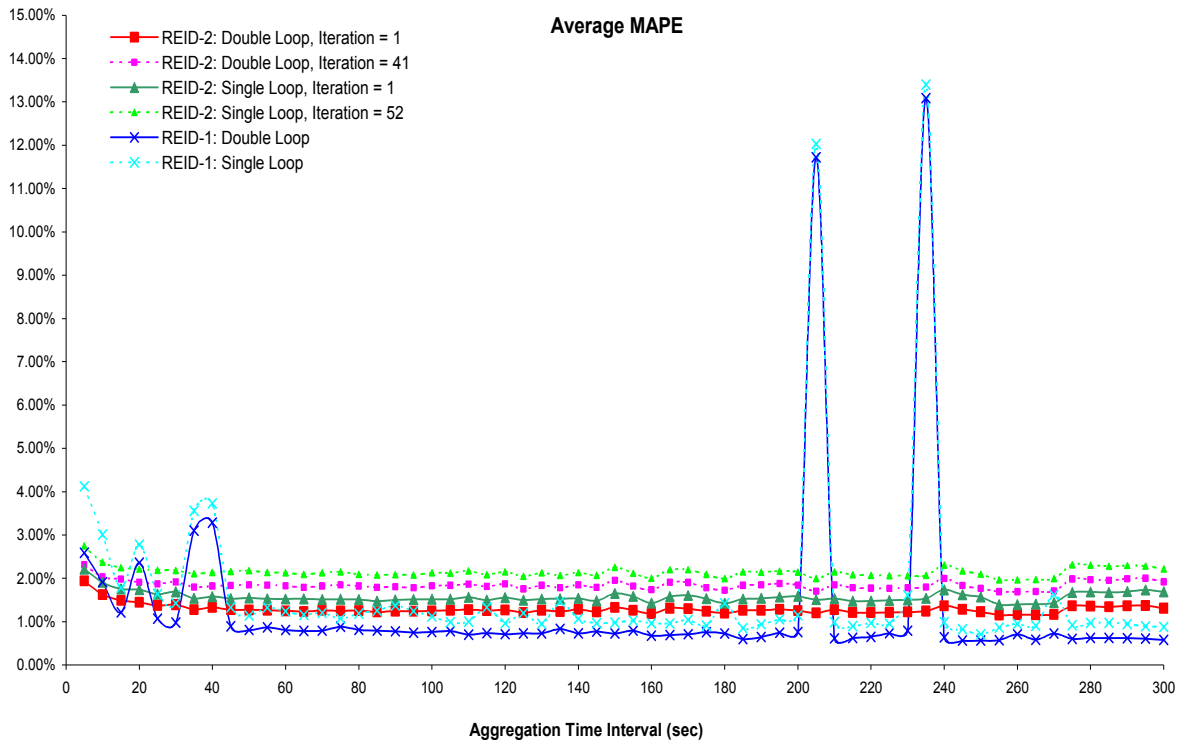
Figure 3-4 Mean absolute percentage error (MAPE) for travel time estimation.

The average travel times for each aggregation time interval are demonstrated in Figure 3-5. It can be observed that for both double and single loop cases, REID-2 has the tendencies to overestimate the travel times. It may be due to the algorithm is more likely unable to catch those vehicles traveling with relatively higher speed. In other words, vehicles traversing with relative higher speed are less likely to be matched by REID-2.

**Figure 3-5 Average estimated travel time accuracy analysis.**

This is explainable since a vehicle traveling at a relatively higher speed will generate fewer data points, and less information can be used for REID-2. That means the errors caused by the interpolation function will emerge as an issue for the magnitude

differences calculation. That is to say, the results of the magnitude differences calculation will involve more interpolation errors for the vehicles traveling at higher speeds (i.e., less possibility to be reidentified). Since it is relatively easy to reidentify vehicles with lower speeds, the estimated travel times for the interpolation method are greater than the true travel times.

Moreover, it can be seen that REID-1 can provide more accurate estimates of travel times than REID-2 does, in general. However, in view of stability, REID-2 leads to more stable average MAPEs than REID-1 does (see Figure 3-4); the estimated travel times follow the trend of the actual travel times (see Figure 3-5). This is because REID-1 brings in more no-match cases, and it is more likely that no vehicle can be reidentified for certain time intervals. If the time window restriction is constructed based on the estimated travel time obtained from the previous time interval, the size of the time window may not be well defined because of the instability of MAPEs. This may cause possibly matched vehicles at upstream detection stations not to be properly included.

Figure 3-6, Figure 3-7, Figure 3-8, and Figure 3-9 demonstrate the selected results of the comparison of estimated travel times given different aggregation periods including 10-seconds, 20-seconds, 30-seconds, 60-seconds, 180-seconds, and 300-seconds. There are zero travel times when the aggregation interval is less than 20 seconds. This is because there is no vehicle passing by the downstream detection station or no vehicle is reidentified at the aggregation interval.
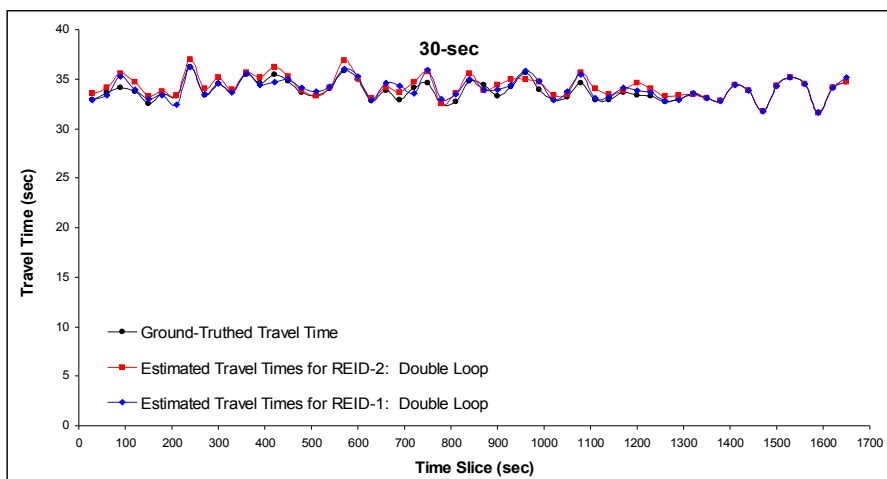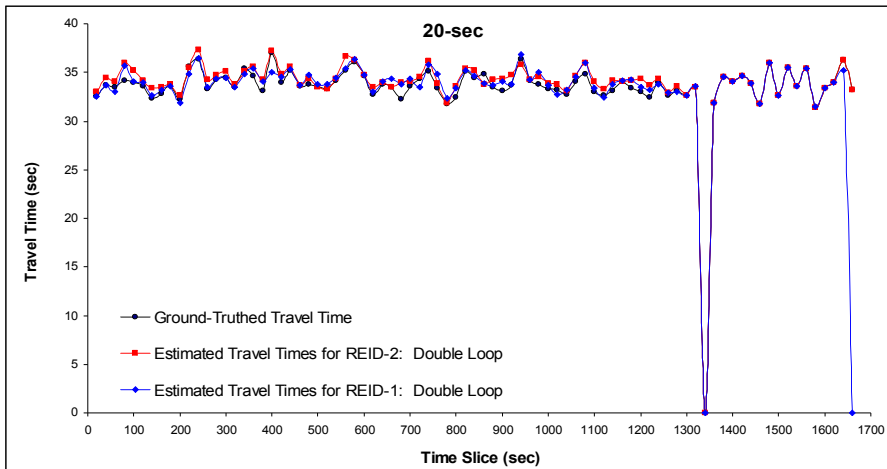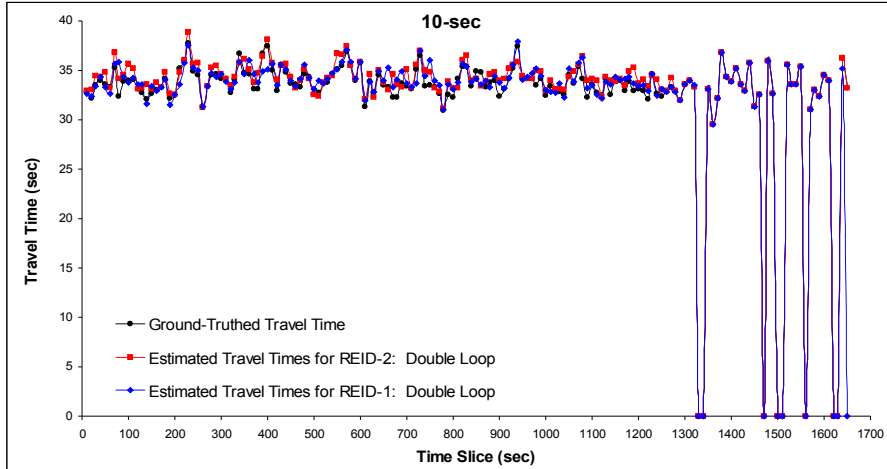
Figure 3-6 Comparisons of travel times (Double loop): 10-sec, 20-sec, and 30-sec.
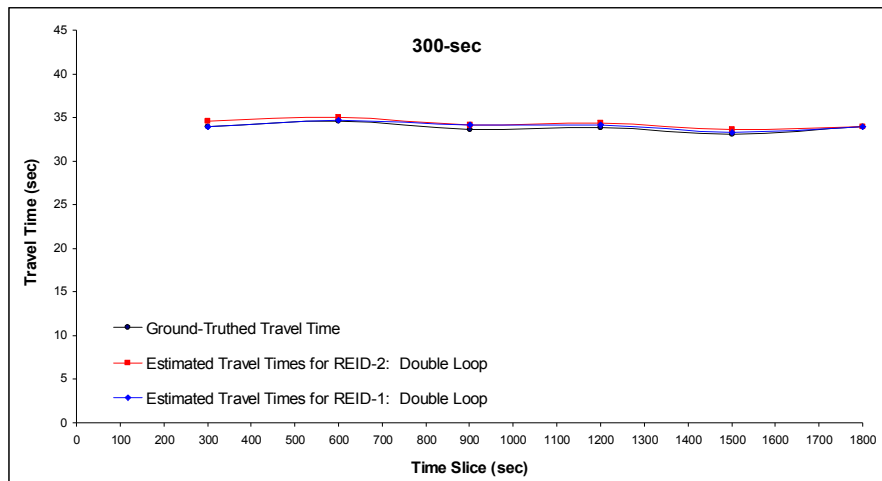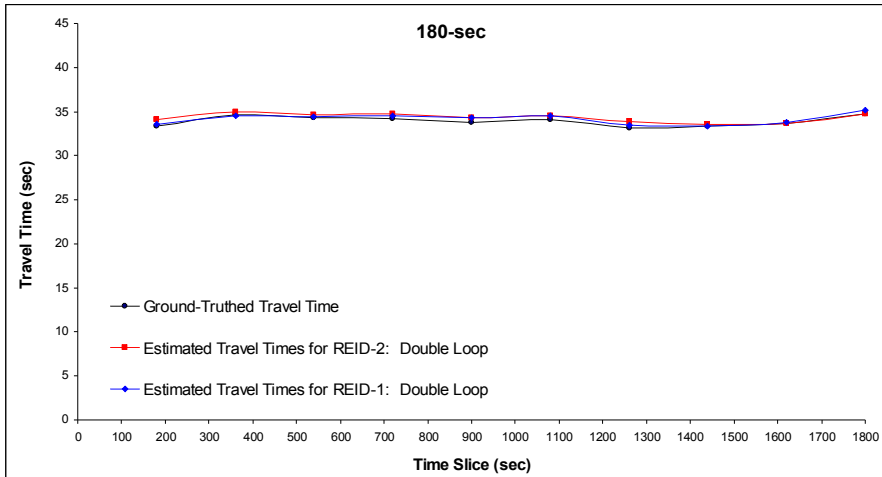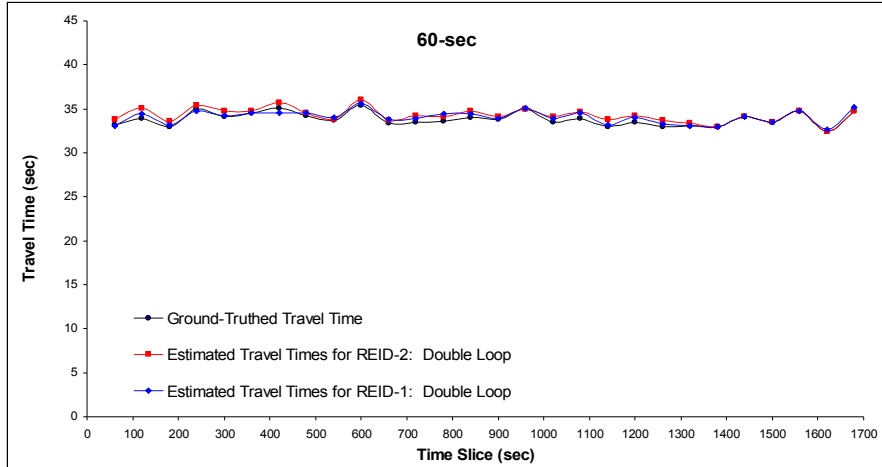
Figure 3-7 Comparisons of travel times (Double loop): 60-sec, 180-sec, and 300-sec.

53
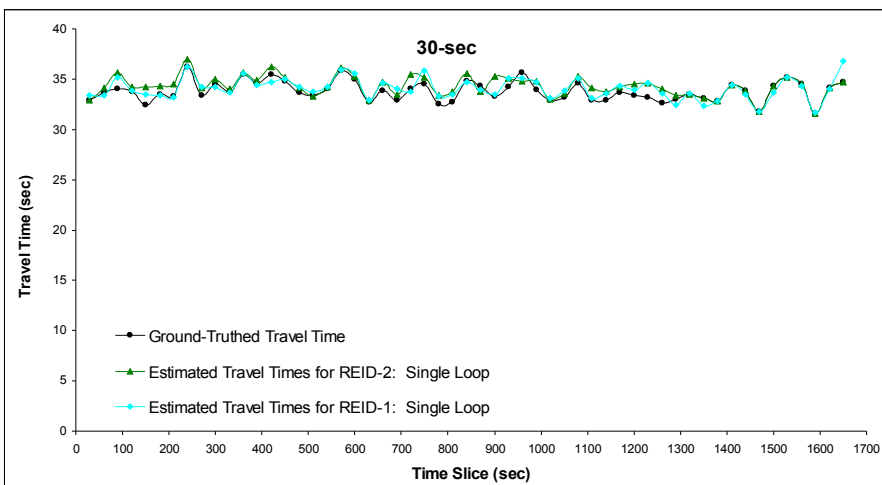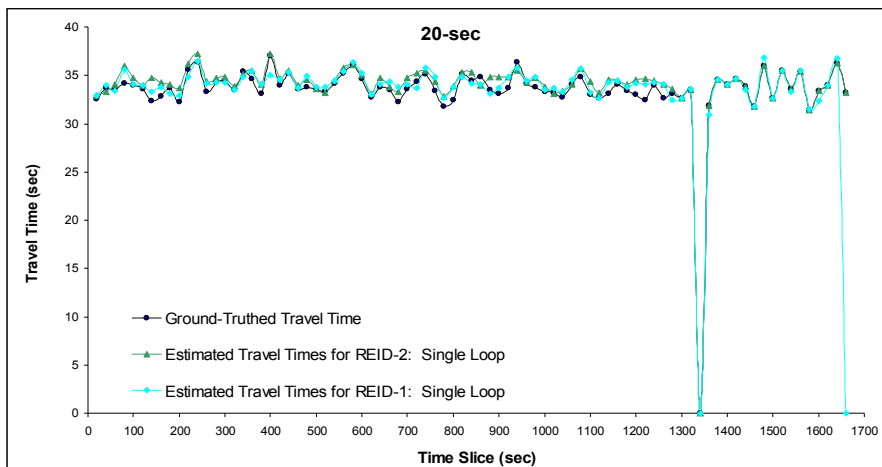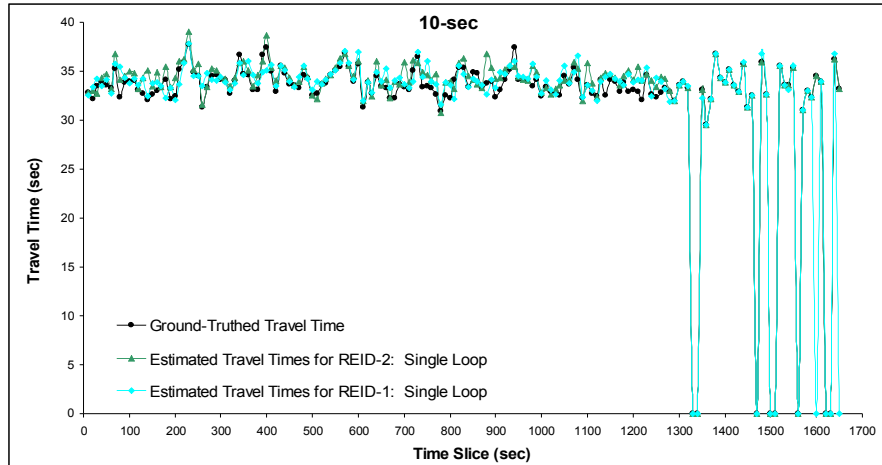
Figure 3-8 Comparisons of travel times (Single loop): 10-sec, 20-sec, and 30-sec.

54
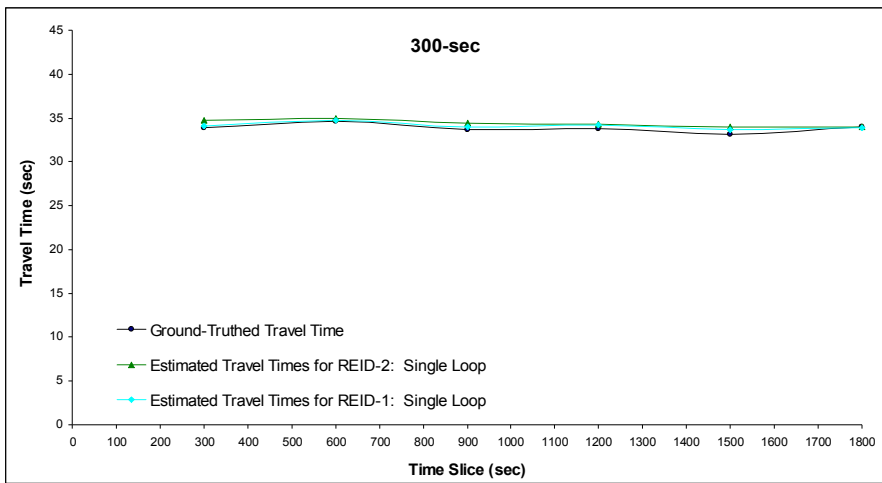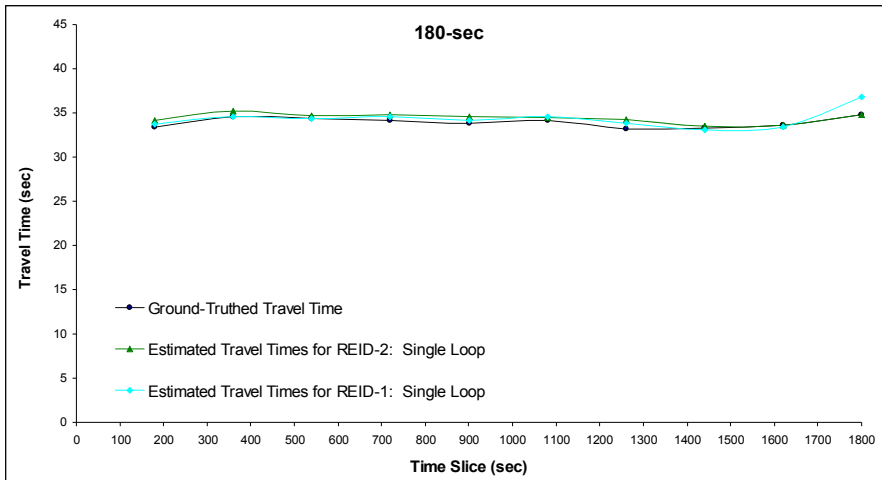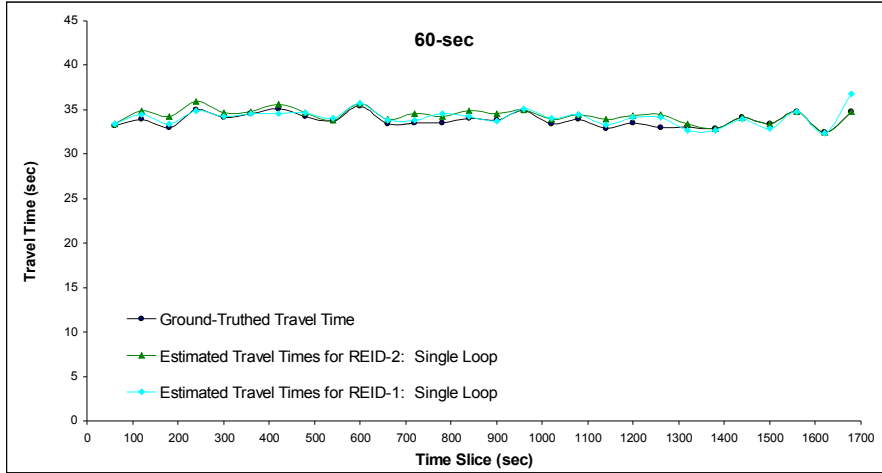
Figure 3-9 Comparisons of travel times (Single loop): 60-sec, 180-sec, and 300-sec.

55

For both single and double loop cases, it can be found that smaller errors and stability can be achieved when the aggregation time interval is greater than 30 seconds. Additionally, the 180-second and 300-second aggregation result in smooth curves and hence they are relatively insensitive to reflect the real world.

3.5 SUMMARY

In this chapter, a new vehicle reidentification algorithm using an interpolation method, named REID-2, was explored. The key idea of the proposed method is to find the minimum magnitude differences given a downstream vehicle and its corresponding upstream candidate vehicles. The case study showed that REID-2 is comparable with REID-1 and is even advantageous because REID-2 involves no speed estimation models, is straightforward, and is readily applied to both single and double loop detectors.

The potential contribution of the proposed method is application to square and round single loop (which in California are far more common than double loop installations) vehicle reidentification, while avoiding issues associated with re-estimation or transferability of the speed models used in the previously developed approach.

The next step is to investigate the feasibility of REID-2 for real-time implementation, and these investigations are presented in Chapter 4. In addition, the study site described in this chapter included only one single freeway section, and REID-2

was implemented under moderate traffic flow conditions. Therefore, further research is

conducted to extend single-sections to multi-sections along a freeway, as demonstrated in

Chapter 5. Different levels of traffic flows are also taken into account in that chapter.

CHAPTER 4 DATA COMPRESSION AND TRANSFORMATION METHOD FOR REAL-TIME VEHICLE REIDENTIFICATION (RTREID-2)

A new vehicle reidentification algorithm (REID-2) developed in Chapter 3 is oriented toward algorithm simplification, but also demonstrates the added benefits of improved performance and much broader potential applicability (to both round and square single inductive loops) compared with earlier methods. However, the basis of REID-2 is directly matching inductive vehicle signatures, which typically consist of 200~1,200 data points (stored as integers, and obtained from IST-222 detector cards) per signature. The size of the vehicle signature may become an issue since the field computational resources in traffic operations and the bandwidth of field communication links are often quite limited.

Therefore, the purpose of this chapter is to investigate if a relatively simple data compression and transformation technique could be applied successfully to the raw inductive signatures of individual vehicles, with the resulting transformed vehicle signatures used as the inputs of the vehicle reidentification system. To achieve this aim, a Piecewise Slope Rate (PSR) approach is utilized to compress and transform the raw vehicle signatures, and the PSR approach is adopted for Real-Time REID-2 (RTREID-2).

4.1 INTRODUCTION

Field computational resources in the traffic operations as well as the bandwidth of field communication links are often quite limited. Accordingly, for real-time implementation of ATMIS strategies, such as vehicle reidentification, there is strong interest in development of field-based techniques and models that can perform satisfactorily while minimizing field computational and communication requirements.

This can be achieved through use of simplified algorithms, and reducing the number and size of data items to be communicated from the field. The relative importance of each of these aspects may vary with different applications, system architectures, and hardware and software environments, but each can play an important role.

The development of REID-2 is oriented toward algorithm simplification. However, the basis of REID-2 is to directly match inductive vehicle signatures, which typically consist of 200~1,200 data points (stored as integers). To compress and transform raw vehicle inductive signatures, a Piecewise Slope Rate (PSR) approach is adopted for Real-Time REID-2 (RTREID-2). If successful, the reduction in computational effort and in computer memory needed to store individual signatures could potentially benefit both the field computational and communication requirements for implementing RTREID-2 in a real-time setting.

4.2 VEHICLE SIGNATURE TRANSFORMATION

As mentioned above, raw vehicle signatures are used as the inputs for REID-2, and each signature typically consists of about 200~1,200 data points. The variation of the data points for each vehicle signature mainly results from different vehicle lengths and traveling speeds. Since the purpose of this chapter is to reduce the size of the input data for REID-2, any approach that is capable of compressing raw vehicle signatures can be considered.

However, in order to compress and transform raw vehicle signatures at the same time (i.e., to reduce the data size and keep as much of the information of the raw signature), a set of piecewise information obtained from the raw vehicle signature is preferred. A simple way to compress and transform the raw vehicle signature is to use slope rate features. While various statistics such as mean, median and others have some potential for this aim, a slope value is more useful. This is because the slope feature can be seen as a linear approximation to the raw vehicle signature.

Therefore, instead of using the whole raw vehicle signature as the input, the proposed method of RTREID-2 uses piecewise slope rate (PSR) values to reidentify individual vehicles. The idea of RTREID-2 is to match vehicle signatures by computing and summing the differences among extracted PSR values. Vehicle matches are then identified by applying a search across the averaged PSR differences, within appropriate time windows. Given a downstream target vehicle and its corresponding upstream

candidate vehicle set, the first three steps for REID-2 are therefore modified and the procedure of RTREID-2 can be summarized in five steps, as illustrated in Figure 4-1:

Step 1: Stretch or shrink vehicle signatures to obtain an identical number of data points per vehicle signature (assigned arbitrarily; say 840 data points, denoted as CASE_840, as shown in Figure 4-1) using a cubic spline interpolation method.

Step 2: Calculate slope rate (SR) at a fixed size of interval (assigned arbitrarily; say every 28 data points, which will generate 30 piecewise slope rate (PSR) values (or PSR = 30) given 840 data points). For example, assume a data point located at $(x_1,\ y_1) = (28,\ 0.2236)$. Given that the slope rate is calculated every 28 data points, the next data point of interest will be located at $(x_2,\ y_2) = (56,\ 0.4747)$. Therefore, the slope rate is:

$$\frac{(y_2 - y_1)}{(x_2 - x_1)} = \frac{(0.4747 - 0.2236)}{(56 - 28)} = 0.007986 .$$

Step 3: Sum up the differences between the PSRs obtained from the downstream target vehicle and the upstream candidate vehicle signatures directly.

Step 4: Find the average of the total PSRs differences obtained from Step 3 (AMD).

Step 5: Perform a minimum AMD search.

created using
BCL easyPDF
Printer Driver
Click here to purchase a license to remove this image
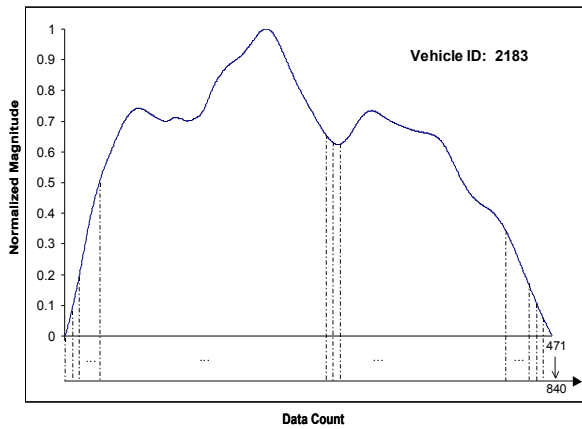
(a) Step 1: Data Interpolation (CASE_840)
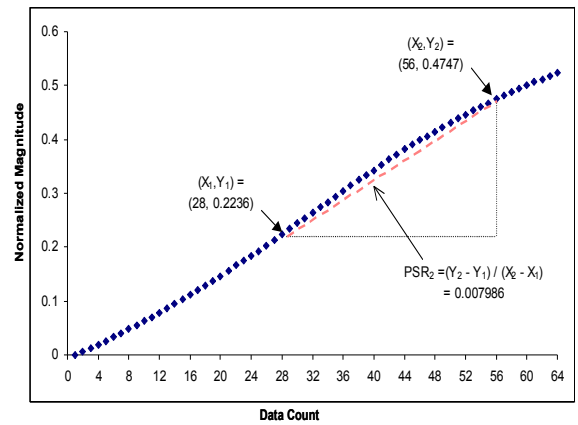
(b) Step 2: Slope Rate Calculation
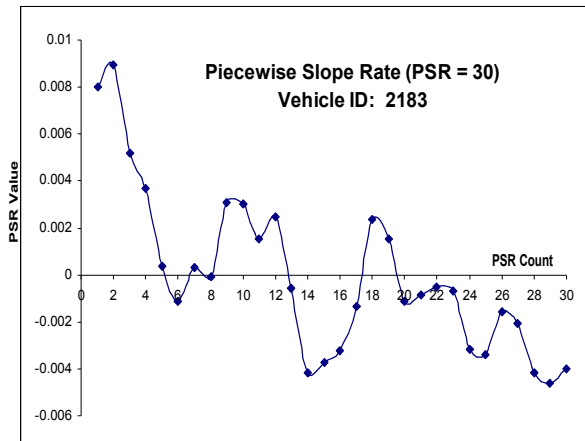
(c) Step 2 (cont): Piecewise Slope Rate Plot
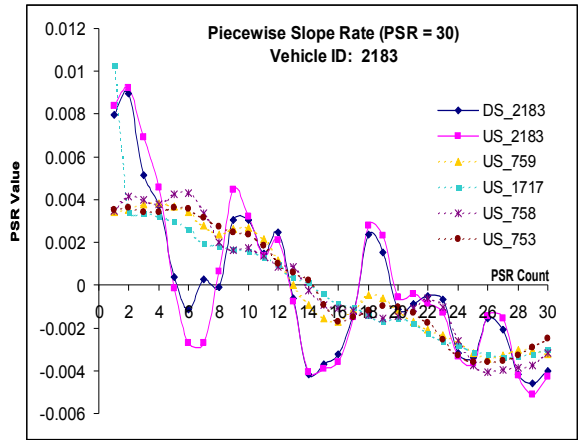
(d) Steps 3 - 5: Vehicle Signature Matching

Figure 4-1 The procedure of RTREID-2.

It must be noted that since the size of the interpolated vehicle signature and the number of PSR values are assigned arbitrarily, a sensitivity analysis is performed in the next section to evaluate the effects caused by these assignments. To facilitate comparison, a case study for implementing RTREID-2 is constructed based on the framework designed in Chapter 3. In addition, five performance indices (Oh, 2003) including total matching rate (TMR), correct matching rate (CMR), mismatching rate (MR), reliability rate (RR), and mean absolute percentage error (MAPE) of estimated travel times are selected for the performance evaluation.

4.3 CASE STUDY

4.3.1 Sensitivity Analysis for Reidentification Performance

For analyzing the effects of the different sizes of the interpolated vehicle signatures, eight cases were constructed for sensitivity analysis. Furthermore, different PSR values were assigned to each case for further evaluation, and the details are tabulated in Table 4-1. The CMR, MR, TMR, and RR were used for performance evaluation. In addition to the four performance indices, a travel time estimation accuracy index (TTEst) was also computed (see Equation 4.1) based on the vehicle reidentification results:

$$TTEst = (1 - MAPE) \times 100\%$$
(4.1)

Table 4-1 Cases for Sensitivity Analysis

# of PSR \ Case_ID	# of Data Points after Performing Interpolation							
	30	60	120	180	280	560	840	1120
	Case_30	Case_60	Case_120	Case_180	Case_280	Case_560	Case_840	Case_1120
PSR = 5	X	X	X	X				
PSR = 7					X	X	X	X
PSR = 10	X	X	X	X	X	X	X	X
PSR = 14					X	X	X	X
PSR = 15	X	X	X	X				
PSR = 20		X	X	X	X	X	X	X
PSR = 28					X	X	X	X
PSR = 30		X	X	X				
PSR = 40					X	X	X	X
PSR = 60			X	X				
PSR = 70					X	X	X	X
PSR = 90				X				
PSR = 140					X	X	X	X
PSR = 280						X	X	X

Representative results of the sensitivity analysis are summarized in Figure 4-2 and Figure 4-3. High values of all indices, except for MR, are preferred. It can be observed from Figure 4-2 that larger sizes (Case_ID) for the interpolated vehicle signature and larger PSR values result in better performance, i.e. higher values of reliability rate (RR). Moreover, all the cases have comparable performance if PSR is equal to or greater than 20. However, with larger PSR values (i.e., PSR > 20), the size of the interpolated vehicle signature has less effect on the overall performance of the travel time estimation (see Figure 4-3).
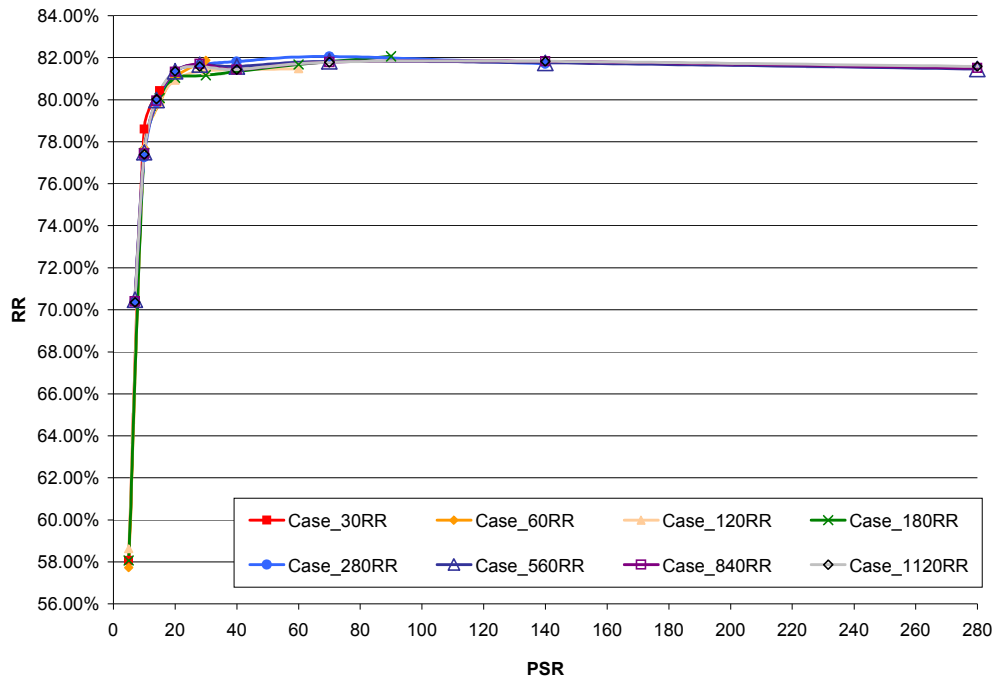
Figure 4-2 Summary of sensitivity analysis based on RR.
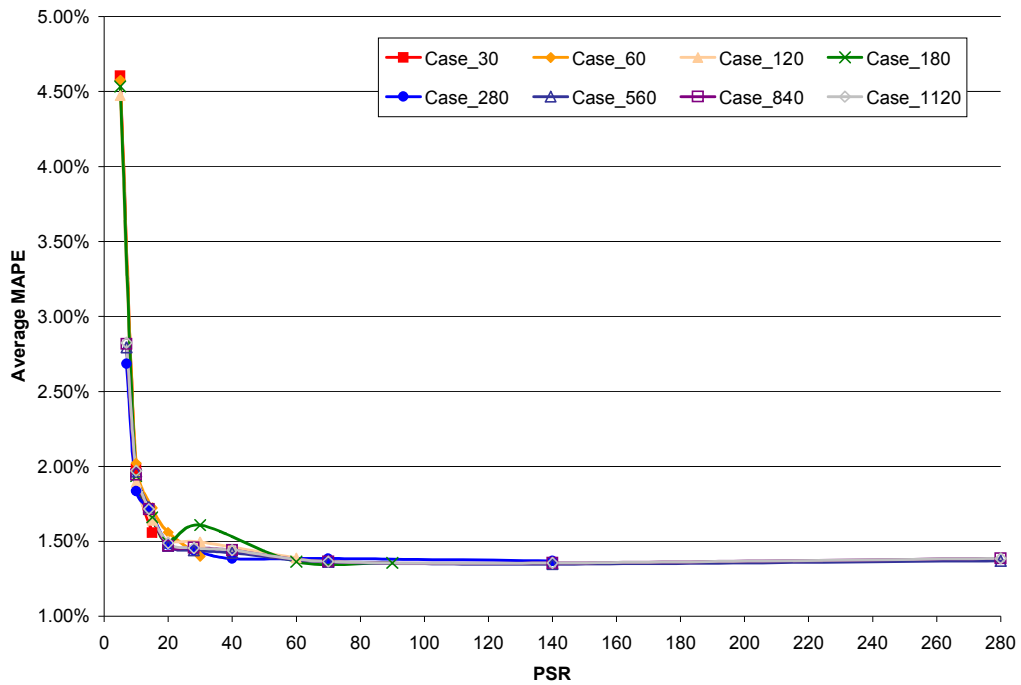
Figure 4-3 Summary of sensitivity analysis based on average MAPE.

65

For computational performance, the computation time included the time to complete the five steps for implementing RTREID-2 and to write the outputs into text files. The results show that the computation time ranges from 0.628 seconds to 1.124 seconds per vehicle and larger PSR values require more computational effort (see Figure 4-4).

Although it was found that CASE_180 with PSR = 90 generated the best performance, smaller PSR values, such as PSR ≤ 30, are preferable to alleviate computational effort. Given PSR ≤ 30, Case_60 with PSR = 30 provided the best outcomes. Hence, both Case_180 with PSR = 90 and Case_60 with PSR = 30 were selected for further evaluation as discussed below.
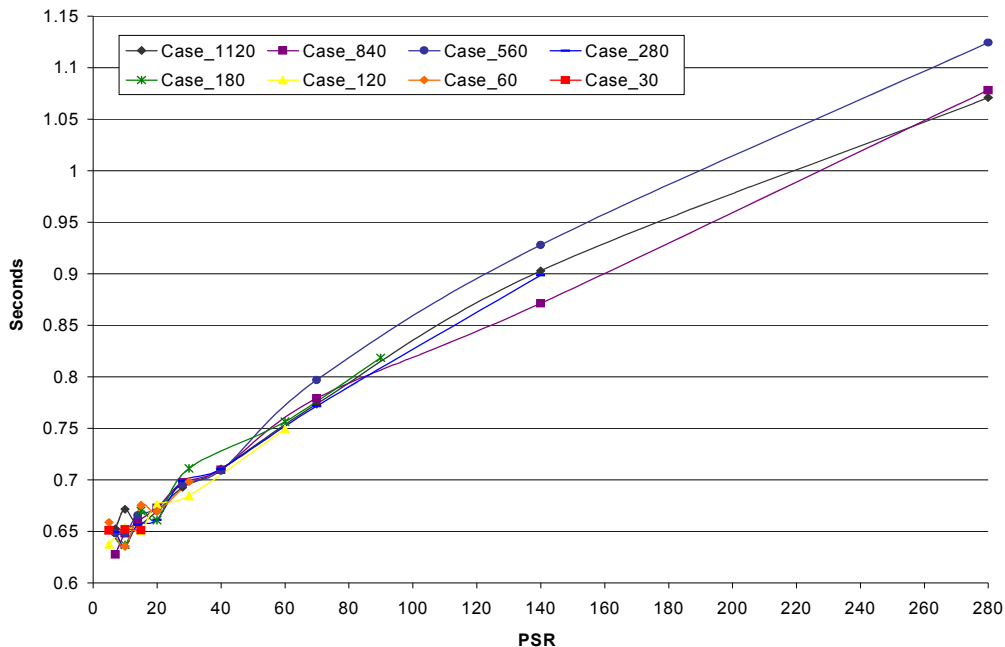
Figure 4-4 Summary of sensitivity analysis based on computational performance.

66

4.3.2 Reidentification Performance

The comparisons of three vehicle reidentification algorithms including REID-1, REID-2, and RTREID-2 are illustrated in Figure 4-5 and Table 4-2. Since the values of MAPE were too small compared with all other performance indices, TTEst was used instead of MAPE for displaying and comparing the results graphically. It can be observed form Figure 4-5 that RTREID-2 is superior to REID-1 and REID-2, and both cases of the RTREID-2 provide the same good performance.
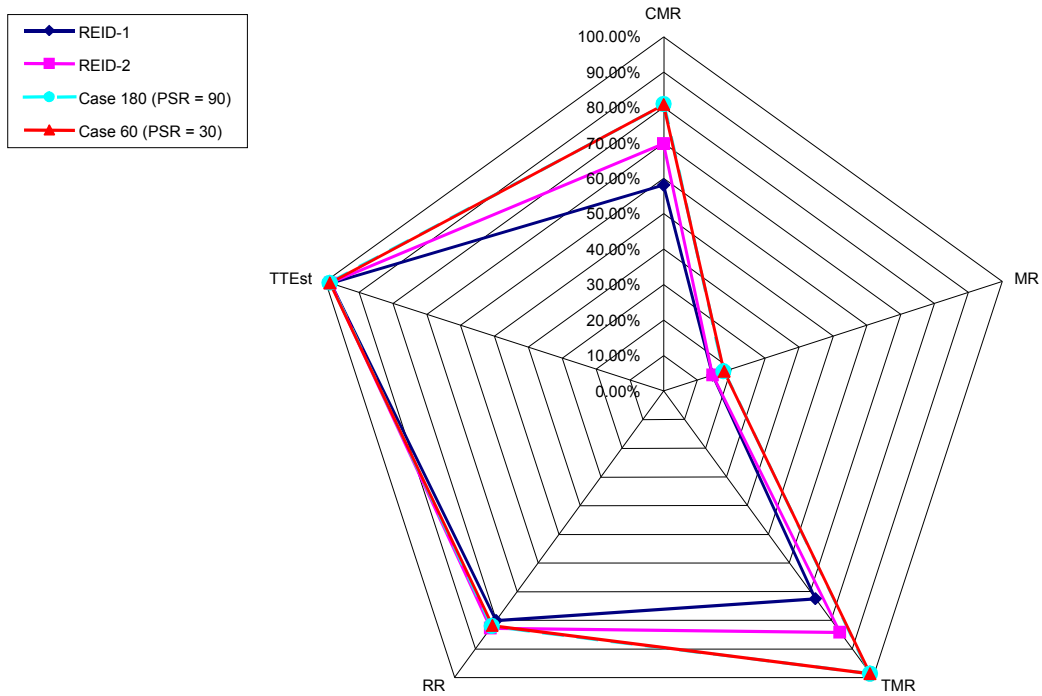
Figure 4-5 Comparisons of three vehicle reidentification algorithms.

It can also be seen from Table 4-2 that the CMR and TMR of RTREID-2 are about 80% and 98% respectively. Both of the performance indices are significantly improved for RTREID-2. Although the MR is also increased for RTREID-2, the reliability rate (RR) of RTREID-2 remains comparable with REID-2. The effects on the different levels of the reliability rate can be examined via the accuracy of the estimated travel times, which will be discussed in the next section. In addition, the computation times for the two cases of RTREID-2 are significantly less than that of REID-2.

Table 4-2 Comparisons of Vehicle Reidentification Algorithms

Methods for Vehicle Reidentification	REID-1*	REID-2**	RTREID-2: Case_60 (PSR = 30)	RTREID-2: Case_180 (PSR = 90)
Correct Matched Volume	1471	1767	2046	2050
Mismatched Volume	366	366	453	448
No Matched Volume	696	400	34	35
Total Matched Volume	1837	2133	2499	2498
Total Volume	2533	2533	2533	2533
Matching Rate	---			
CMR	58.07%	69.76%	80.77%	80.93%
MR	14.45%	14.45%	17.88%	17.69%
NMR	27.48%	15.79%	1.34%	1.38%
TMR	72.52%	84.21%	98.66%	98.62%
RR	80.08%	82.84%	81.87%	82.07%
Computation Time (seconds per vehicle)	N/A	1.549	0.698	0.818

* REID-1 is the lexicographic method (Jeng and Ritchie, 2005)
** REID-2 is the interpolation method (Jeng and Ritchie, 2005)

The results are quite encouraging since the CMR and TMR of both cases of RTREID-2 are superior to those of REID-1 and REID-2. The comparable RR implies that RTREID-2 can achieve similar performance to REID-2 using the transformed vehicle signatures as input data. Since Case_60 with PSR = 30 is comparable to Case_180 with PSR = 90, the number of data points required by a transformed vehicle signature can be 20~40 data points, which is about 80.00%~98.33% less than the original raw vehicle signature.

Moreover, it is worth noting that in addition to inheriting the major potential contributions of REID-2, the higher CMR and TMR together with the comparable RR of RTREID-2 imply a potential to correctly reidentify more vehicles without suffering the degradation of system reliability. In other words, the high CMR, TMR, and RR of RTREID-2 show the potential contribution of tracking a vehicle more successfully along its path leading to a destination.

4.3.3 Travel Time Accuracy Evaluation

The results of travel time accuracy evaluation are shown in Figure 4-6, Figure 4-7, Figure 4-8, and Figure 4-9. Given different aggregation time periods, selected results from the comparison of estimated travel times are demonstrated in Figure 4-6 and Figure 4-7. It was found that smaller errors and stability could be obtained when the aggregation interval was greater than 30 seconds, which is similar to the previous studies discussed in Chapter 3.
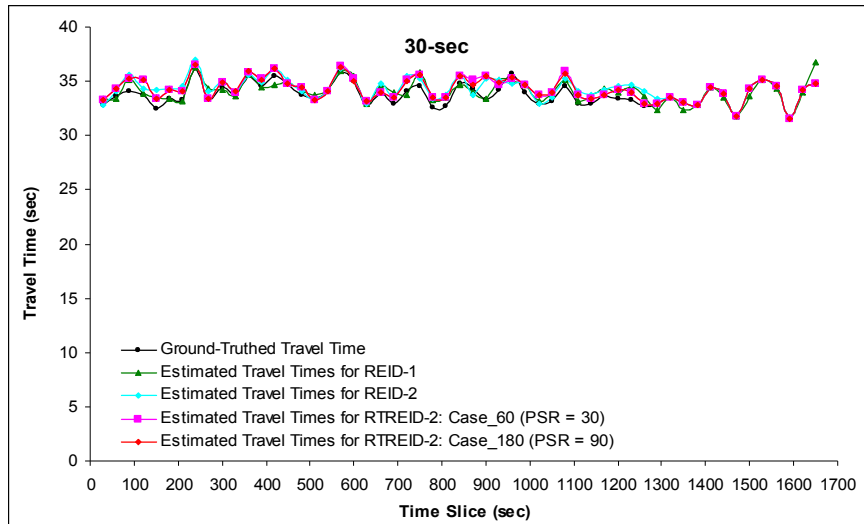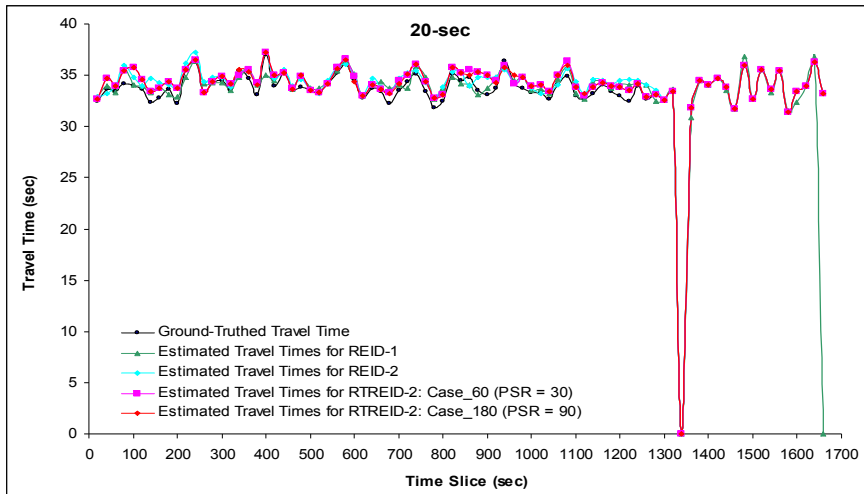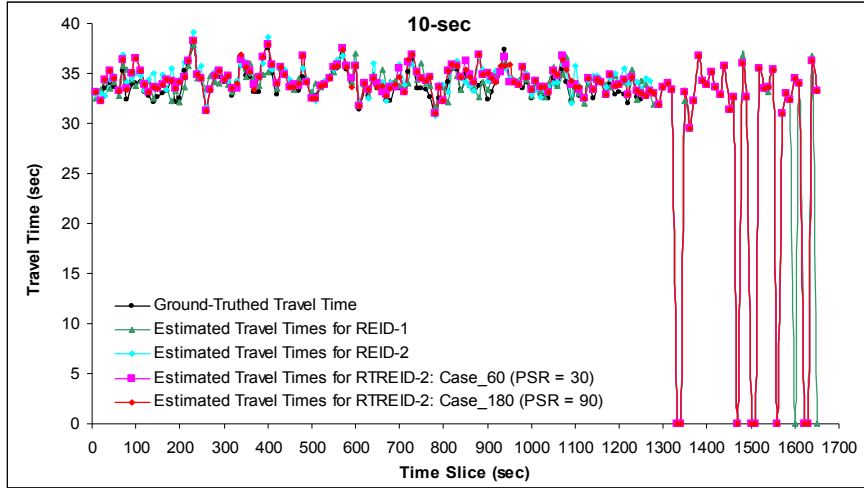
Figure 4-6 Comparisons of travel times: 10-sec, 20-sec, and 30-sec.
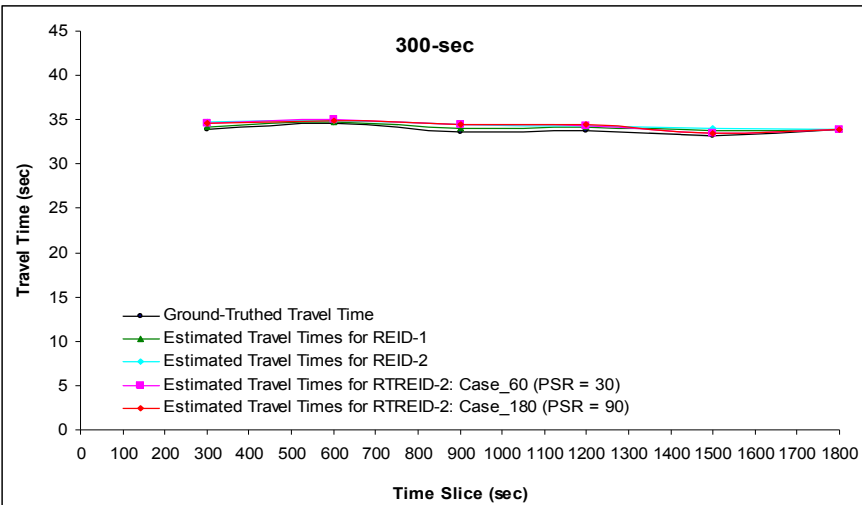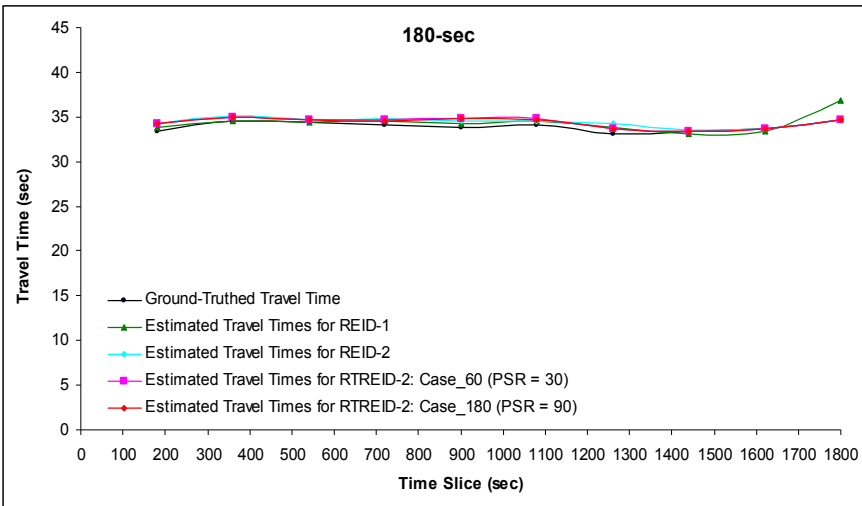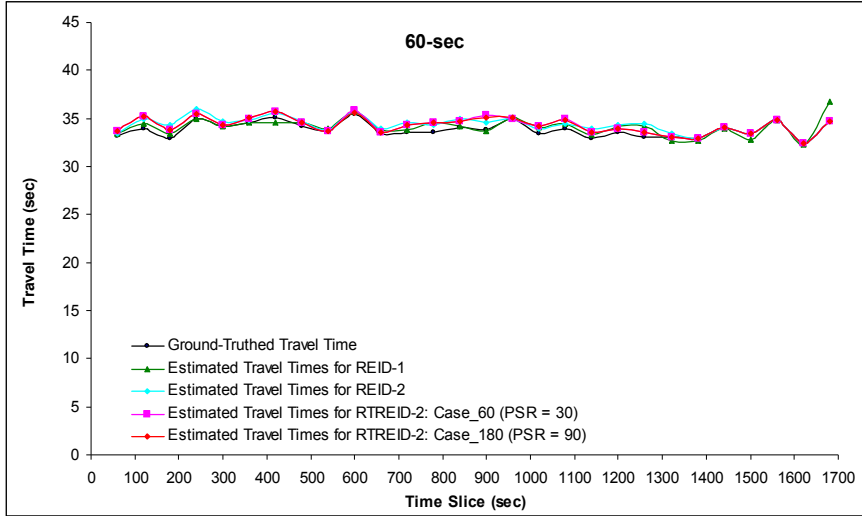
Figure 4-7 Comparisons of travel times: 60-sec, 180-sec, and 300-sec.

Figure 4-8 depicts the average travel times for each aggregation time interval. It can be observed that the estimated travel times of both cases of RTREID-2 follow the trend of the actual travel times very well. In addition, the two cases of RTREID-2 generate similar results as compared with REID-2, and have a tendency to overestimate the travel time slightly. This may be due to the system not capturing some vehicles traveling at relatively high speed, which is observed from the previous studies shown in Chapter 3. Since it is relatively easy to reidentify vehicles with lower speeds, the estimated travel times for the interpolation method are higher than the true travel times.
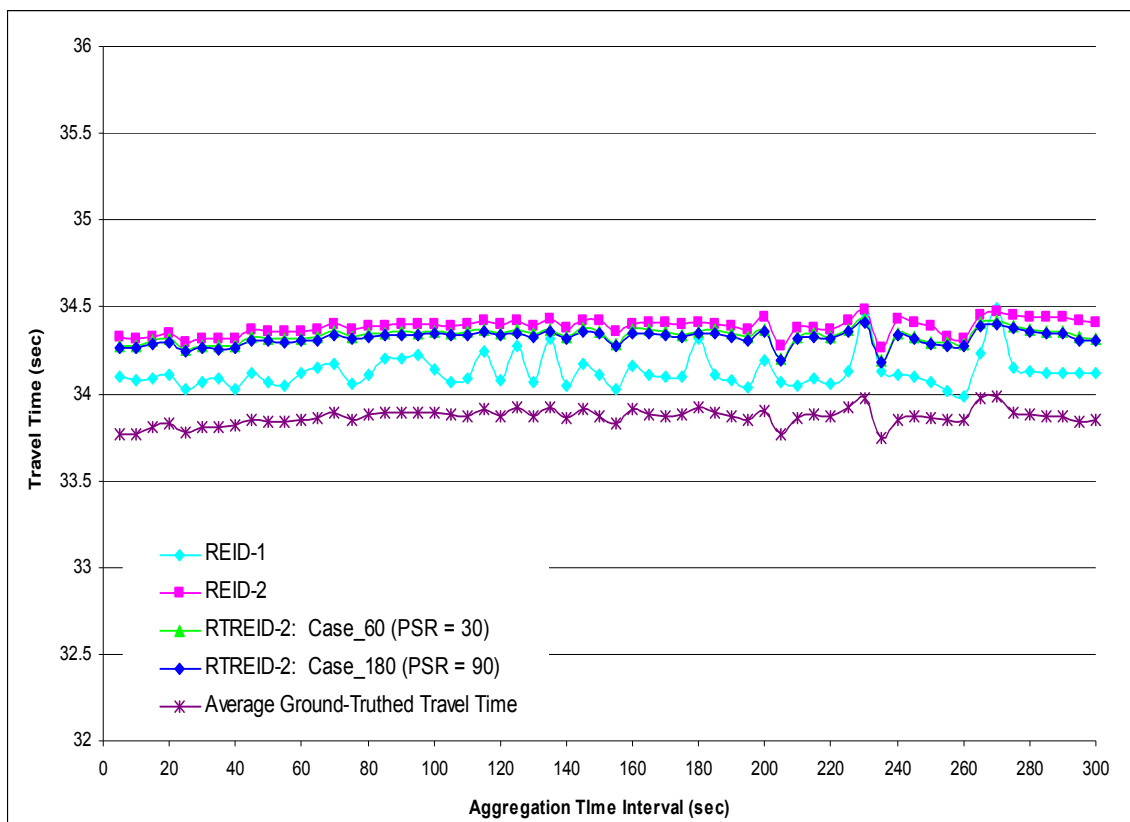
Figure 4-8 Average estimated travel time accuracy analysis.

The average MAPEs for each aggregation time interval are shown in Figure 4-9. There are 60 aggregation periods ranging from 5-seconds to 300-seconds. Overall, the average MAPEs are within the range of 1.23% to 1.79% for RTREID-2. Although, in general, REID-1 can provide slightly more accurate travel time estimates, in view of stability, both REID-2 and RTREID-2 lead to more stable average MAPEs than REID-1 does. This is because it is more likely that no vehicle can be reidentified for certain time intervals for REID-1, and this may cause possibly matched vehicles at upstream detection stations to not be properly included in the candidate vehicle set (see Chapter 3).
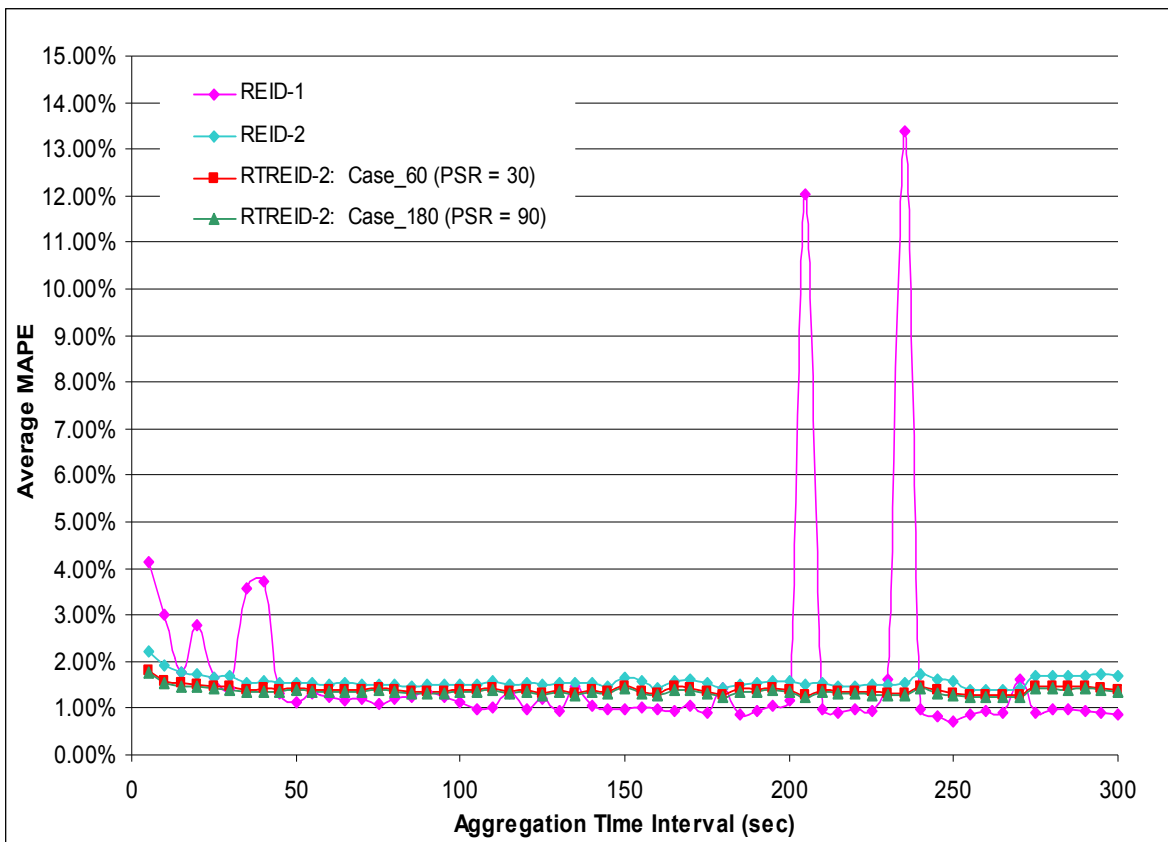
Figure 4-9 Mean absolute percentage error (MAPE) for travel time estimation.

4.4 SUMMARY

In this Chapter, RTREID-2, a modified vehicle reidentification algorithm based on REID-2 using a piecewise slope rate (PSR) data compression method for vehicle signature transformation, was developed. The results of this investigation, including sensitivity analyses, vehicle reidentification performance, and the accuracy of section travel time measurement, are very promising and suggest that the reduction in both computational effort and computer memory needed to store individual signatures with this approach could potentially benefit real-time implementation.

It was found that excellent results could be obtained when a raw vehicle signature was represented by only 30 piecewise slope rates, based on a total of only 60 interpolated data points. This compares with a typical raw signature size of 200-1200 data points. Qualitative experience with RTREID-2, which employs this data compression scheme, indicates that the computational requirements are much lower than those needed for REID-2.

The case study demonstrated that RTREID-2 inherits the potential benefits of REID-2. Moreover, it was observed that RTREID-2 performed better than REID-1 and REID-2, and high values of the indices CMR, TMR, and RR of the RTREID-2 implied a potential to track a vehicle more successfully along its path. On the basis of this study,

the applicability of RTREID-2 to real-time freeway corridor implementation as well as

the different levels of traffic flow condition are investigated in Chapter 5.

CHAPTER 5 FREEWAY PERFORMANCE

MEASUREMENTS BASED ON RTREID-2

As mentioned in Chapter 2, section-related or link-based data can arguably provide more reliable and accurate inputs for traffic surveillance and performance measurement systems. To obtain section-related data, vehicle reidentification plays an important role since section performance measurements can be generated easily via a vehicle reidentification system. Among vehicle reidentification systems, ILD-based systems are cost-effective because the ILDs are largely installed in the field, and are essentially anonymous systems with few if any privacy concerns.

Accordingly, RTREID-2, using inductive loop signature-based methods for vehicle reidentification, is dedicated to meet the needs for real-time implementation and section performance measurement. Therefore, RTREID-2 is applied along a freeway corridor in this chapter for further investigation. This chapter reports the results of a 6.2-mile freeway corridor implementation of RTREID-2 under congested morning peak-period conditions. Although RTREID-2 has been designed for real-time operation, this initial corridor investigation is conducted off-line. The corridor contained mostly round inductive loop detectors with some square loops, providing an opportunity to assess the applicability and transferability of RTREID-2 to homogenous and heterogeneous loop detection systems.

5.1 BACKGROUND STATEMENT

RTREID-2 developed in Chapter 4 utilizes inductive loop signature-based methods for vehicle reidentification and is dedicated to meet the needs for real-time implementation and section performance measurement. A Piecewise Slope Rate (PSR) approach is applied to transform the raw vehicle signatures obtained from square loops. The key advantage of RTREID-2 is straightforward application to square, as well as potentially round, inductive loop detectors in a single loop configuration. In other words, implementing RTREID-2 can eliminate the requirement for either double-loop speed trap configurations or single loop speed estimation models.

However, the development of RTREID-2 was conducted under moderate flow conditions along a single section of freeway. In addition, the detection stations were equipped with square double loops, whereas round single loop detection stations are far more common than square loop detection stations in many locations, including California. A further evaluation of RTREID-2 for a freeway corridor under congested traffic condition using round loops data is therefore desired to assess its ability to meet real world needs.

Therefore, this chapter presents a case study for a 6.2-mile freeway corridor implementation of RTREID-2 under congested morning peak-period conditions. The corridor consists of four round loop detection stations and two square loop detection

created using
BCL easyPDF
Printer Driver
Click here to purchase a license to remove this image

stations. Thus the applicability and transferability of RTREID-2 to homogenous and heterogeneous loop detection systems can be evaluated.

The resulting data will be analyzed at the level of single freeway sections and then the whole corridor. For single-section freeway analysis, the repeatability of RTREID-2 will be first examined using square single loop data. Then the applicability of RTREID-2 will be assessed using round single loop data. The transferability of RTREID-2 to a heterogeneous detection system including one square single loop detection station and one round single loop detection station will also be investigated.

For freeway corridor analysis, RTREID-2 will be firstly implemented for each single-section within the corridor, and the results obtained from each single-section will be aggregated to represent the performance along the corridor.

In this study, 60 interpolated data points will be used in Step 1 and 30 PSR values will be used in Step 2 for RTREID-2 since this assignment has been found to have good performance in Chapter 4. Five indices will be adopted for evaluating the performances of RTREID-2, including total matching rate (TMR), correct matching rate (CMR), mismatching rate (MR), reliability rate (RR), and mean absolute percentage error (MAPE) of estimated travel times.

5.2 STUDY SITE DESCRIPTION AND DATA COLLECTION

5.2.1 Study Site Description

The study site spanned six detection stations along a 6.2-mile corridor in the northbound direction of the I-405 interstate freeway in the City of Irvine, California (see Figure 5-1). The freeway consisted of one high occupancy lane, and between five and seven mainline lanes along this corridor. A buffer lane that separated the high occupancy lane from the other mainline lanes existed from the south end of the study corridor and extended to the Jeffrey interchange, except for a stretch at the vicinity of the Sand Canyon interchange that allowed entry into and exit from the high occupancy lane as shown in Figure 5-1.

Two detection stations, Laguna Canyon 1 and Sand Canyon, were equipped with square double loops embedded in each lane of the freeway. All other detection stations were equipped with round single loops. The loop detectors at each detection station were connected to IST-222 advanced loop detector cards via a card file interface. These detector cards were in turn connected to an industrial PC running the Microsoft Windows 2000 operating system via the USB interface.
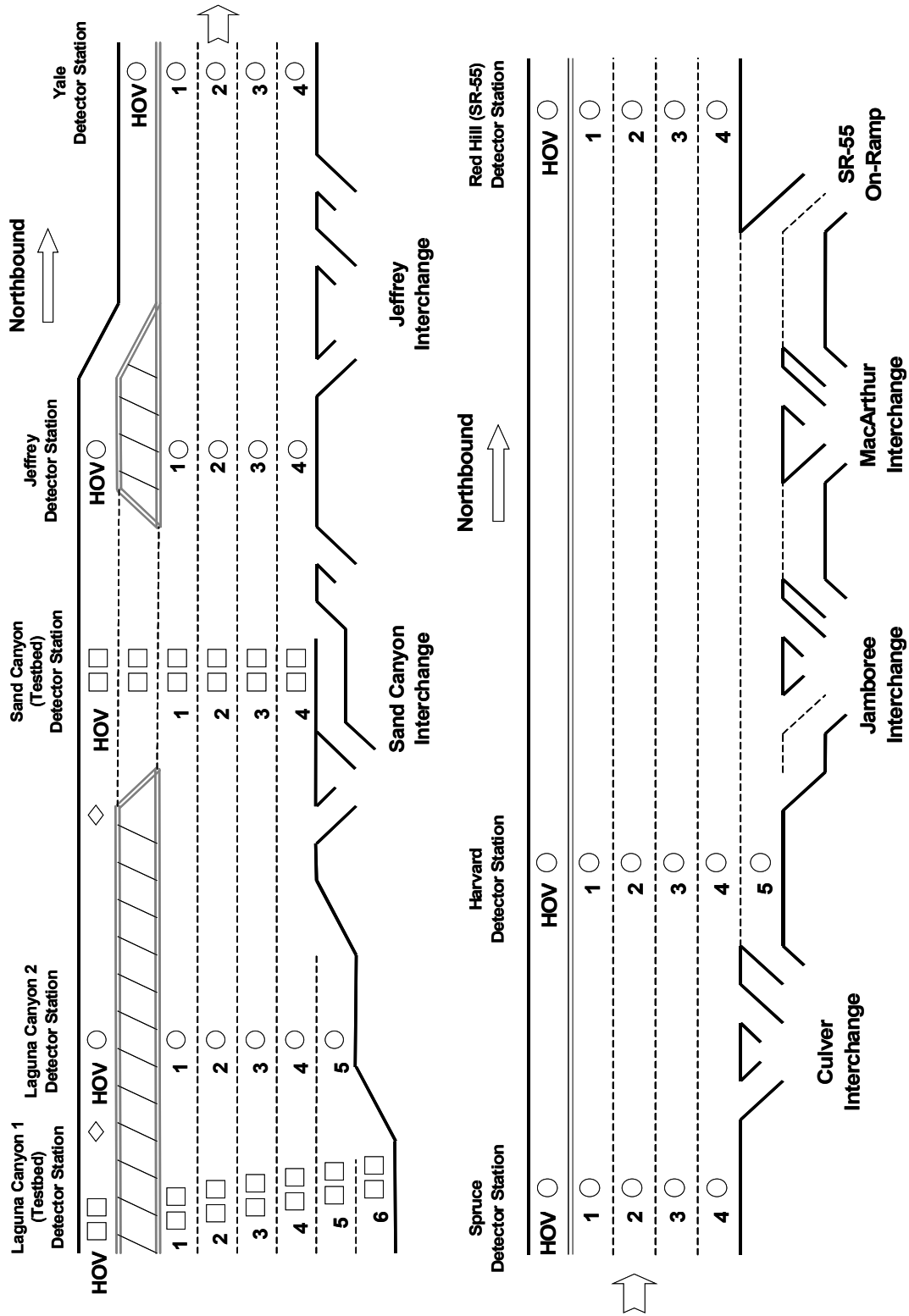
Figure 5-1 Study site: Northbound I-405 in Irvine, California

All detector equipments as well as industrial PCs were housed in existing traffic cabinets located by the side of the shoulder at each detection station. The advanced detector cards process inductance signals induced by vehicles passing over the loops and operate at a rate of 1200 samples per second. A proprietary client program stores these signals in continuous mode in binary format to the PC hard drive for future off-line analysis.

The industrial PCs at each detector station were synchronized with an external clock just prior to each data collection to ensure accurate analysis of travel time information. Where video coverage was provided, the clocks of the camcorders were also synchronized to ensure accurate ground-truthing of video information with inductance signature records. The synchronization was performed manually, with an expected accuracy within fractions of a second. It was found that drifting of the clocks in each device was generally negligible, and did not significantly adversely affect the accuracy of the travel time investigation.

5.2.2 Data Collection and Description

Two data collection exercises were conducted during the morning peak hours in this corridor. Data collection I was performed on March 11th, 2005, for the sub-corridor from Laguna Canyon 1 to Jeffrey, and was used for single-section analysis. Data collection II was performed on November 17th, 2005 throughout the entire corridor and was used for freeway corridor analysis.

For data collection I, camcorders were used to monitor traffic from the on and off ramps along the corridor in addition to detector station locations (as shown in Figure 5-2) to obtain a complete ground-truth dataset. In data collection II, five control vehicles were used for collecting travel time information. The control vehicles were equipped with a GPS unit providing an accuracy of within 3 feet. These GPS offered data logging at one-second intervals, and provided physical position as well as speed information.

The precise positioning obtained from these units allows accurate matching of control vehicle signatures. Since the GPS data was used for determining section and corridor travel times, the drivers of control vehicles were instructed to utilize the floating-car driving technique to obtain travel-time data in the traffic stream.
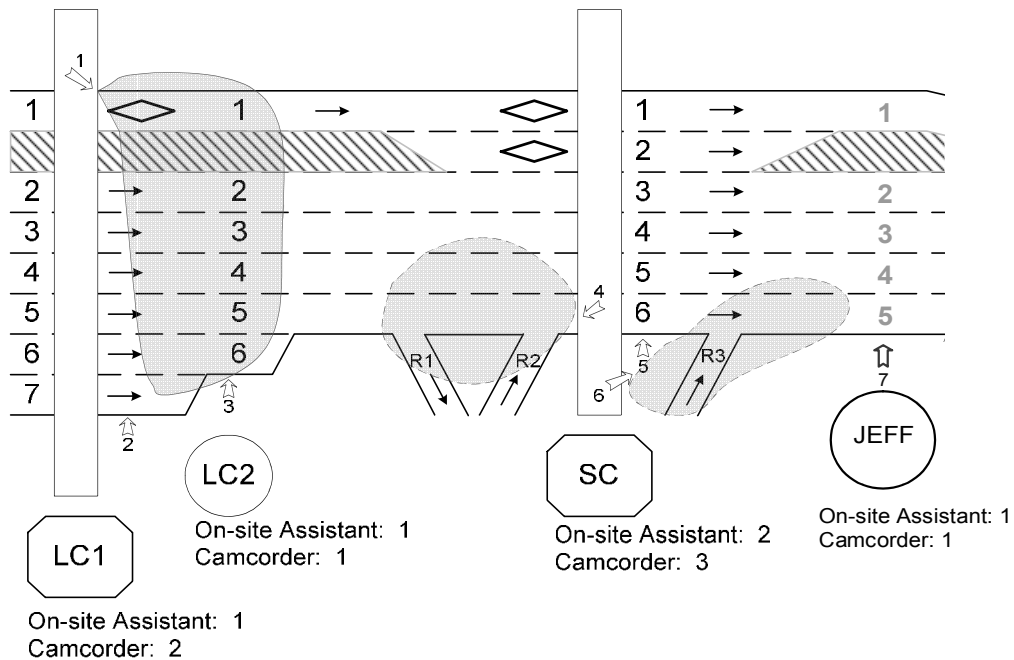
Figure 5-2 Camcorder locations for data collection I

5.2.2.1 Data Description for Single-Section Freeway analysis

To evaluate the repeatability of RTREID-2 and its applicability to round-to-round loops and square-to-round loops, the dataset obtained from data collection I was used which included about 6.5 minutes of vehicle signatures and video-ground-truthed data. The traffic flows at Laguna Canyon 1, Laguna Canyon 2, Sand Canyon, and Jeffrey during this period were 1250 vehicles-per-hour-per-lane (VPHPL), 1894 VPHPL, 1458 and 1578 VPHPL, respectively.

Laguna Canyon 1 and Sand Canyon detection stations were considered for the square-to-square loops case study with 834 ground-truthed vehicle signatures between these detection stations. The Laguna Canyon 2 and Jeffrey detection stations were considered for the round-to-round loops case study, with 957 ground-truthed vehicle signatures between the stations. For the square-to-round loops case study, Sand Canyon and Jeffrey were chosen, with 992 vehicle signatures. The size of the time window was the same for all vehicles for each case described above and was calculated based on the mean travel time.

During signature analysis, it was found that detectors at lane 3 in Laguna Canyon 1 and at lane 6 in Laguna Canyon 2 produced abnormal vehicle signatures that were not due to driver behavior. It was observed that signature records of vehicle types such as passenger cars and minivans that typically produce larger magnitude inductive signatures

created using
BCL easyPDF
Printer Driver
Click here to purchase a license to remove this image

among the vehicle population were found to have a somewhat squashed peak in lane 3 at
Laguna Canyon 1. Samples of such signatures are shown in Figure 5-3.

Normal Signatures   **Abnormal Signatures**
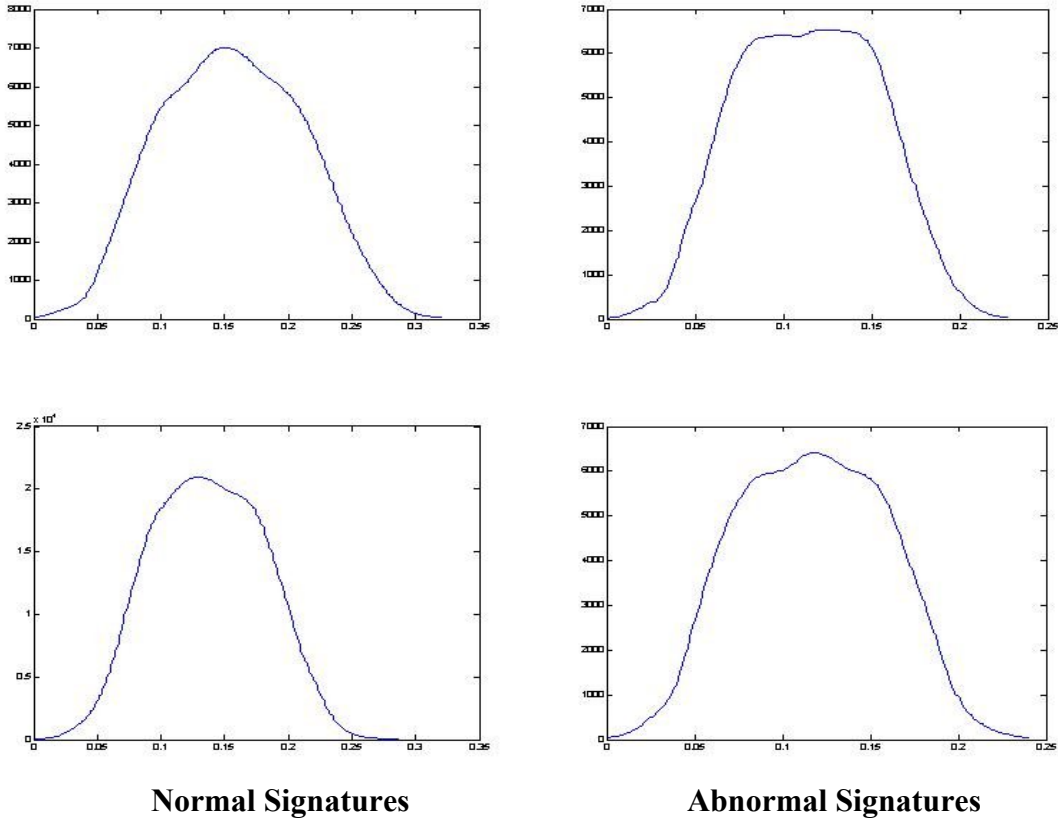
Laguna Canyon 1—Lane 3

Figure 5-3 Comparison between normal and abnormal signatures (LC1).

In addition, some abnormal signatures with inverted peaks were observed in lane
6 at Laguna Canyon 2. These observed abnormalities prevent low profile vehicles from
obtaining a larger recorded inductance magnitude change than they should otherwise
have with good detectors. Samples of such signatures are shown in Figure 5-4. The
reasons for these abnormal signatures could not be precisely determined.

Normal Signatures   **Abnormal Signatures**
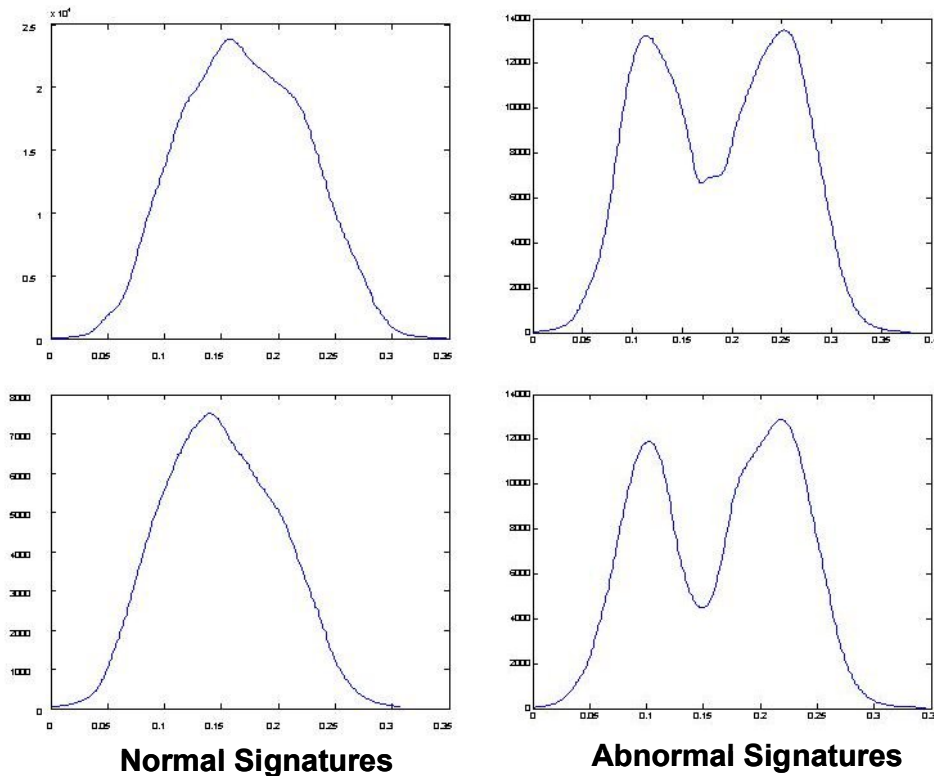
Laguna Canyon 2—Lane 6

Figure 5-4 Comparison between normal and abnormal signatures (LC2).

Moreover, the stop-and-go vehicles under congestion caused abnormal vehicle signatures. This is because a vehicle is less likely to maintain constant speed when it travels over a detector under congestion. Samples of such signatures are shown in Figure 5-5. These abnormalities would adversely affect applications of vehicle signature studies such as vehicle signature-based reidentification (Sun et al., 1999; Jeng and Ritchie, 2006; Jeng and Ritchie, 2005), speed estimation (Sun and Ritchie, 1999), and level-of-service (Oh, Tok, and Ritchie, 2005) models where good quality signatures are essential.
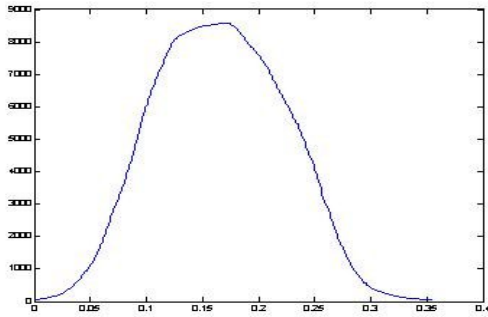
| **Normal Signatures** | **Abnormal Signatures** |
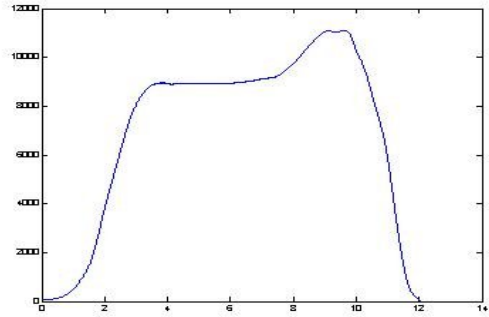
Laguna Canyon 2—Lane 3
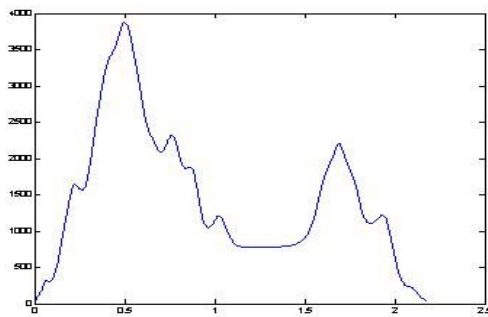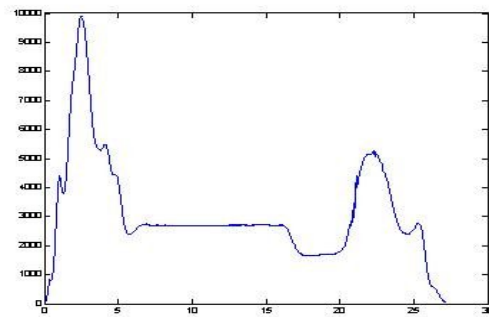
| **Normal Signatures** | **Abnormal Signatures** |

Jeffrey—Lane 4

Figure 5-5 Comparison between normal and abnormal signatures (LC2 and Jeff).

5.2.2.2 Data Description for Freeway Corridor analysis

To perform corridor (i.e., from Laguna Canyon 1 to Red Hill) travel time estimation, the corridor was divided into five sections comprising Laguna Canyon 1 – Sand Canyon, Sand Canyon – Jeffrey, Jeffrey – Yale, Yale – Harvard, and Harvard – Red Hill. The dataset was obtained from data collection II, and included 3.5 hours of vehicle signature data and GPS data between 6:00am and 10:00am. The traffic flow is illustrated in Figure 5-6.
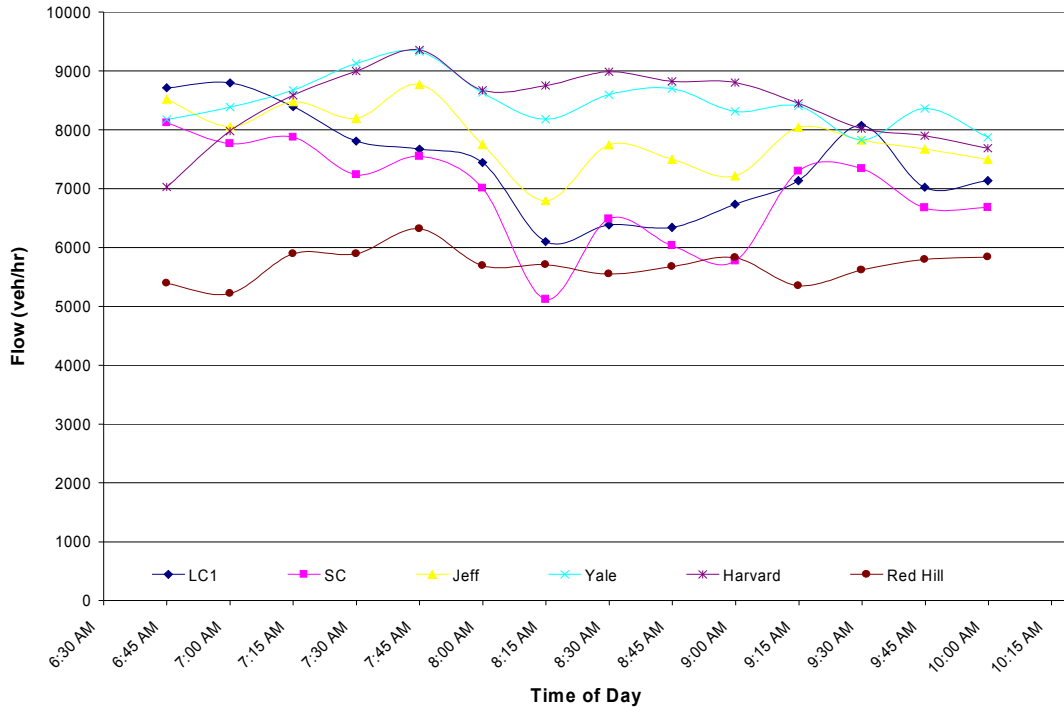
(a) Traffic flow by vehicle per hour
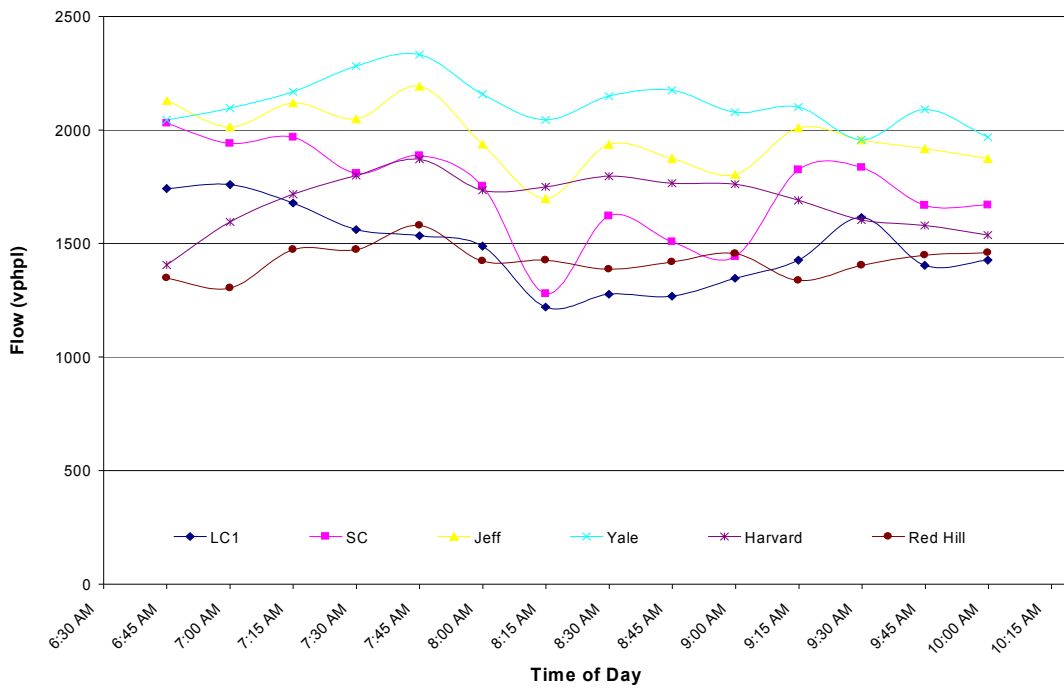
(a) Traffic flow by vehicle per hour per lane

Figure 5-6 Traffic flow observation of freeway corridor analysis.

RTREID-2 was first implemented for each of these sections. The estimated travel times thus obtained from each section were summed to represent the estimated travel time for the corridor. The estimated travel times were calculated every 30 seconds. Then the time window restriction was recalculated according to the latest estimated travel times obtained from the past 30 seconds.

5.3 SINGLE-SECTION FREEWAY ANALYSIS

5.3.1 Reidentification Performance

The reidentification performances for the single-section freeway analysis are tabulated in Table 5-1. For the square-to-square loops case, it was found that the reidentification performance for this dataset decreased when compared with the previous study discussed in Chapter 4. The correct match rate (CMR) was previously 80.77% but it decreased to 54.20% in this study. The previous study also demonstrated a potential of up to 81.87% system reliability, while the reliability rate (RR) in this case study is 56.15%.

However, it must be noted that as mentioned in the Data Collection section, this dataset involved problematic vehicle signatures. The abnormal signatures were observed in lane 3 at Laguna Canyon 1, which contributes 24.10% of the total number of vehicles. Those abnormalities were not easy to detect via the signature quality examination module, and 97.51% of the abnormal signatures are passenger cars. The effects of this were

spread out along the freeway section spatially as well as temporally; thus, the reidentification performances were affected and degraded.

Table 5-1 RTREID-2 Reidentification Performance

(a) Matched Volume

Matched Volume (Vehicles)	Loops Configuration (Upstream/Downstream)		
	Square/Square	Round/Round	Square/Round
Correct Matched Volume	452	485	507
Mismatched Volume	353	444	455
Total Matched Volume	805	929	962
Total Volume	834	957	992

(b) Performance Index

Performance Index	Loops Configuration (Upstream/Downstream)		
	Square/Square	Round/Round	Square/Round
Correct Matching Rate (CMR)	54.20%	50.68%	51.11%
Mismatching Rate (MR)	42.33%	46.39%	45.87%
Total Matching Rate (TMR)	96.52%	97.07%	96.98%
Reliability Rate (RR)	56.15%	52.21%	52.70%

For the round-to-round loops case, the *CMR* is 50.68% and the *RR* is 52.21%. Again, 7.52% of the vehicle signatures were found to be problematic in lane 6 at Laguna Canyon 2. Since 95.83% of the abnormal signatures were passenger cars, the effects were again observed along both space and time dimensions. Although abnormalities of the vehicle signatures may account for the degradation of the reidentification performance, further investigations are suggested to address vehicle signature data quality issues and the improvement of system reliability for the round loops detection system.

For the square-to-round loops case, RTREID-2 was applied directly, disregarding the fact that characteristics of vehicle signatures obtained from square loops may differ from round loops. It is found that a *CMR* of 51.11% and a *RR* of 52.70% could be obtained. Although further studies are required to improve the RR for a square-to-round loop system, these results are deemed sufficient for application to travel estimation and O-D estimation.

In fact, a probe vehicle study by Van Aerde et al. (1993) showed that "a 20% level of market penetration" is reliable for freeway link travel time estimation. In addition, for O-D estimation, 50% market penetration yields less than about 18% root-mean square error. Therefore, RTREID-2 is capable of providing reliable results for travel estimation and O-D estimation.

5.3.2 Travel Time Accuracy Evaluation

Single-section travel time accuracy evaluation results are shown in Figures 5-7 and Figure 5-8. Figure 5-7 illustrates the selected results of the estimated travel times given an aggregation time interval of 30 seconds, which has be shown to yield smaller errors and better stability in Chapter 3 and Chapter 4. It can be observed from Figure 5-7 that the estimated travel times of all the three cases follow the trend of the actual travel times quite well.
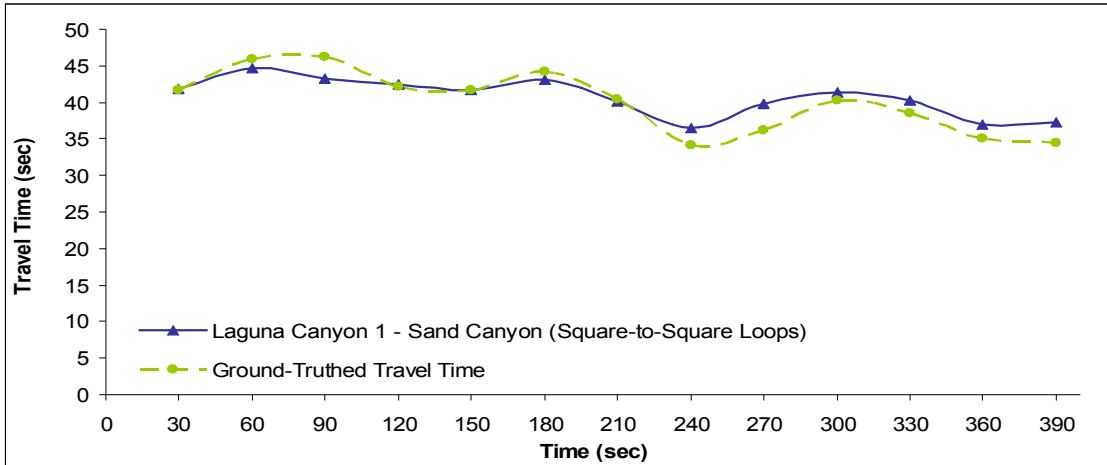
(a) Square-to-square loops case.
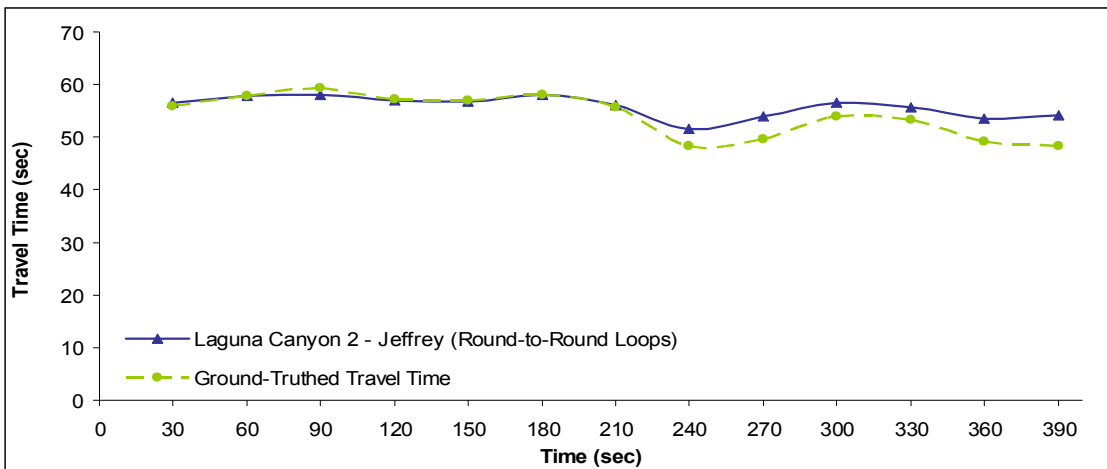
(b) Round-to-round loops case.
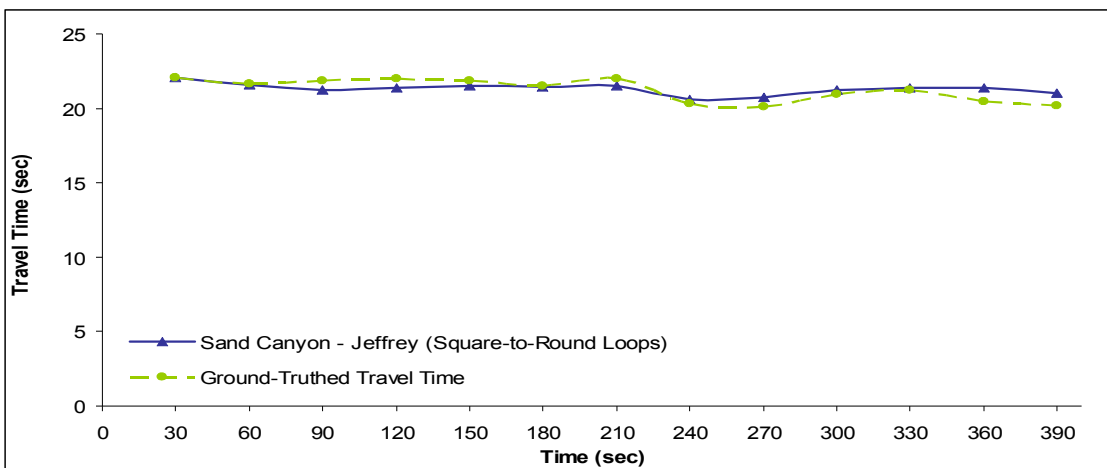
(c) Square-to-round loops case.

Figure 5-7 Results of single-section freeway travel time estimation.

91

The average MAPEs for different aggregation time intervals are presented in Figure 5-8. It is expected that the square-to-round loops case will perform better since no abnormal signature data was observed within this section. For square-to-square loops and round-to-round loops cases, the average MAPEs are within the range of 2.40% to 5.98%. The square-to-round loops case generates better performance, with the average MAPEs within the range of 1.63% to 2.72%.
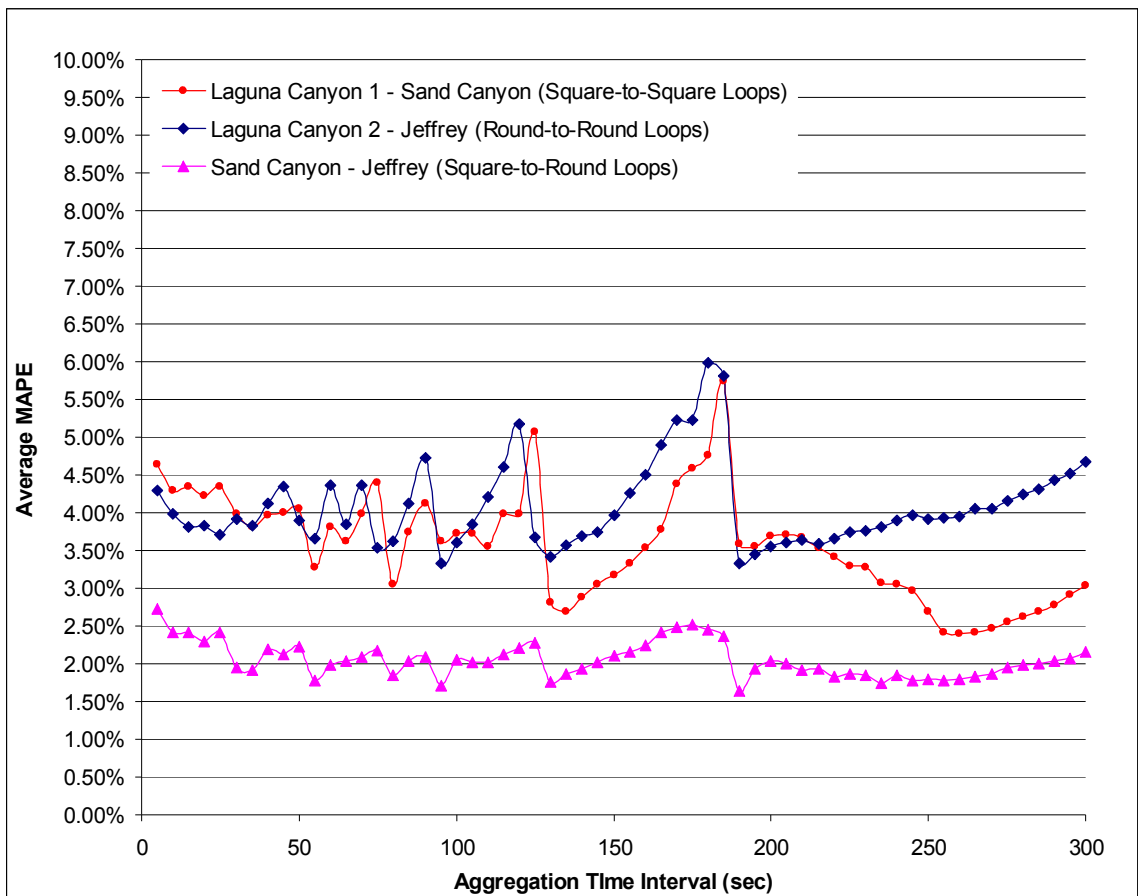
Figure 5-8 Average estimated travel time accuracy analysis for single-section freeway.

These results are encouraging because it can be seen that with system reliability (i.e., *RR*) above 52%, very good travel time estimates can be obtained from RTREID-2. In addition, as mentioned in Section 5.2.2, the datasets for square-to-square loops and round-to-round loops contain some problematic vehicle signatures. These results support the potential of implementing RTREID-2 for generating freeway performance measurements under congested conditions.

5.4 FREEWAY CORRIDOR ANALYSIS

5.4.1 Section Travel Time and Speed Estimations

As mentioned in the Data Collection section for freeway corridor analysis, RTREID-2 was first implemented for each single section along the corridor and the estimated travel times were calculated every 30 seconds. Moreover, since travel time information can be directly obtained from RTREID-2, space-mean-speed measurements can also be calculated. The results of section travel times and speed estimations are shown from Figures 5-9 to 5-13.

It can be seen from Figure 5-9(a) to Figure 5-13(a) that the estimated travel times generally follow the trend of the GPS travel times very well. Although the estimated travel times have some large variations during this congested time period in these five freeway sections, large variations of the GPS travel times are also observed during the same period for those sections.
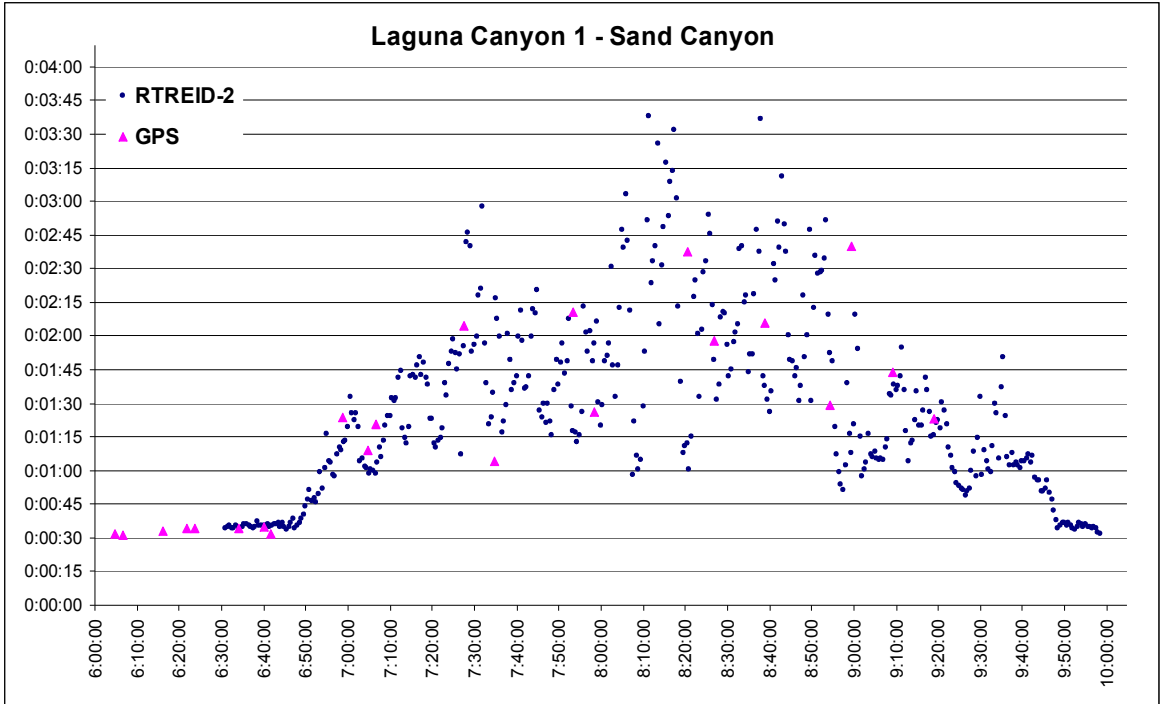
(a) Travel time estimation.
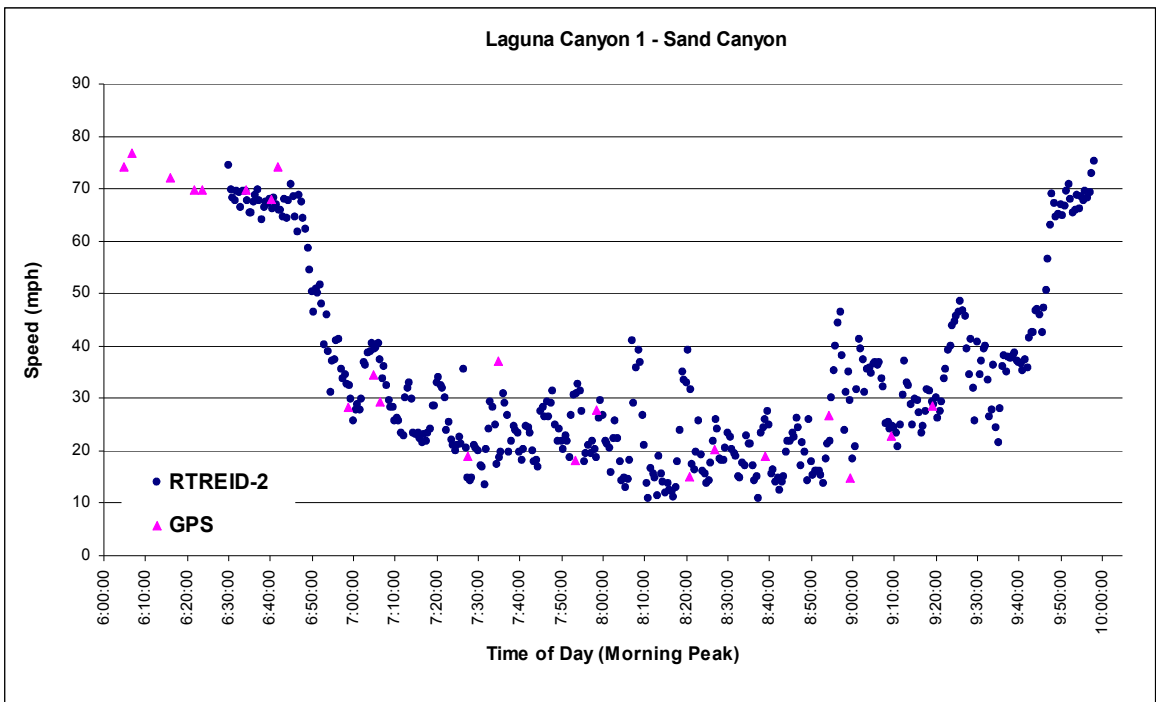
(b) Speed estimation.

Figure 5-9 Freeway corridor analysis: Laguna Canyon 1—Sand Canyon section

travel time and speed estimations.

94
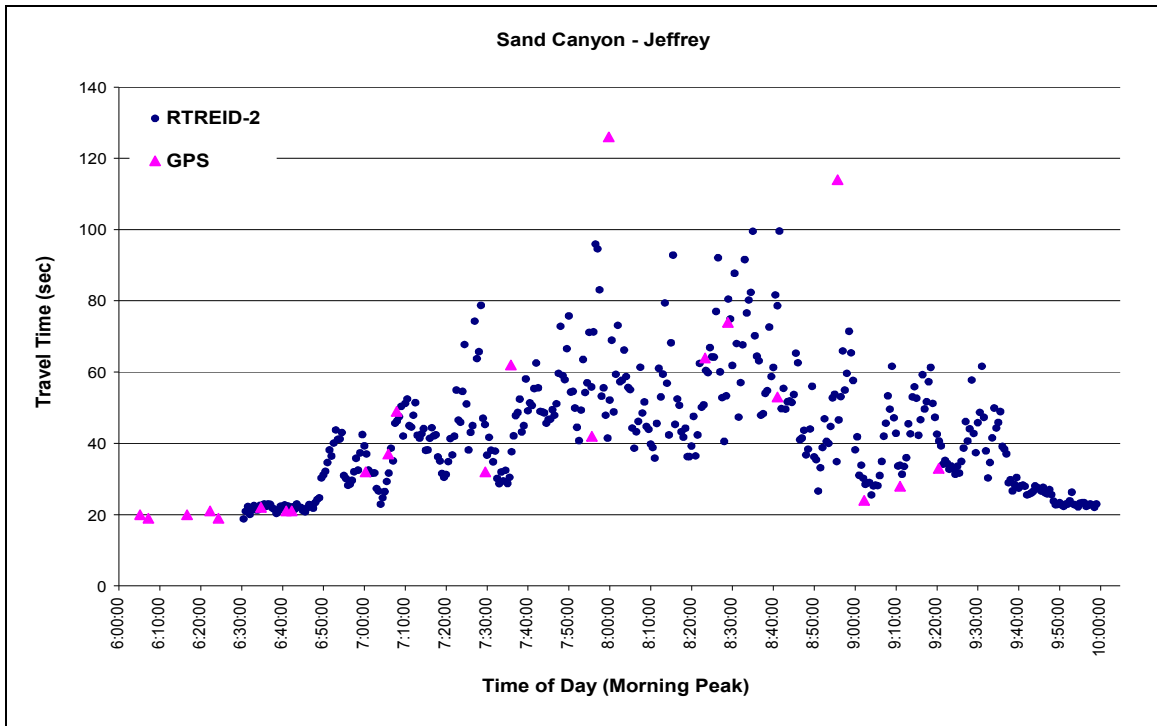
(a) Travel time estimation.
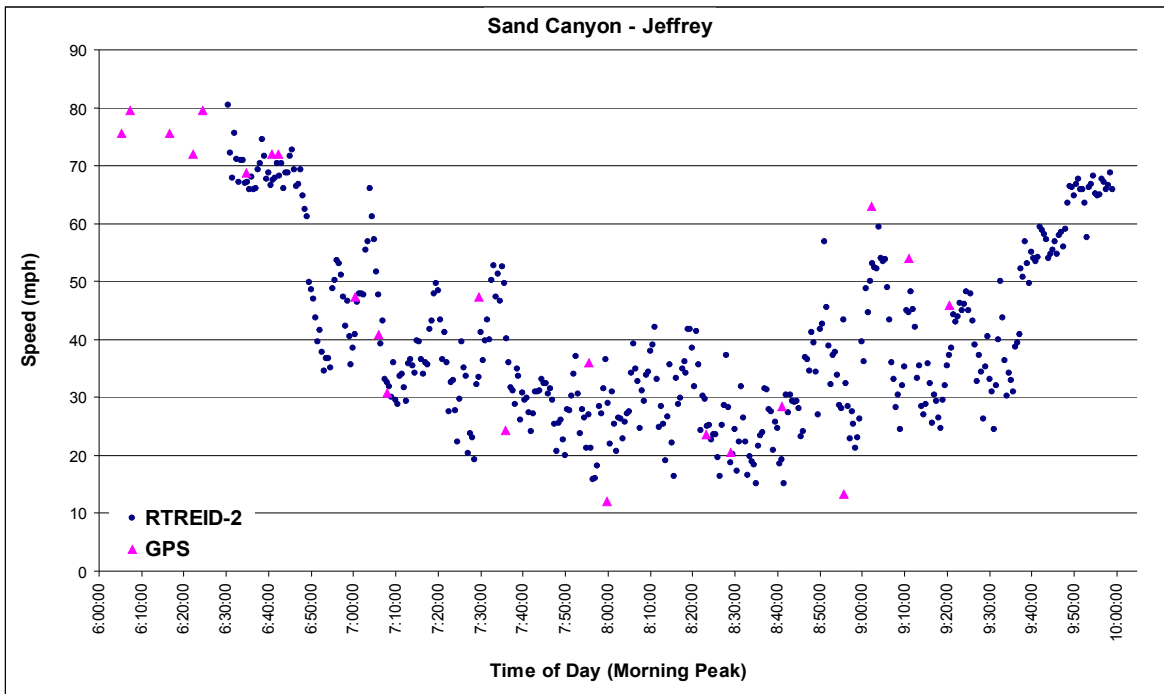
(b) Speed estimation.

Figure 5-10 Freeway corridor analysis: Sand Canyon—Jeffrey section travel time and speed estimations.
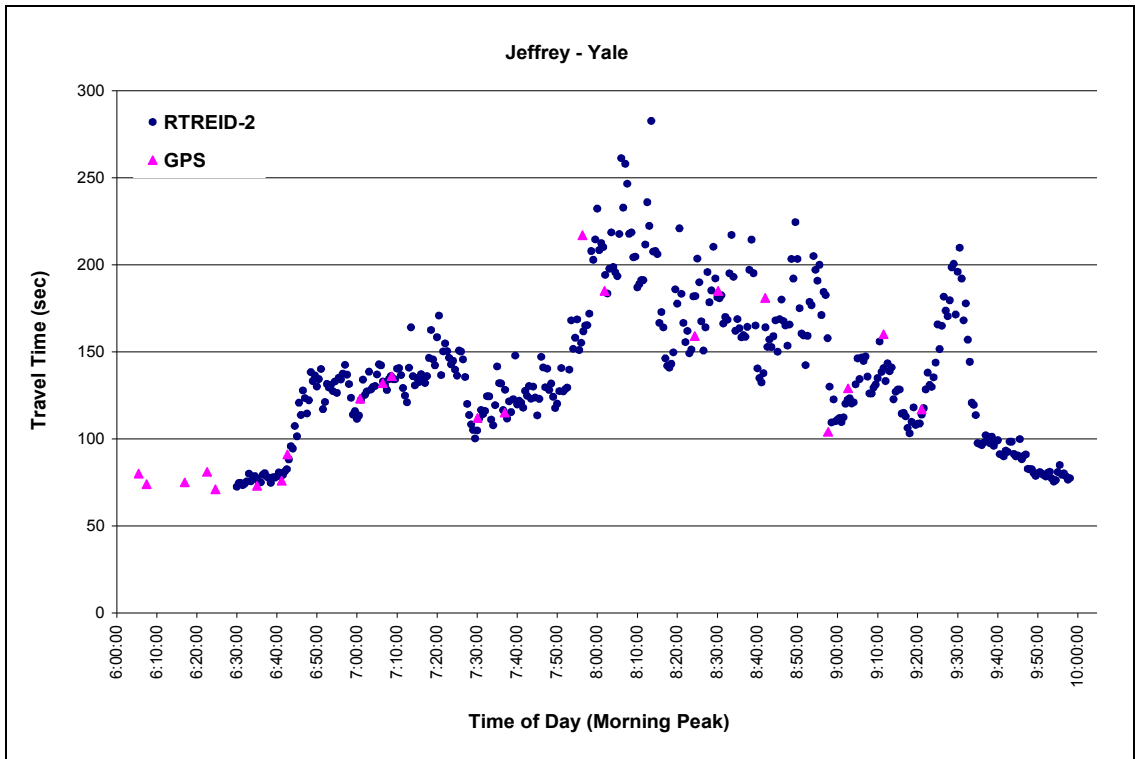
(a) Travel time estimation.
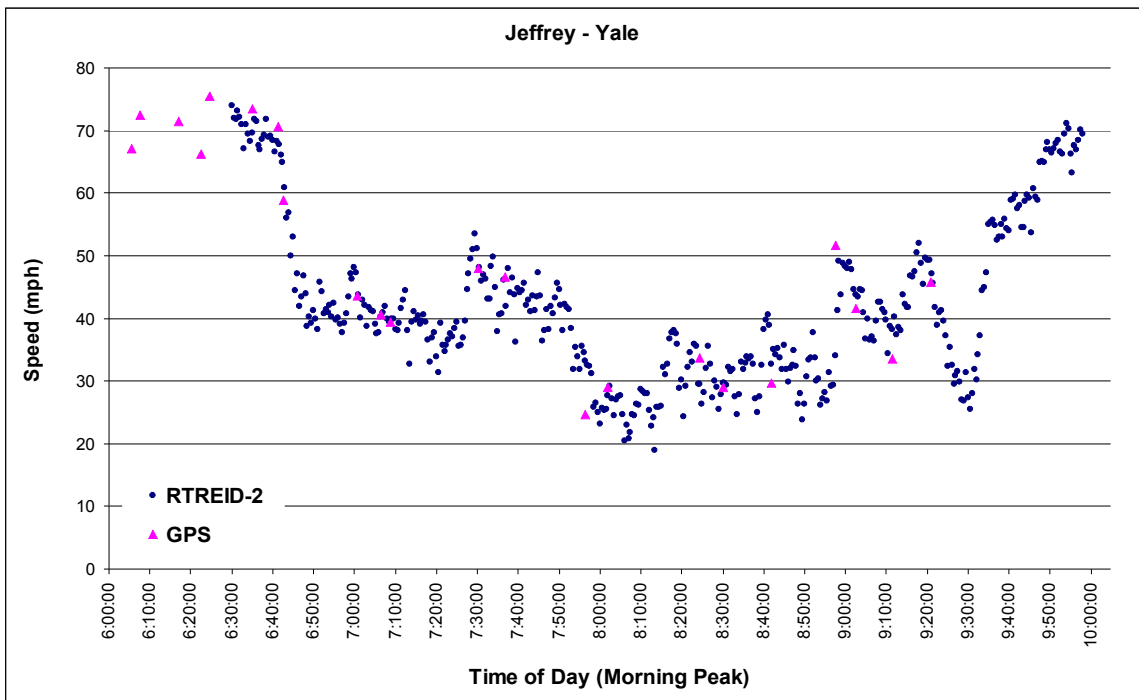
(d) Speed estimation.

Figure 5-11 Freeway corridor analysis: Jeffrey—Yale section travel time and speed estimations.
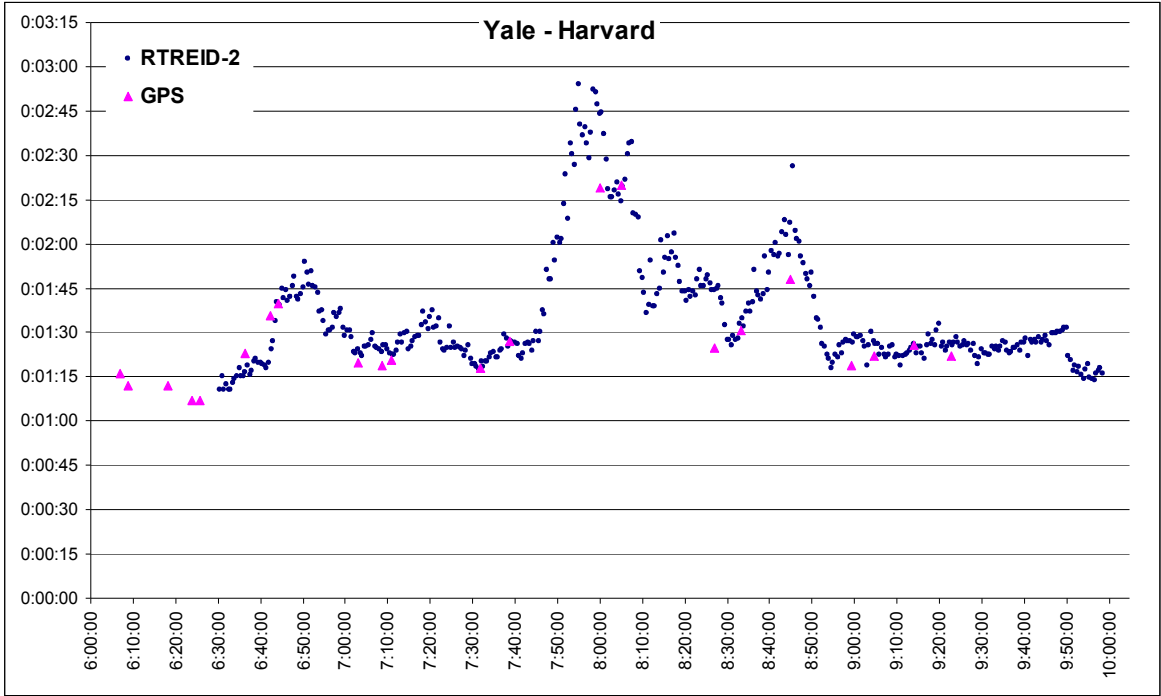
(a) Travel time estimation.
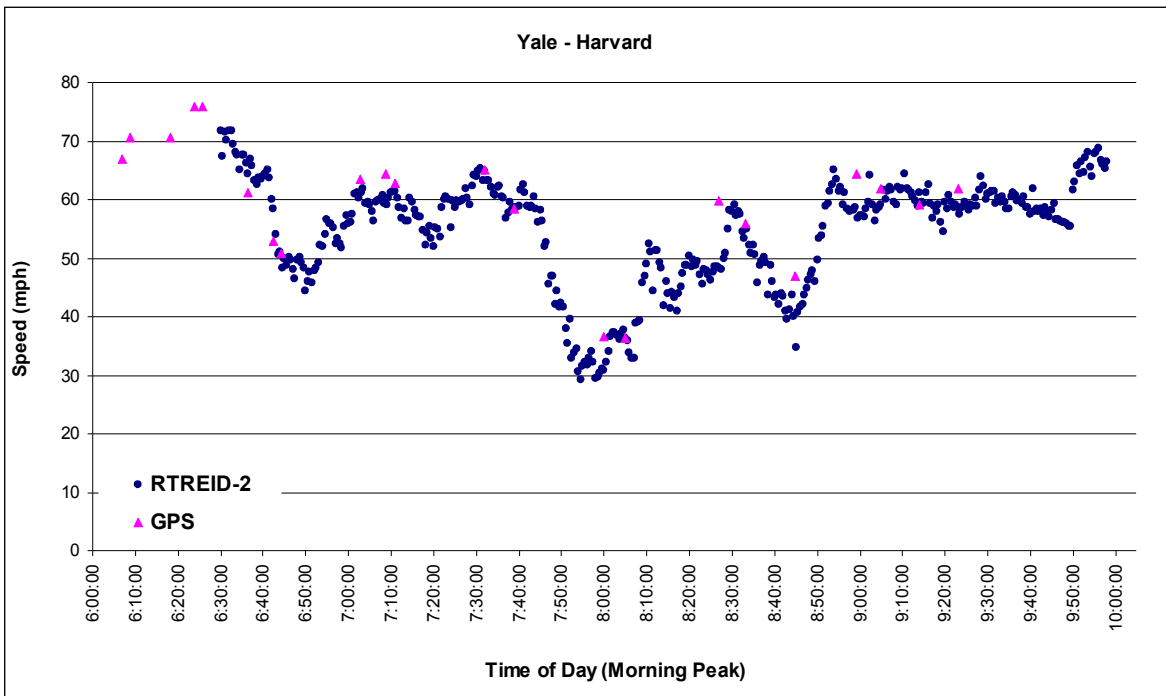
(b) Speed estimation.

Figure 5-12 Freeway corridor analysis: Yale—Harvard section travel time and speed estimations.

97
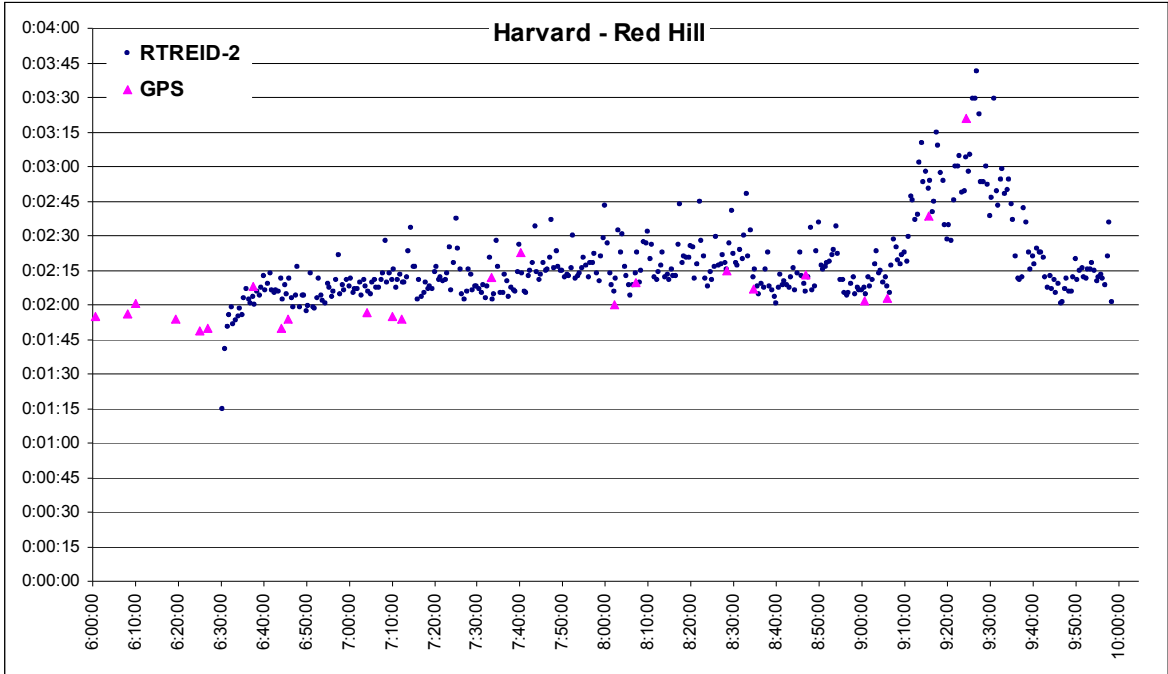
(a) Travel time estimation.
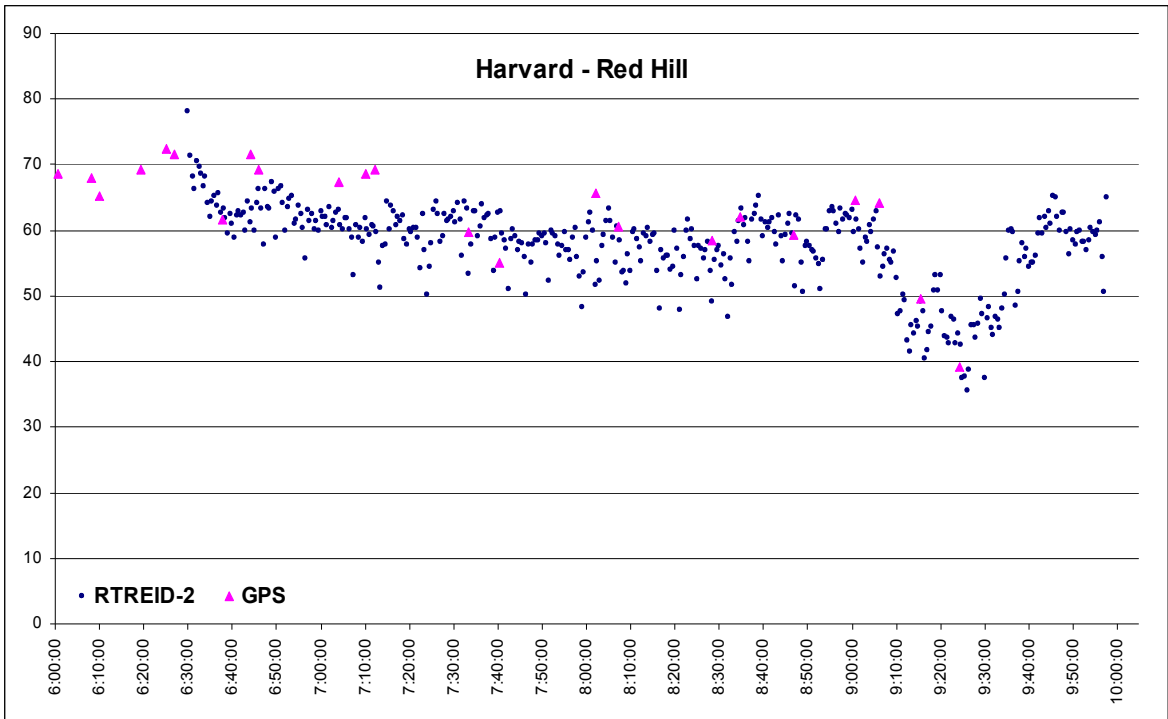
(b) Speed estimation.

Figure 5-13 Freeway corridor analysis: Harvard—Red Hill section travel time and

speed estimations.

Moreover, as shown in Figure 5-9(b) to Figure 5-12(b), congestion was first observed around 6:40am and peaks around 8:00-8:10am when speeds varied between 20 to 30mph. The congestion was alleviated after 9:30am, and the traffic in these four sections was back to normal around 10:00am. The Harvard—Red Hill section behaved differently from the other sections. The congestion at this section was first observed around 9:00am and peaks around 9:30am but the speed did not go below 35mph. The congestion did not stay long and the traffic alleviated after 9:40am.

5.4.2 Corridor Travel Time and Speed Estimations

The corridor travel time and speed estimations were obtained from aggregating the results of the section estimations. The results are presented in Figure 5-14. It can be seen from Figure 5-14 that the RTREID-2 results follow the GPS travel times and speeds of the corridor quite closely.

In addition, it can be seen from the RTREID-2 results in Figure 5-14(b) that the onset of corridor congestion was around 6:40am and reaches morning peak around 8:00am when the speed dropped to 30mph. The congestion situation lingered for one and half hours and the corridor traffic returned to "normal" speeds around 10:00am.

99
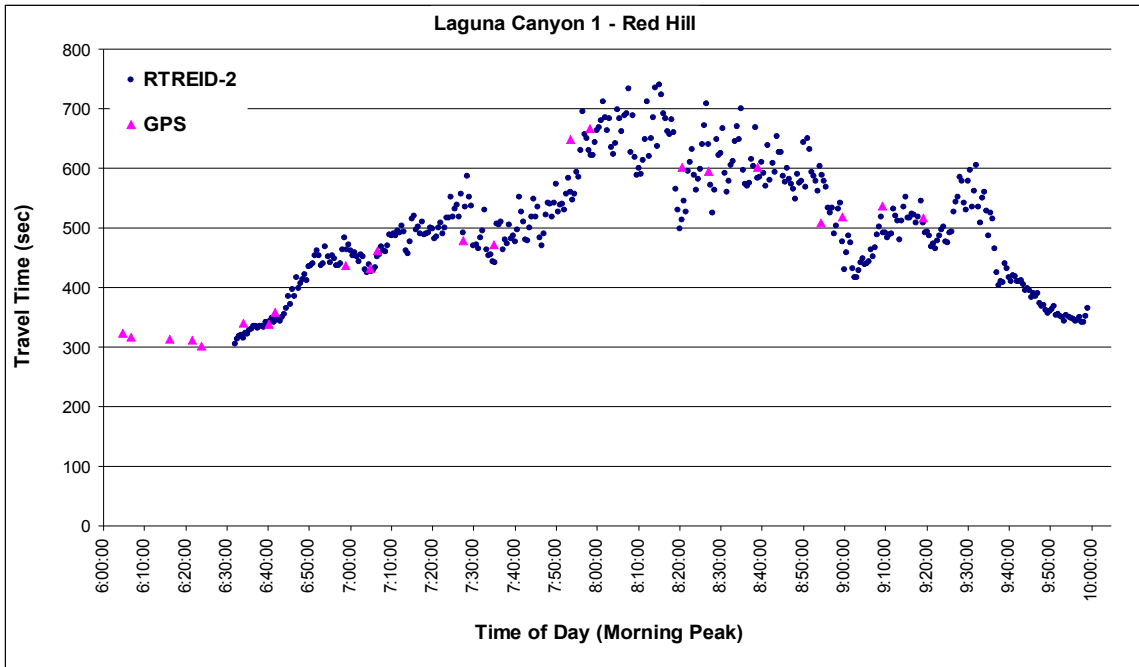
(a) Travel time estimation.
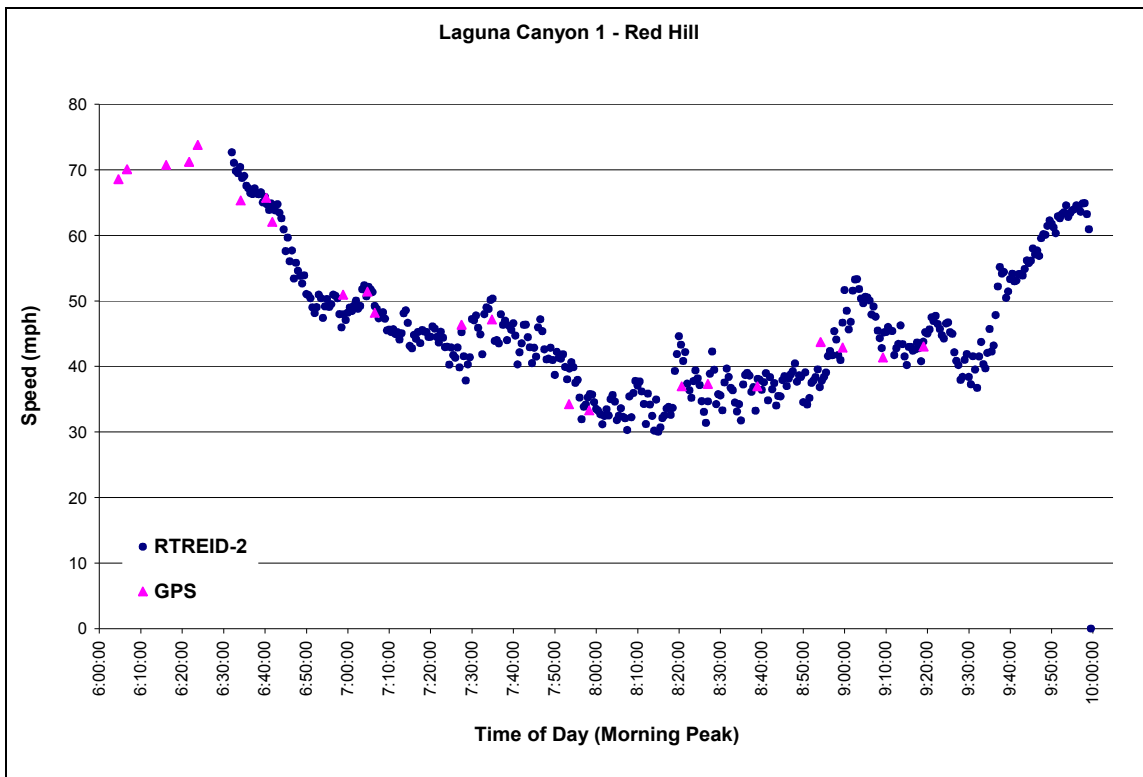
(b) Speed estimation.

Figure 5-14 Freeway corridor analysis: Corridor travel time and speed estimations.

5.5 SUMMARY

This chapter reported the results of a 6.2-mile freeway corridor implementation of RTREID-2 to provide traffic performance measurements under congested morning peak-period conditions. The corridor consisted of both round inductive loop detectors and square loops, providing an opportunity to assess the applicability and transferability of RTREID-2 to homogenous and heterogeneous loop detection systems.

Although problematic signature data were observed from single-section freeway analysis, the results are encouraging because with system reliability above 52%, very good travel time estimates can be obtained from RTREID-2. The results also demonstrated the potential of implementing RTREID-2 for generating freeway performance measurements under congested conditions.

Furthermore, for freeway corridor analysis, excellent results were obtained compared with GPS measurements from control vehicles. The RTREID-2 travel times and speeds followed the GPS travel times and speeds quite closely in all cases. The results suggest that RTREID-2 has the potential to be implemented successfully in a congested freeway corridor, utilizing either or both round or square inductive loop detectors.

CHAPTER 6 APPLICATION OF THE PSR APPROACH TO VEHICLE CLASSIFICATION

Vehicle class is an important characteristic of traffic measurement, and classification information can contribute to many important applications in various transportation fields. Foe instance, vehicle classification is helpful to monitor heavy vehicle traffic for road maintenance and safety, for modeling traffic flow, and for obtaining performance measurements based on each vehicle class for traffic surveillance. In this chapter, a vehicle classification model, which is an application of the PSR approach, is introduced. A heuristic method combined with decision tree and K-means clustering approaches is proposed to develop a vehicle classification model. The features used in the proposed model are extracted from PSR values.

6.1 BACKGROUND STATEMENT

According to various predefined classes, vehicle classification is the process of separating vehicles based on given vehicle features. Vehicle classification information is useful in different transportation applications including vehicle reidentification, road management and maintenance, roadway design, emissions evaluation, multi-mode traffic modeling development, transportation planning, traffic control, traffic signal design (especially for public transit), traffic safety improvement, toll systems assessment, etc.

For example, heavier vehicles such as trucks and oversized vehicles possess different performance characteristics from light vehicles and passenger cars. The former have longer braking distances and at slower speeds on average, occupy more road space, may be lane-restricted, and hence, cause more damage to pavements. Monitoring those heavy vehicles on a roadway will help to design pavements, estimate the life of current road surface and schedule road maintenance. With vehicle classification information, traffic agencies can efficiently allocate resources for roadway design.

Obtaining vehicle classes is also useful for evaluating environmental impacts since the degree of airborne and noise emissions vary between different vehicle classes. Moreover, in terms of traffic flow modeling, more reliable modeling and simulation of the real world can be achieved by observing the heterogeneity of traffic. For traffic control, since vehicle class is one of the important traffic measurements, it may help to convey and predict traffic conditions accurately through traffic control strategies.

Furthermore, the severity of traffic accidents is highly correlated with vehicle types (Garrott et al., 1999), because the speeds are usually significantly different between trucks and passenger cars, and trucks are much larger than passenger cars. Therefore, improvement of freeway safety can also benefit from vehicle classification information.

Various detection technologies (Davies, 1986) have been investigated and applied to perform vehicle classification, such as imaging-based sensors including infrared imaging, video imaging, and laser range imaging systems (Lu et al., 1992; Yuan et al,

1994; Gupte et al., 2002), acoustic signature analysis (Nooralahiyan et al., 1997), magnetic sensor (Cheung et al., 2006), and inductive signature systems (Pursula and Pikkarainen, 1994; Sun et al., 2003; Ritchie et al., 2005).

To apply inductive vehicle signature data to vehicle classification, Pursula et al. (1994) firstly proposed a classification scheme that consisted of seven vehicle classes. Their approach adopted a Self-Organizing Feature Map (SOFM) and the classification rate of the training data set was around 80%. More recently, Sun et al. (2003) suggested two methods for vehicle classification utilizing the inductive vehicle signature data. One method employed heuristic discriminant algorithms and multi-objective optimization for training the heuristic algorithms, and the classification rates were around 81%-91%. SOFM was applied to the second method and results with 80% classification rates were obtained.

These two studies demonstrate the potential of developing vehicle classification models using inductive vehicle signature data. However, both Pursula and Sun's studies utilized double inductive loop signatures for model development. Although Sun et al. suggested adopting a single loop estimation model for single loop data, their model has to be re-calibrated. Therefore, a new vehicle classification model, which is part of RTREID-2, is introduced.

The proposed model is not only capable of categorizing vehicle types based on the Federal Highway Administration (FHWA) scheme (USDOT, 2007) but is also capable of

grouping vehicles into more detailed classes. Since the proposed model is intended for real-time implementation, this dissertation suggests a simple but efficient method that is based on a heuristic decision tree approach combined with the K-means clustering method.

This heuristic multi-level decision tree method classifies vehicles by applying K-means clustering approach to decide on the number of branches at each step using the most distinguishable PSR feature, which is extracted from single square loop detector data. Moreover, a dataset obtained from single round loop detector is applied to test transferability of the developed algorithm. The advantages of the proposed method are its transferability without model re-calibration, and employing the current infrastructure. In addition, this approach will also help to enhance the use of single loop detectors for vehicle classification.

6.2 VEHICLE CLASSIFICATION SCHEME

There are three vehicle classification schemes applied to develop the proposed vehicle classification model. Table 6-1 displays the FHWA classification scheme, which consists of thirteen vehicle classes and the figures of each vehicle class are illustrated in Figure 6-1. In Table 6-2, FHWA-I classification scheme is designed based on FHWA classification scheme but extends to fifteen vehicle classes according to data availability. In Table 6-3, the Real-time Traffic Performance Measurement System (RTPMS) classification scheme collapses the FHWA classes into five vehicle classes.

Table 6-1 FHWA Classification Scheme

FHWA Class	Description
1	Motorcycles
2	Passenger Cars
3	Two Axle, Four Tire Single Units
4	Buses
5	Two Axle, 6 Tire Single Units
6	Three Axle Single Units
7	Four or More Axle Single Units
8	Four or Less Axle Single Trailers
9	Five Axle Single Trailers
10	Six or More Axle Single Trailers
11	Five or Less Axle Multi-Trailers
12	Six Axle Multi-Trailers
13	Seven or More Axle Multi-Trailers

The FHWA-1 classification scheme attempts to distinguish vehicle with trailer from other vehicles and four classes are designed to display those cases. Buses are classified into three classes including regular buses, 20' buses, and 30' buses. In addition, bobtail tractor, and goose-neck trailer and moving van are classified as new vehicle classes due to their apparent characteristics.

The design of the RTPMS classification scheme aims to classify vehicles into few groups so that the vehicle classification information can be displayed and understood easily. Therefore, vehicles are grouped into five vehicle classes including passenger cars, small single unit trucks, buses, medium/large single unit trucks, and trailer trucks (see Table 6-3).

1 MOTORCYCLES

2 PASSENGER CARS

3 FOUR TIRE, SINGLE UNIT

4 BUSES

5 TWO AXLE, SIX TIRE SINGLE UNIT

6 THREE AXLE, SINGLE UNIT

7 FOUR OR MORE AXLE, SINGLE UNIT

8 FOUR OR LESS AXLE, SINGLE TRAILER

9 FIVE-AXLE, SINGLE TRAILER

10 SIX OR MORE AXLE, SINGLE TRAILER

11 FIVE OR LESS AXLE, MULT-TRAILER

12 SIX AXLE, MULT-TRAILER

13 SEVEN OR MORE AXLE, MULTI-TRAILER
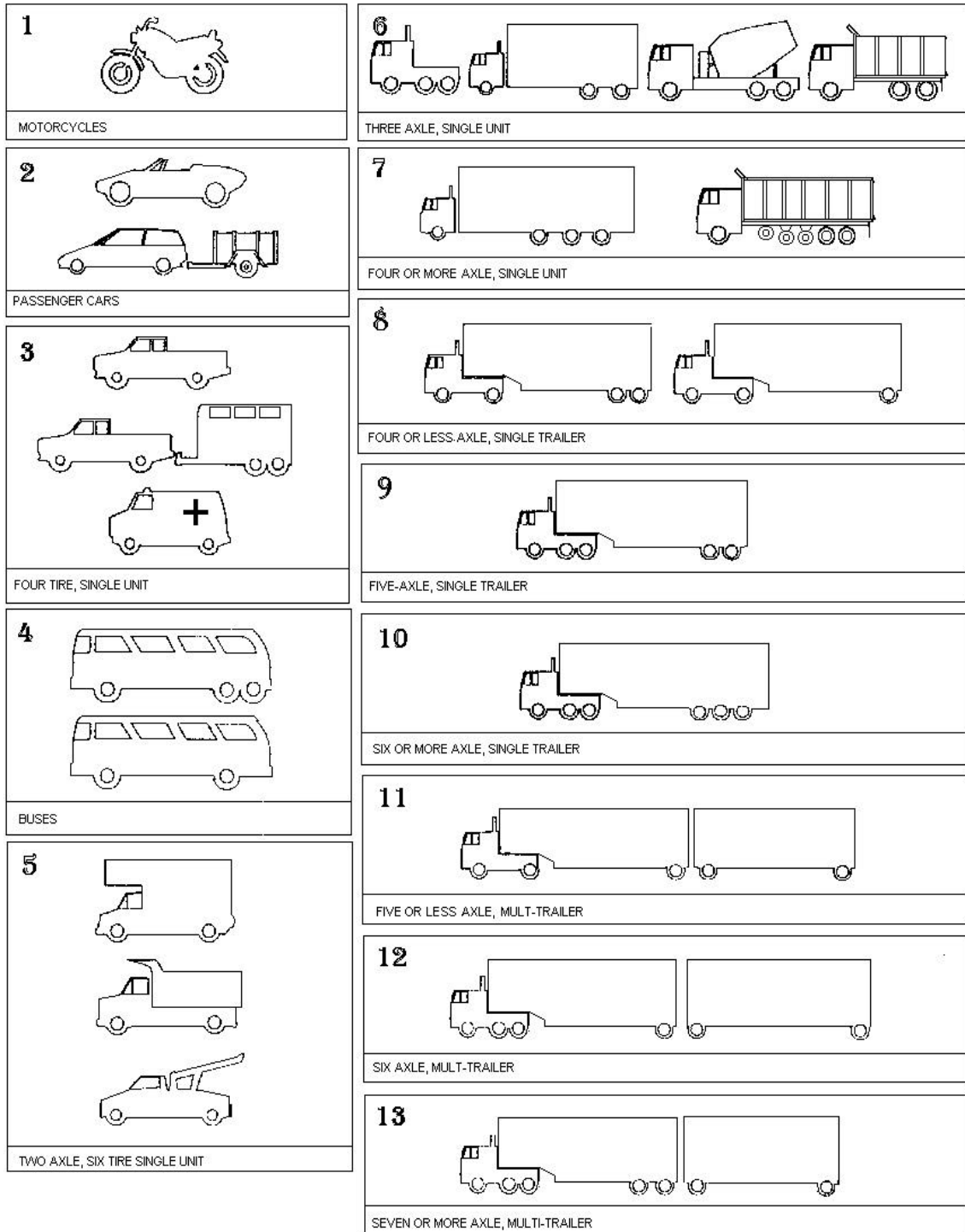
Source: USDOT, 2007

Figure 6-1 FHWA classification scheme.

Table 6-2 FHWA-I Classification Scheme

FHWA-I Class	Description
1	Passenger Cars
2	Two Axle, Four Tire Single Units
3	Buses
4	Two Axle, 6 Tire Single Units
5	Three Axle Single Units
6	Four or Less Axle Single Trailers
7	Five Axle Single Trailers
8	Class 1 + Trailer
9	Class 2 + Trailer
10	Class 4 + Trailer
11	Class 5 + Trailer
12	Bobtail Tractor (Semi Without Any Trailers)
13	Goose-neck Trailer or Moving Van
14	30' Buses
15	20' Buses

Table 6-3 RTPMS Classification Scheme

RTPMS Class	Description
1	Passenger Cars
2	Small Single Unit Trucks
3	Buses
4	Medium/Large Single Unit Trucks
5	Trailer Trucks

The proposed vehicle classification model will be developed based on the FHWA-I classification scheme (as shown in Table 6-2). Once vehicle classes are generated for the FHWA-I classification scheme, the classification results can be re-assigned to the FHWA classification scheme and RTPMS classification scheme according to Table 6-4 and Table 6-5.

Table 6-4 FHWA-1 Classification Scheme vs. FHWA Classification Scheme

FHWA-I Class	Description	FHWA Class	Description
1	Passenger Cars	2	Passenger Cars
2	Two Axle, Four Tire Single Units	3	Two Axle, Four Tire Single Units
3	Buses	4	Buses
4	Two Axle, 6 Tire Single Units	5	Two Axle, 6 Tire Single Units
5	Three Axle Single Units	6	Three Axle Single Units
6	Four or Less Axle Single Trailers	8	Four or Less Axle Single Trailers
7	Five Axle Single Trailers	9	Five Axle Single Trailers
8	Class 1 + Trailer	2	Passenger Cars
9	Class 2 + Trailer	3	Two Axle, Four Tire Single Units
10	Class 4 + Trailer	5	Two Axle, 6 Tire Single Units
11	Class 5 + Trailer	6	Three Axle Single Units
12	Bobtail Tractor (Semi Without Any Trailers)	6	Three Axle Single Units
13	Goose Neck Trailer or Moving Van	9	Five Axle Single Trailers
14	30' Buses	4	Buses
15	20' Buses	4	Buses

Table 6-5 FHWA-1 Classification Scheme vs. RTPMS Classification Scheme

FHWA-I Class	Description	RTPMS Class	Description
1	Passenger Cars	1	Passenger Cars
2	Two Axle, Four Tire Single Units	2	Small Single Unit Trucks
3	Buses	3	Buses
4	Two Axle, 6 Tire Single Units	2	Small Single Unit Trucks
5	Three Axle Single Units	4	Medium/Large Single Unit Trucks
6	Four or Less Axle Single Trailers	5	Single Trailer Trucks
7	Five Axle Single Trailers	5	Single Trailer Trucks
8	Class 1 + Trailer	1	Passenger Cars
9	Class 2 + Trailer	2	Small Single Unit Trucks
10	Class 4 + Trailer	2	Small Single Unit Trucks
11	Class 5 + Trailer	4	Medium/Large Single Unit Trucks
12	Bobtail Tractor (Semi Without Any Trailers)	2	Small Single Unit Trucks
13	Goose Neck Trailer or Moving Van	5	Single Trailer Trucks
14	30' Buses	3	Buses
15	20' Buses	3	Buses

6.3 VEHICLE CLASSIFICATION ALGORITHM DEVELOPMENT

A heuristic decision tree method combined with K-means clustering method is employed for the development of the proposed vehicle classification model in this dissertation. To split the tree at each level, K-means clustering method is adopted to decide the number of

branches utilizing most distinguishable PSR feature. This approach helps to reduce the dimension of possible vehicle classes at each level.

K-means clustering method creates clusters with a self-organized approach. The advantages of K-means clustering method are "its simplicity, efficiency, and self-organization, as well as its minimization of the mean square error" (Looney, 1997). Although one limitation of this method is that the number K of clusters must be provided, the K is known in this study. Since the K can not exceeds the number of vehicle classes at each decision node (denoted as Q), several runs with different K values (where the $K \leq Q$) are made and the K that yields minimum total misclassified cases is selected.

For PSR feature extraction, the PSR values are plotted for each vehicle class and are shown from Figure 6-2 to Figure 6-6. As shown in those PSR plots, the first eight PSR values are greater than zero for class 1 and class 2, while some of the first eight PSR values for other classes are most likely below zero. Therefore, a feature named PSR_8_IDX is derived to distinguish small vehicle classes (PSR_8_IDX = 1) and large truck classes (PSR_8_IDX = 2) as depicted in Equation 6.1 and Equation 6.2. Furthermore, considering the needs for real-time implementation, simple statistics are extracted from PSR values including mean, standard deviation, and median.
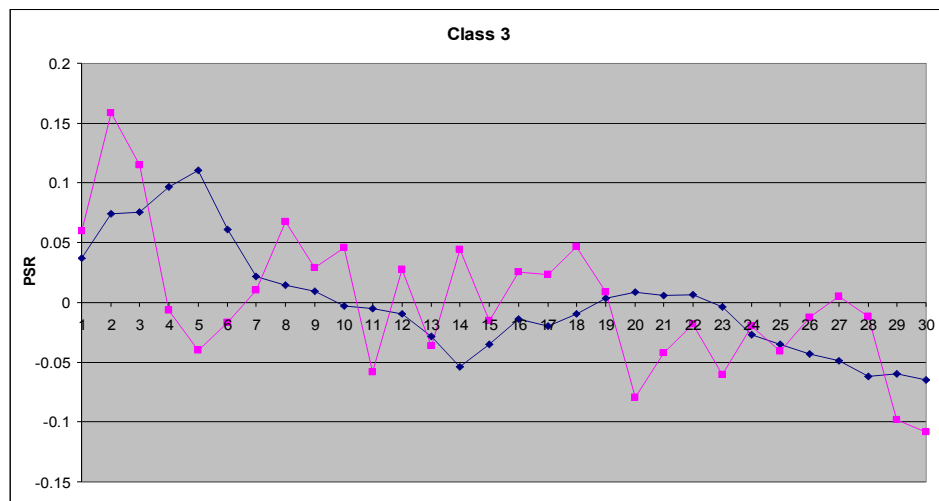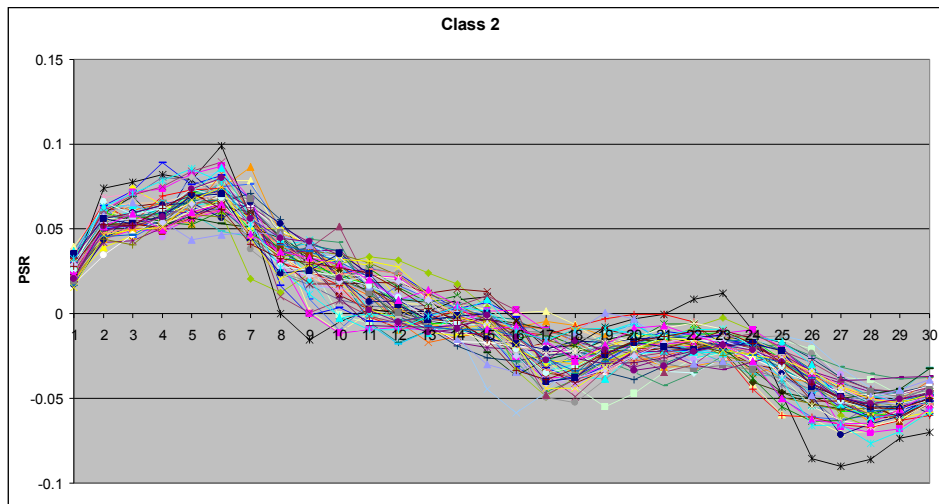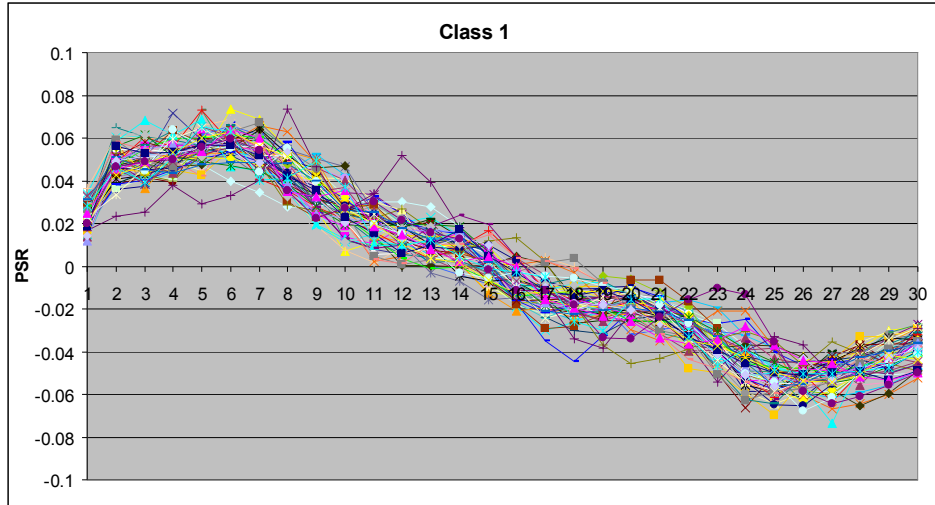
Figure 6-2 PSR plots: Class 1, Class 2, and Class 3.
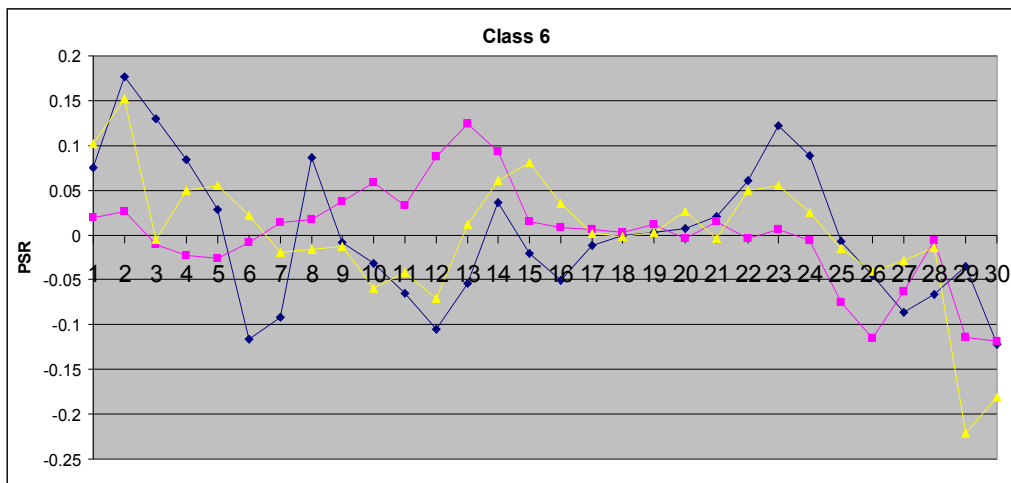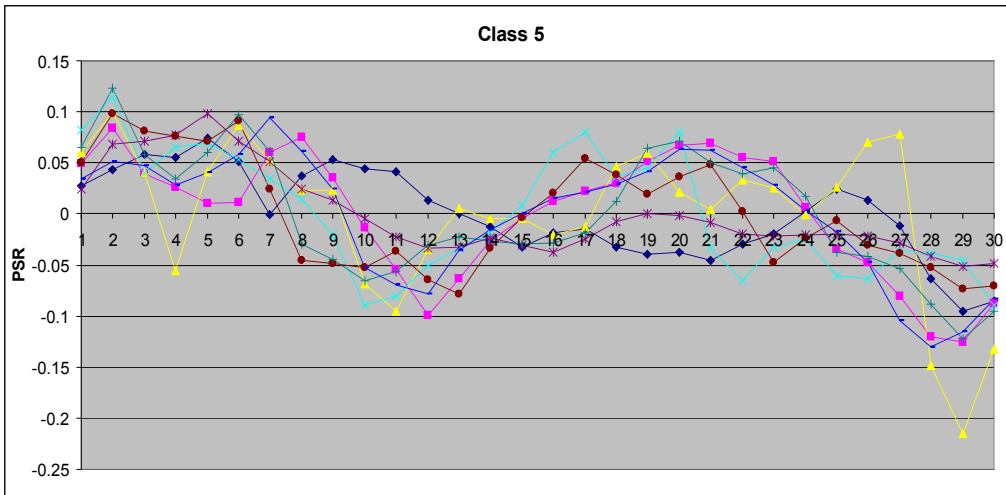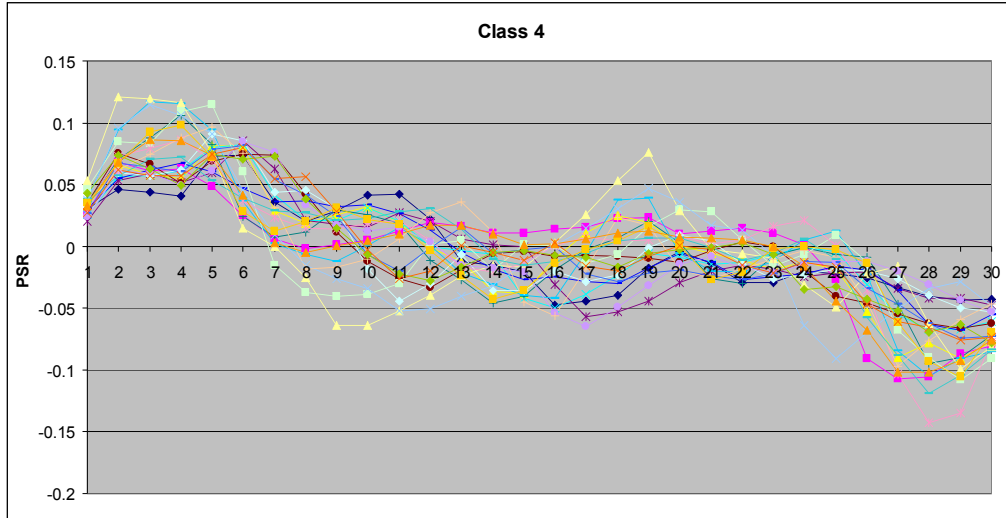
Figure 6-3 PSR plots: Class 4, Class 5, and Class 6.
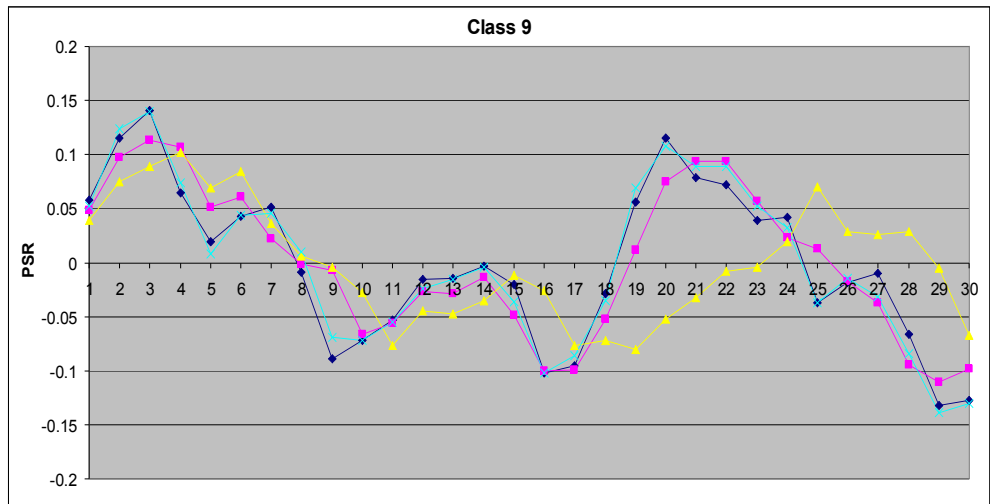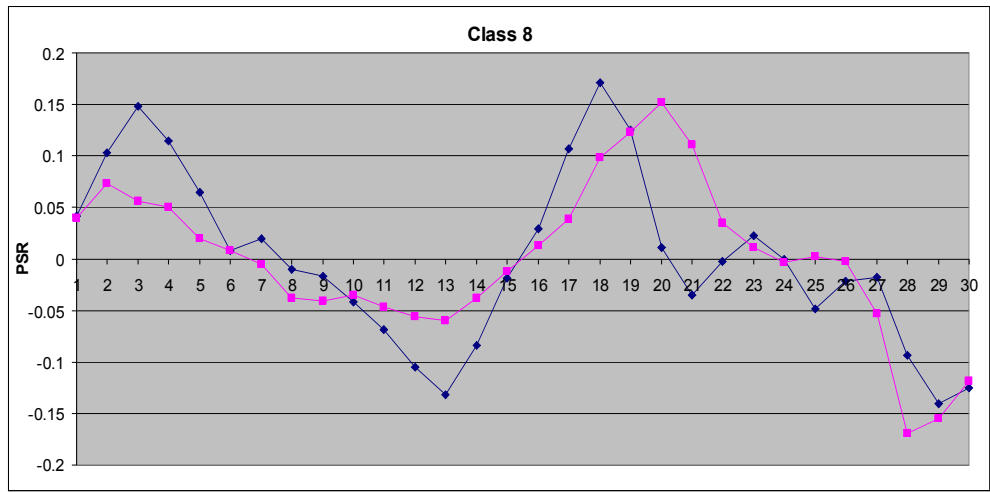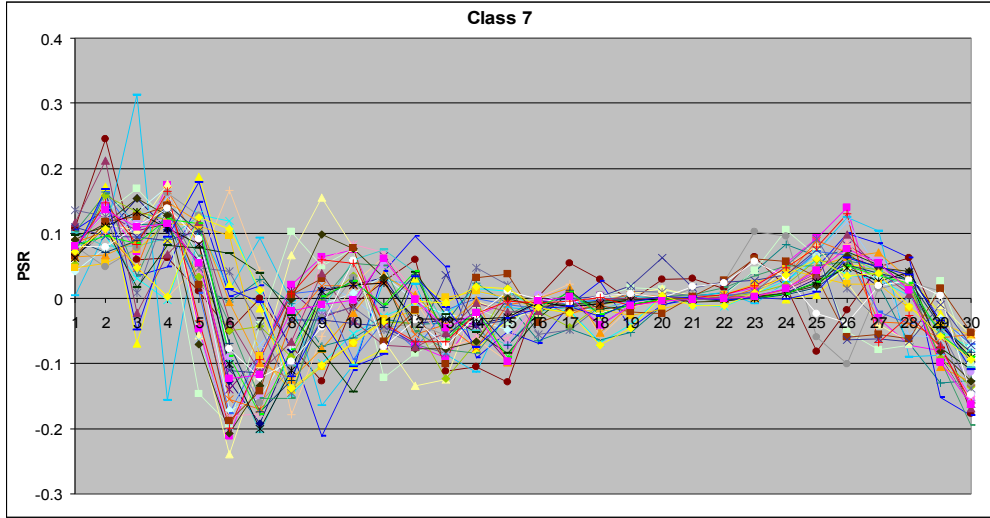
Figure 6-4 PSR plots: Class 7, Class 8, and Class 9.
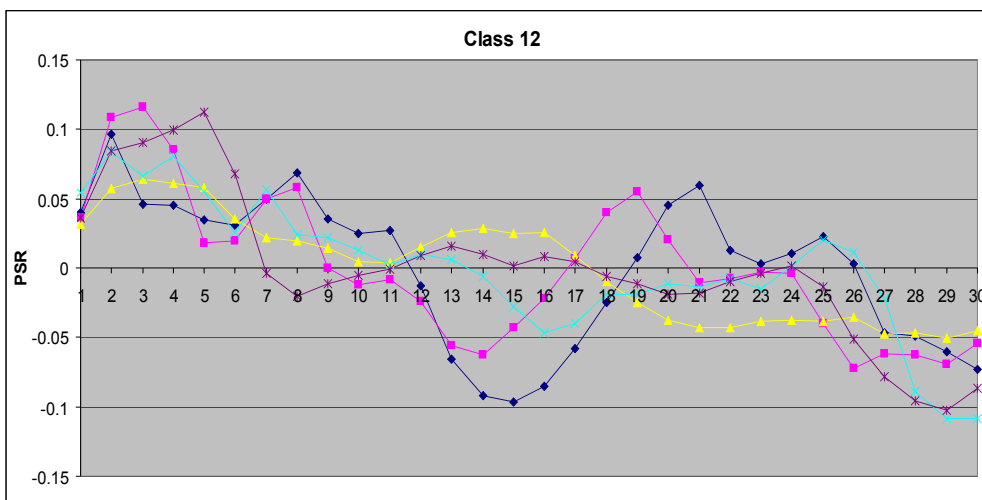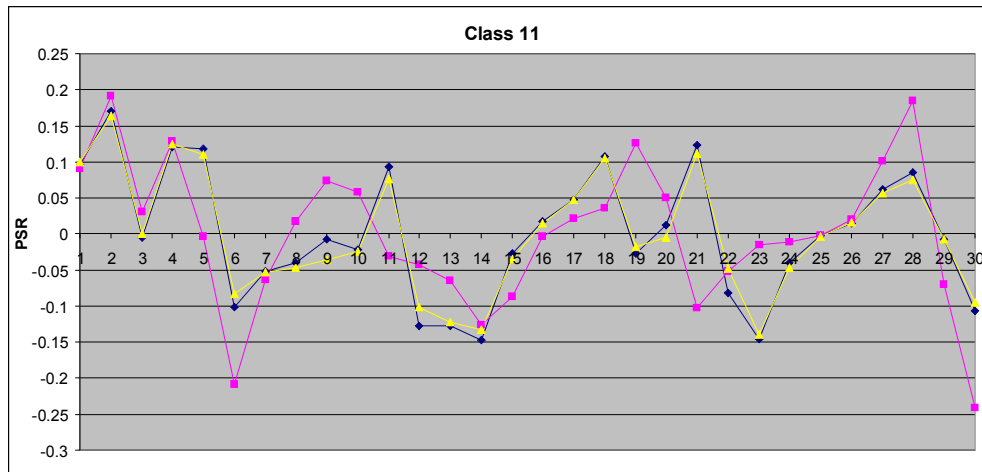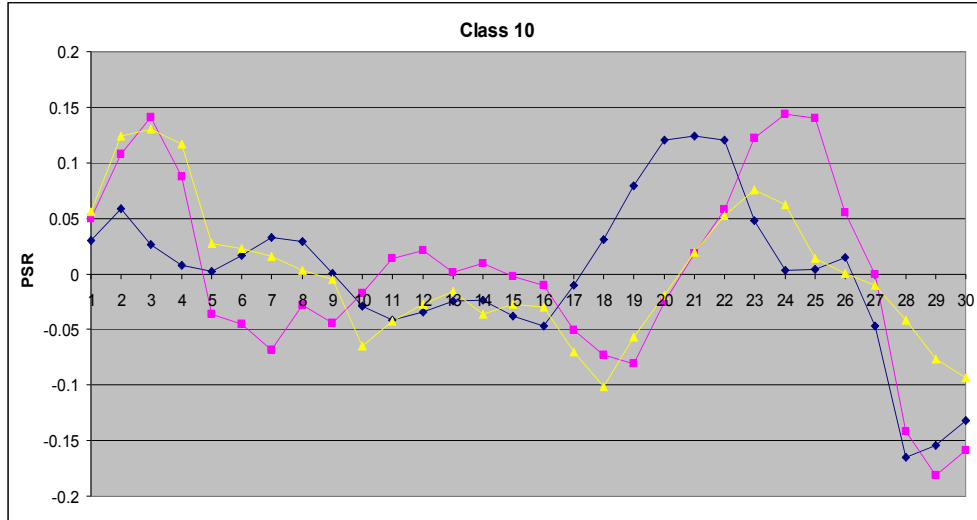
Figure 6-5 PSR plots: Class 10, Class 11, and Class 12.
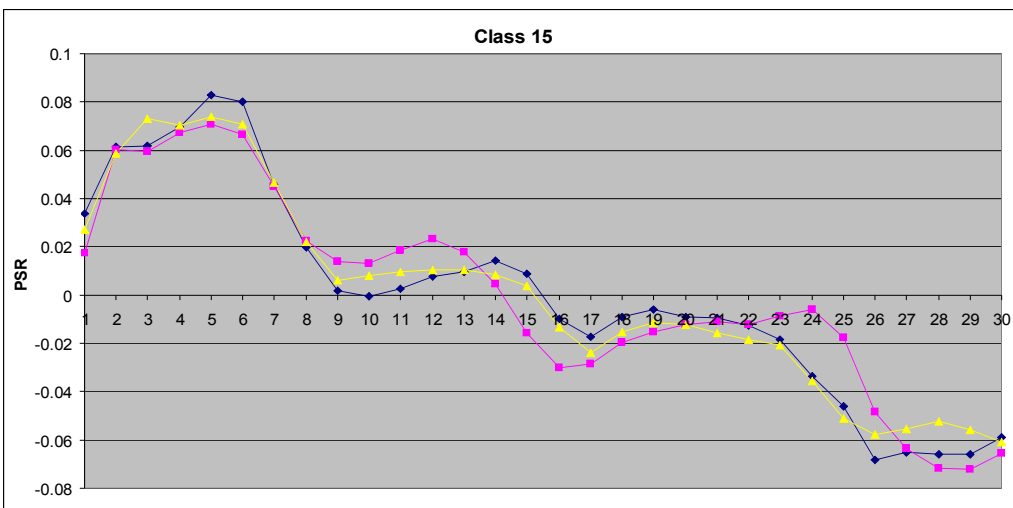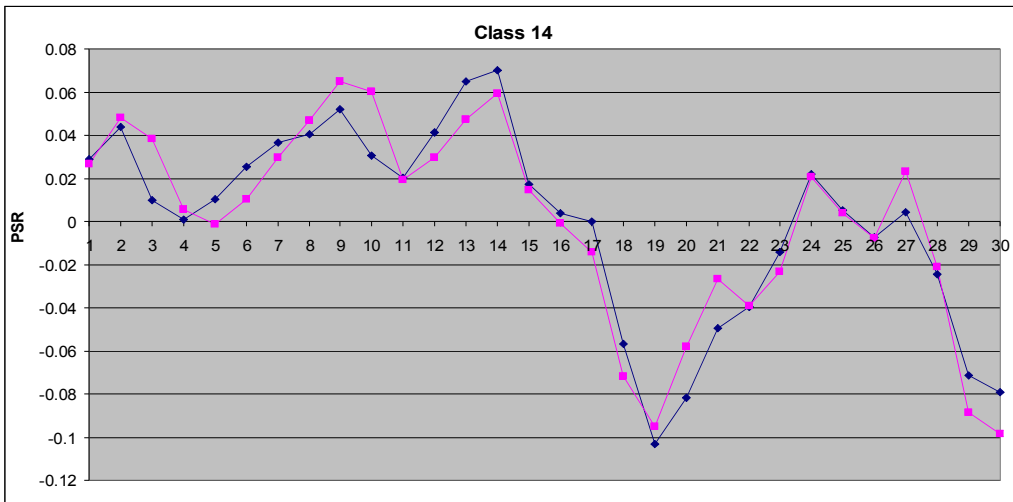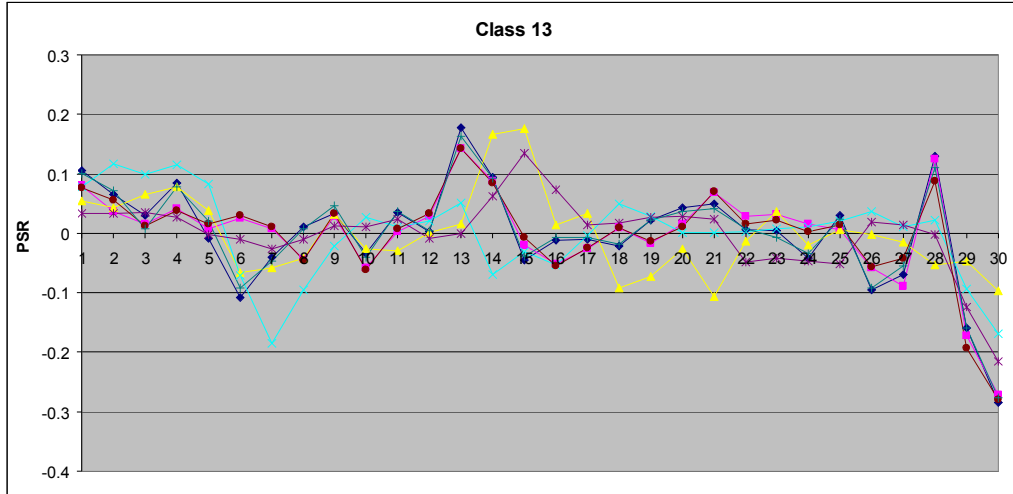
Figure 6-6 PSR plots: Class 13, Class 14, and Class 15.

$$PSR\_8\_IDX = 1 \qquad if \quad PSR_i \le PV, \quad for \quad i = 2 \cdots 8 \qquad (6.1)$$

$$PSR\_8\_IDX = 2 \qquad if \quad PSR_i > PV, \quad for \quad i = 2 \cdots 8 \qquad (6.2)$$

where

PSR_i : ith PSR value

$SORT\_PSR_i$: ith sorted PSR value

$PV = 0.008$

In order to obtain more information from the PSRs, they are categorized into five groups for each individual vehicle. The statistics are calculated for each group:

Group I Features: MEAN_1_15, STD_1_15, MDN_1_15, XMDN_1_15 (see Equations 6.3-6.6)

Group II Features: MEAN_16_30, STD_16_30, MDN_16_30, XMDN_16_30 (see Equations 6.7-6.10)

Group III Features: MEAN_1_10, STD_1_10, MDN_1_10, XMDN_1_10 (see Equations 6.11-6.14)

Group IV Features: MEAN_11_20, STD_11_20, MDN_11_20, XMDN_11_20

(see Equations 6.15-6.18)

Group V Features: MEAN_21_30, STD_21_30, MDN_21_30, XMDN_21_30

(see Equations 6.19-6.22)

$$MEAN\_1\_15 = \frac{\sum_{i=1}^{15} PSR_i}{15} \tag{6.3}$$

$$STD\_1\_15 = \sqrt{\frac{\sum_{i=1}^{15} (PSR_i - MEAN\_1\_15)^2}{14}} \tag{6.4}$$

$$MDN\_1\_15 = SORT\_PSR_8 \tag{6.5}$$

$$XMDN\_1\_15 = PSR_8 \tag{6.6}$$

$$MEAN\_16\_30 = \frac{\sum_{i=16}^{30} PSR_i}{15} \tag{6.7}$$

$$STD\_16\_30 = \sqrt{\frac{\sum_{i=16}^{30} (PSR_i - MEAN\_16\_30)^2}{14}} \tag{6.8}$$

$$MDN\_16\_30 = SORT\_PSR_{23} \tag{6.9}$$

$$XMDN\_16\_30 = PSR_{23} \tag{6.10}$$

$$MEAN\_1\_10 = \frac{\sum_{i=1}^{10} PSR_i}{10} \tag{6.11}$$

$$STD\_1\_10 = \sqrt{\frac{\sum_{i=1}^{10}\left(PSR_i - MEAN\_1\_10\right)^2}{9}} \tag{6.12}$$

$$MDN\_1\_10 = \frac{\left(SORT\_PSR_5 + SORT\_PSR_6\right)}{2} \tag{6.13}$$

$$XMDN\_1\_10 = \frac{\left(PSR_5 + PSR_6\right)}{2} \tag{6.14}$$

$$MEAN\_11\_20 = \frac{\sum_{i=11}^{20} PSR_i}{10} \tag{6.15}$$

$$STD\_11\_20 = \sqrt{\frac{\sum_{i=11}^{20}\left(PSR_i - MEAN\_11\_20\right)^2}{9}} \tag{6.16}$$

$$MDN\_11\_20 = \frac{(SORT\_PSR_{15} + SORT\_PSR_{16})}{2} \qquad (6.17)$$

$$XMDN\_11\_20 = \frac{(PSR_{15} + PSR_{16})}{2} \qquad (6.18)$$

$$MEAN\_21\_30 = \frac{\sum_{i=21}^{30} PSR_i}{10} \qquad (6.19)$$

$$STD\_21\_30 = \sqrt{\frac{\sum_{i=21}^{30}(PSR_i - MEAN\_21\_30)^2}{9}} \qquad (6.20)$$

$$MDN\_21\_30 = \frac{(SORT\_PSR_{25} + SORT\_PSR_{26})}{2} \qquad (6.21)$$

$$XMDN\_21\_30 = \frac{(PSR_{25} + PSR_{26})}{2} \qquad (6.22)$$

6.4 CASE STUDY

6.4.1 Data Description

To develop the proposed vehicle classification model, the dataset obtained from data collection I (as described in Chapter 5), which included about 6.5 minutes of vehicle

signature and video-ground-truthed data, was used. This dataset was divided into two sub-dataset, calibration dataset and testing dataset for model development. The two sub-datasets are illustrated in Table 6-6. Since abnormal vehicle signature data were observed in lane 3 at Laguna Canyon 1 and in lane 6 at Laguna Canyon 2, those data were discarded to enhance the development process.

Table 6-6 Dataset Description

	Calibration Dataset		**Test Dataset**	
Location	Laguna Canyon 1	Sand Canyon	Laguna Canyon 2	Jeffrey
Lane	7 lanes	5 lanes	6 lanes	5 lanes
Time Period	March 11th, 2005 6:50-6:57 AM		March 11th, 2005 6:50-6:57 AM	
Loop Configuration	Square loop detector		Round loop detector	
Dataset traffic count	3718		3914	

After the PSR_8_IDX is computed, vehicles were categorized into two groups: small vehicles and large trucks. The PSR features that applied to each group are depicted in Figure 6-7. Thirteen PSR features were applied to the small vehicles group, while nine PSR features were applied to large trucks group. The heuristic decision tree thus obtained is illustrated in Figure 6-8 and Figure 6-9. As shown in Figure 6-8, the tree for the small vehicles group has seven levels and twenty-four nodes. In addition, it can be observed from Figure 6-9 that the tree for the large trucks group has three levels and there are fifteen nodes.
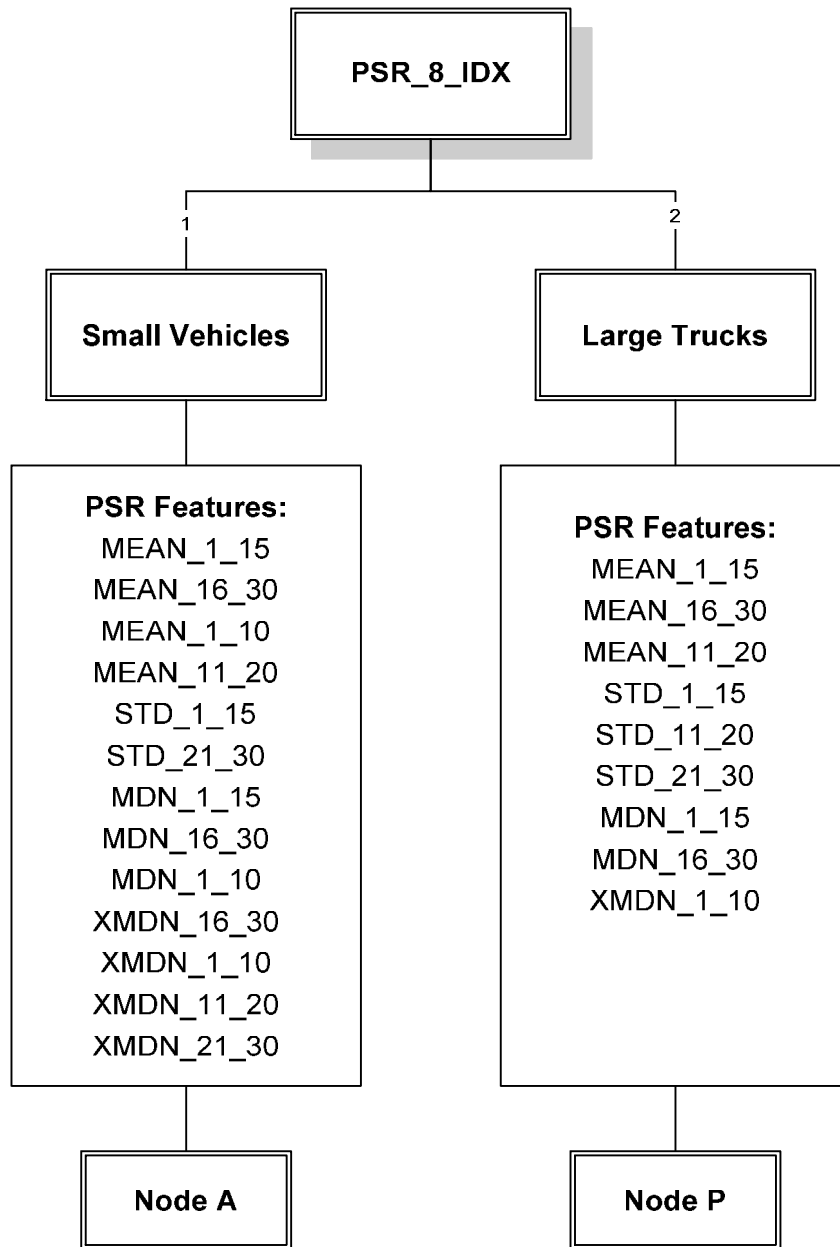
Figure 6-7 PSR features applied to small vehicle group and large trucks group.
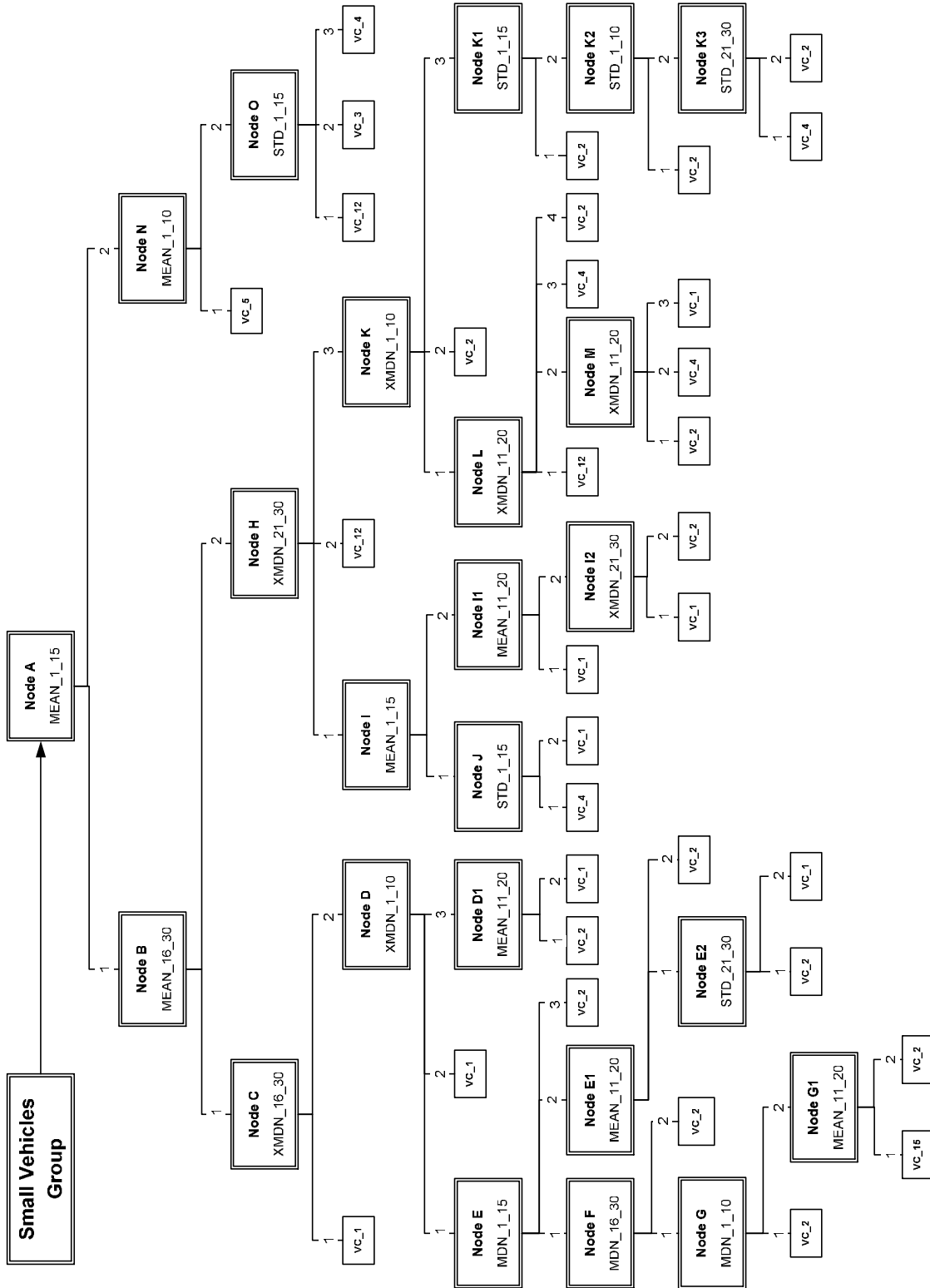
Figure 6-8 Vehicle classification flow chart: small vehicles group.

Figure 6-9 Vehicle classification flow chart: large trucks group.

6.4.2 Calibration Results

The calibration results are tabulated in Table 6-7. It can be seen from Table 6-7 that the three classification schemes yield similar performance. The results are very encouraging since the proposed model can successfully separate small vehicles from large trucks, and classify vehicles based on the FHWA classification scheme using single loop detector data without any axle information.

Table 6-7 Vehicle Classification Result Summary: Calibration Dataset

	Correct Classified Vehicle	Performance
FHWA Classification Scheme	3577	96.2%
FHWA-I Classification Scheme	3577	96.2%
RTPMS Classification Scheme	3587	96.5%

The detailed results according to the three proposed vehicle classification schemes are demonstrated in Table 6-8, Table 6-9, and Table 6-10. Table 6-8 presents the FHWA-I vehicle classification category. It can be observed that classification rates are lower in class 4, class 5, and class 15, which are "Two Axle, 6 Tire Single Units," "Three Axle Single Units," and "20' Buses" respectively. The misclassifications among class 1, class 2, class 4, and class 15 are due to similarity of signatures. For class 5, the misclassification is caused by varied characteristics within class 5 as observed in Figure 6-3.

Table 6-8 FHWA-I Vehicle Classification Category: Calibration Dataset

Performance		Predicted Vehicle Class															Volume by Class	Classification Rate
3577	96.2%	1	2	3	4	5	6	7	8	9	10	11	12	13	14	15		
FHWA-I Vehicle Class	1	2960	39	0	2	0	0	0	0	0	0	0	1	0	0	0	3002	98.6%
	2	75	525	0	6	1	0	0	0	0	0	0	0	0	0	1	608	86.3%
	3	0	0	2	0	0	0	0	0	0	0	0	0	0	0	0	2	100.0%
	4	0	3	0	18	1	0	0	0	0	0	0	1	0	0	0	23	78.3%
	5	0	0	0	1	7	0	1	0	0	0	0	0	1	0	0	10	70.0%
	6	0	0	0	0	0	3	0	0	0	0	0	0	0	0	0	3	100.0%
	7	0	0	0	0	1	1	34	0	0	1	2	0	0	0	0	39	87.2%
	8	0	0	0	0	0	0	0	2	0	0	0	0	0	0	0	2	100.0%
	9	0	0	0	0	0	0	0	1	5	0	0	0	0	0	0	6	83.3%
	10	0	0	0	0	0	0	0	0	0	3	0	0	0	0	0	3	100.0%
	11	0	0	0	0	0	0	0	0	0	0	3	0	0	0	0	3	100.0%
	12	0	0	0	0	0	0	0	0	0	0	0	5	0	0	0	5	100.0%
	13	0	0	0	0	0	1	0	0	0	0	0	0	6	0	0	7	85.7%
	14	0	0	0	0	0	0	0	0	0	0	0	0	0	2	0	2	100.0%
	15	0	1	0	0	0	0	0	0	0	0	0	0	0	0	2	3	66.7%
Estimated Volume by Class		3035	568	2	27	10	5	35	3	5	4	5	7	7	2	3	3718	
Estimated Vehicle Composition		81.6%	15.3%	0.1%	0.7%	0.3%	0.1%	0.9%	0.1%	0.1%	0.1%	0.1%	0.2%	0.2%	0.1%	0.1%	100%	

Table 6-9 FHWA Vehicle Classification Category: Calibration Dataset

Performance		Predicted Vehicle Class													Volume by Class	Classification Rate
3577	96.2%	1	2	3	4	5	6	7	8	9	10	11	12	13		
FHWA Vehicle Class	1	-	-	-	-	-	-	-	-	-	-	-	-	-	-	-
	2	0	2962	39	0	2	1	0	0	0	0	0	0	0	3004	98.6%
	3	0	76	530	1	6	1	0	0	0	0	0	0	0	614	86.3%
	4	0	0	1	6	0	0	0	0	0	0	0	0	0	7	85.7%
	5	0	0	3	0	21	2	0	0	0	0	0	0	0	26	80.8%
	6	0	0	0	0	1	15	0	0	2	0	0	0	0	18	83.3%
	7	-	-	-	-	-	-	-	-	-	-	-	-	-	-	-
	8	0	0	0	0	0	0	0	3	0	0	0	0	0	3	100.0%
	9	0	0	0	0	1	3	0	2	40	0	0	0	0	46	87.0%
	10	-	-	-	-	-	-	-	-	-	-	-	-	-	-	-
	11	-	-	-	-	-	-	-	-	-	-	-	-	-	-	-
	12	-	-	-	-	-	-	-	-	-	-	-	-	-	-	-
	13	-	-	-	-	-	-	-	-	-	-	-	-	-	-	-
Estimated Volume by Class		0	3038	573	7	31	22	0	5	42	0	0	0	0	3718	
Estimated Vehicle Composition		0%	81.7%	15.4%	0.2%	0.8%	0.6%	0.0%	0.1%	1.1%	0.0%	0.0%	0.0%	0.0%	100%	

127

Table 6-10 RTPMS Vehicle Classification Category: Calibration Dataset

Performance		Predicted Vehicle Class					Volume by Class	Classification Rate
3587	**96.5%**	**1**	**2**	**3**	**4**	**5**		
RTPMS Vehicle Class	**1**	2962	42	0	0	0	3004	98.6%
	2	76	566	2	2	0	646	87.6%
	3	0	1	5	1	0	7	71.4%
	4	0	1	0	9	2	12	75.0%
	5	0	1	0	3	45	49	91.8%
Estimated Volume by Class		3038	611	7	15	47	**3718**	
Estimated Vehicle Composition		81.7%	16.4%	0.2%	0.4%	1.3%	100%	

The outcomes presented in Table 6-9 and Table 6-10 demonstrate the potential of the proposed vehicle classification model. The FHWA classification scheme and RTPMS classification scheme results are very encouraging because the correct classification rates are around 96% for both schemes. Moreover, for the FHWA classification scheme, the worst case still maintains 80% correct classification rate.

6.4.3 Transferability Analysis

In order to perform model transferability analysis for round loop configuration, a dataset collected at different locations was applied. The testing results are presented in Table 6-11. As shown in Table 6-11, the three classification schemes again yield similar performances. Although the performances are degraded compared with calibration dataset, the results are very promising since correct classification rates are around 93% for the three classification schemes.

Table 6-11 Vehicle Classification Result Summary: Test Dataset

	Correct Classified Vehicle	Performance
FHWA Classification Scheme	3641	93.0%
FHWA-I Classification Scheme	3640	93.0%
RTPMS Classification Scheme	3661	93.5%

Table 6-12, Table 13, and Table 6-14 present the classification results in detail according to the three proposed vehicle classification schemes. It can be observed from Table 6-12 that classification rates are lower in class 3, class 4, and class 6, which are "Buses," "Two Axle, 6 Tire Single Units," and "Four or Less Axle Single Trailers" respectively. For class 4, the misclassifications pattern is similar compared with calibration dataset. For class 3 and class 6, further investigations are needed due to lack of enough samples.

Despite high misclassification rates occurring in class 3 and class 6, the results are significant enough to conclude reliable model transferability. It is worth nothing that the classification performances of the three proposed classification schemes are around 93%, which demonstrates the potential of employing the procedure of the proposed vehicle classification model for a detection system with single round loop configuration.

Table 6-12 FHWA-I Vehicle Classification Category: Test Dataset

Performance		Predicted Vehicle Class															Volume by Class	Classification Rate
3640	93.0%	1	2	3	4	5	6	7	8	9	10	11	12	13	14	15	Class	Rate
FHWA-I Vehicle Class	1	3027	124	0	13	0	0	0	0	0	0	0	4	0	0	2	3170	95.5%
	2	79	546	1	11	8	0	0	0	0	0	0	1	0	0	1	647	84.4%
	3	0	0	0	1	0	0	0	0	0	1	0	0	0	0	0	2	0.0%
	4	0	4	0	12	3	0	0	0	0	1	0	1	0	0	0	21	57.1%
	5	0	1	1	1	6	0	1	0	0	0	0	0	0	0	0	10	60.0%
	6	0	0	1	0	0	1	0	0	0	0	0	0	0	0	0	2	50.0%
	7	0	0	0	0	1	2	34	0	0	0	2	0	0	0	0	39	87.2%
	8	0	0	0	0	0	0	0	2	0	0	0	0	0	0	0	2	100.0%
	9	0	0	0	0	0	0	1	0	4	0	0	0	0	1	0	6	66.7%
	10	0	0	0	0	1	0	0	0	0	1	0	0	0	0	0	2	50.0%
	11	0	0	0	0	0	0	0	0	0	0	3	0	0	0	0	3	100.0%
	12	0	0	1	0	0	0	0	0	0	0	0	1	0	0	0	2	50.0%
	13	0	0	0	1	0	2	0	0	0	1	0	0	2	0	0	6	33.3%
	14	0	0	0	0	0	0	0	0	0	0	0	0	0	1	0	1	100.0%
	15	1	0	0	0	0	0	0	0	0	0	0	0	0	0	0	1	0.0%
Estimated Volume by Class		3107	675	4	39	19	5	36	2	4	4	5	7	2	2	3		3914
Estimated Vehicle Composition		79.4%	17.2%	0.1%	1.0%	0.5%	0.1%	0.9%	0.1%	0.1%	0.1%	0.1%	0.2%	0.1%	0.1%	0.1%		100%

Table 6-13 FHWA Vehicle Classification Category: Test Dataset

Performance		Predicted Vehicle Class													Volume by Class	Classification Rate
3641	**93.0%**	**1**	**2**	**3**	**4**	**5**	**6**	**7**	**8**	**9**	**10**	**11**	**12**	**13**		
FHWA Vehicle Class	**1**	-	-	-	-	-	-	-	-	-	-	-	-	-	-	-
	2	0	3029	124	2	13	4	0	0	0	0	0	0	0	3172	95.5%
	3	0	79	550	3	11	9	0	0	1	0	0	0	0	653	84.2%
	4	0	1	0	1	2	0	0	0	0	0	0	0	0	4	25.0%
	5	0	0	4	0	14	5	0	0	0	0	0	0	0	23	60.9%
	6	0	0	1	2	1	10	0	0	1	0	0	0	0	15	66.7%
	7	-	-	-	-	-	-	-	-	-	-	-	-	-	-	-
	8	0	0	0	1	0	0	0	1	0	0	0	0	0	2	50.0%
	9	0	0	0	0	2	3	0	4	36	0	0	0	0	45	80.0%
	10	-	-	-	-	-	-	-	-	-	-	-	-	-	-	-
	11	-	-	-	-	-	-	-	-	-	-	-	-	-	-	-
	12	-	-	-	-	-	-	-	-	-	-	-	-	-	-	-
	13	-	-	-	-	-	-	-	-	-	-	-	-	-	-	-
Estimated Volume by Class		0	3109	679	9	43	31	0	5	38	0	0	0	0	**3914**	
Estimated Vehicle Composition		0%	79.4%	17.3%	0.2%	1.1%	0.8%	0.0%	0.1%	1.0%	0.0%	0.0%	0.0%	0.0%	**100%**	

Table 6-14 RTPMS Vehicle Classification Category: Test Dataset

Performance		Predicted Vehicle Class					Volume by Class	Classification Rate
3661	**93.5%**	**1**	**2**	**3**	**4**	**5**		
RTPMS Vehicle Class	**1**	3029	141	2	0	0	3172	95.5%
	2	80	584	4	12	1	681	85.8%
	3	0	1	1	2	0	4	25.0%
	4	0	1	2	7	2	12	58.3%
	5	0	2	0	3	40	45	88.9%
Estimated Volume by Class		3109	729	9	24	43	**3914**	
Estimated Vehicle Composition		79.4%	18.6%	0.2%	0.6%	1.1%	100%	

Moreover, it must be noted that abnormal vehicle signatures were discarded at the model development stage as described in section 6.4.1. Since these abnormalities may not be recognized and filtered out in real-time implementation, the proposed vehicle classification model was also applied to the same test dataset but all of the problematic vehicle signatures were included.

Therefore, 282 problematic vehicle signatures observed in lane 6 at Laguna Canyon 2 were added to the test dataset. Because the abnormalities were observed from vehicle types with low profile vehicles (e.g., passenger car, minivan, and some trucks), it is expected that the classification rates of those groups will be affected more compared with other vehicle classes.

The results are summarized in Table 6-15. As shown in Table 6-15, although the overall performance for the three classification schemes declines, about 90%-91% classification rate could be still obtained. Moreover, detailed results for the three schemes are presented in Table 6-16, Table 17, and Table 6-18

Table 6-15 Vehicle Classification Result Summary: Test Dataset with Problematic Vehicle Signature

	Correct Classified Vehicle	Performance
FHWA Classification Scheme	3794	90.4%
FHWA-I Classification Scheme	3792	90.4%
RTPMS Classification Scheme	3818	91.0%

Table 6-16 FHWA-I Vehicle Classification Category: Test Dataset with Problematic Vehicle Signature

FHWA-I Classification Scheme		Problematical Data Excluded		Problematical Data Included	
Vehicle Class	Descriptions	Volume by Class	Classification Rate	Volume by Class	Classification Rate
1	Passenger Cars	3170	95.5%	3395	**92.8%**
2	Two Axle, Four Tire Single Units	647	84.4%	689	**82.9%**
3	Buses	2	0.0%	2	**0.0%**
4	Two Axle, 6 Tire Single Units	21	57.1%	24	**50.0%**
5	Three Axle Single Units	10	60.0%	12	**58.3%**
6	Four or Less Axle Single Trailers	2	50.0%	2	50.0%
7	Five Axle Single Trailers	39	87.2%	39	87.2%
8	Passenger (Class 2) + Trailer	2	100.0%	2	100.0%
9	Class 3 + Trailer	6	66.7%	6	66.7%
10	Class 5 + Trailer	2	50.0%	3	**33.3%**
11	Class 6 + Trailer	3	100.0%	3	100.0%
12	Bobtail Tractor (Semi Without Any Trailers)	2	50.0%	5	**20.0%**
13	Goose Neck Trailer or Moving Van	6	33.3%	7	42.9%
14	30' Buses	1	100.0%	4	75.0%
15	20' Buses	1	0.0%	3	0.0%

133

Table 6-17 FHWA Vehicle Classification Category: Test Dataset with Problematic Vehicle Signature

FHWA Classification Scheme		Problematical Data Excluded		Problematical Data Included	
Vehicle Class	Descriptions	Volume by Class	Classification Rate	Volume by Class	Classification Rate
1	Motorcycles	-	-	-	-
2	Passenger Cars	3172	95.5%	3397	**92.8%**
3	Two Axle, Four Tire Single Units	653	84.2%	695	**82.7%**
4	Buses	4	25.0%	9	33.3%
5	Two Axle, 6 Tire Single Units	23	60.9%	27	**51.9%**
6	Three Axle Single Units	15	66.7%	20	**60.0%**
7	Four or More Axle Single Units	-	-	-	-
8	Four or Less Axle Single Trailers	2	50.0%	2	50.0%
9	Five Axle Single Trailers	45	80.0%	46	80.4%
10	Six or More Axle Single Trailers	-	-	-	-
11	Five or Less Axle Multi-Trailers	-	-	-	-
12	Six Axle Multi-Trailers	-	-	-	-
13	Seven or More Axle Multi-Trailers	-	-	-	-

Table 6-18 RTPMS Vehicle Classification Category: Test Dataset with Problematic Vehicle Signature

RTPMS Classification Scheme		Problematical Data Excluded		Problematical Data Included	
Vehicle Class	Descriptions	Volume by Class	Classification Rate	Volume by Class	Classification Rate
1	Passenger Cars	3172	95.5%	3397	**92.8%**
2	Small Single Unit Trucks	681	85.8%	728	**84.1%**
3	Buses	4	25.0%	9	33.3%
4	Medium/Large Single Unit Trucks	12	58.3%	14	64.3%
5	Single Trailer Trucks	45	88.9%	48	87.5%

It can be observed from Table 6-16 to Table 6-18 that as expected, classification rates are degraded for "Passenger Cars" and "Two Axle, Four Tire Single Units." Furthermore, the results again demonstrate the potential of deploying the proposed vehicle classification model in real-time.

6.5 SUMMARY

This chapter showed the application of PSR features in developing vehicle classification for real-time implementation. Vehicle class is an important characteristic of traffic measurement and can contribute to many important transportation applications including vehicle reidentification, road maintenance, emissions evaluation, traffic modeling development, transportation planning, traffic control, traffic safety improvement, toll systems assessment, etc.

Considering real-time implementation, a simple but efficient vehicle classification model, which utilizes heuristic decision tree combined with K-means clustering method, was suggested. The proposed real-time vehicle classification model is not only capable of categorizing vehicle types based on the FHWA scheme, but is also capable of grouping vehicles into more detailed classes.

Three vehicle classification schemes, FHWA, FHWA-I, and RTPMS classification schemes, were applied to develop the proposed vehicle classification model. A dataset obtained from square single loop detector was utilized to perform vehicle classification task based on the FHWA-I classification scheme. Moreover, a dataset obtained from round single loop detector was applied to test transferability of the proposed model.

The results are very encouraging since the proposed real-time vehicle classification model can successfully classify vehicles using single loop detector data without any explicit axle information, and the results demonstrate reliable model transferability. In addition, the advantages of the proposed vehicle classification model are its simplicity, and employing the current detection infrastructure. Furthermore, due to the small proportion of large trucks, future studies are suggested to improve classification rates for vehicle classes under the large trucks group.

CHAPTER 7 DESIGN OF REAL-TIME TRAFFIC PERFORMANCE MEASUREMENT SYSTEM (RTPMS)

As mentioned in Chapter 4, field computational resources and the bandwidth of field communication links, are often quite limited for traffic operations. Therefore, RTREID-2 and the proposed real-time vehicle classification model are developed to address those issues. The next step is to investigate development of a real-time freeway performance measurement system in a real-world setting. Accordingly, the design of a Real-time Traffic Performance Measurement System (RTPMS) is presented in this chapter. The framework of RTPMS is based on RTREID-2. The overall system can be divided into two sub-systems: field data preprocessing system and performance measurement system. Each of the sub-systems is discussed in detail. A simulation of RTPMS is also conducted in this chapter to access its feasibility.

7.1 RTPMS DEPLOYMENT FRAMEWORK

RTPMS can be divided into two sub-systems: field data preprocessing system and performance measurement system. The field data preprocessing system includes all field computers that obtain and process raw vehicle signature data. The performance measurement system consists of four severs to generate and display real-time performance measurements. The details of the two subsystems are described in Section 7.3. The framework of the RTPMS is illustrated in Figure 7-1.
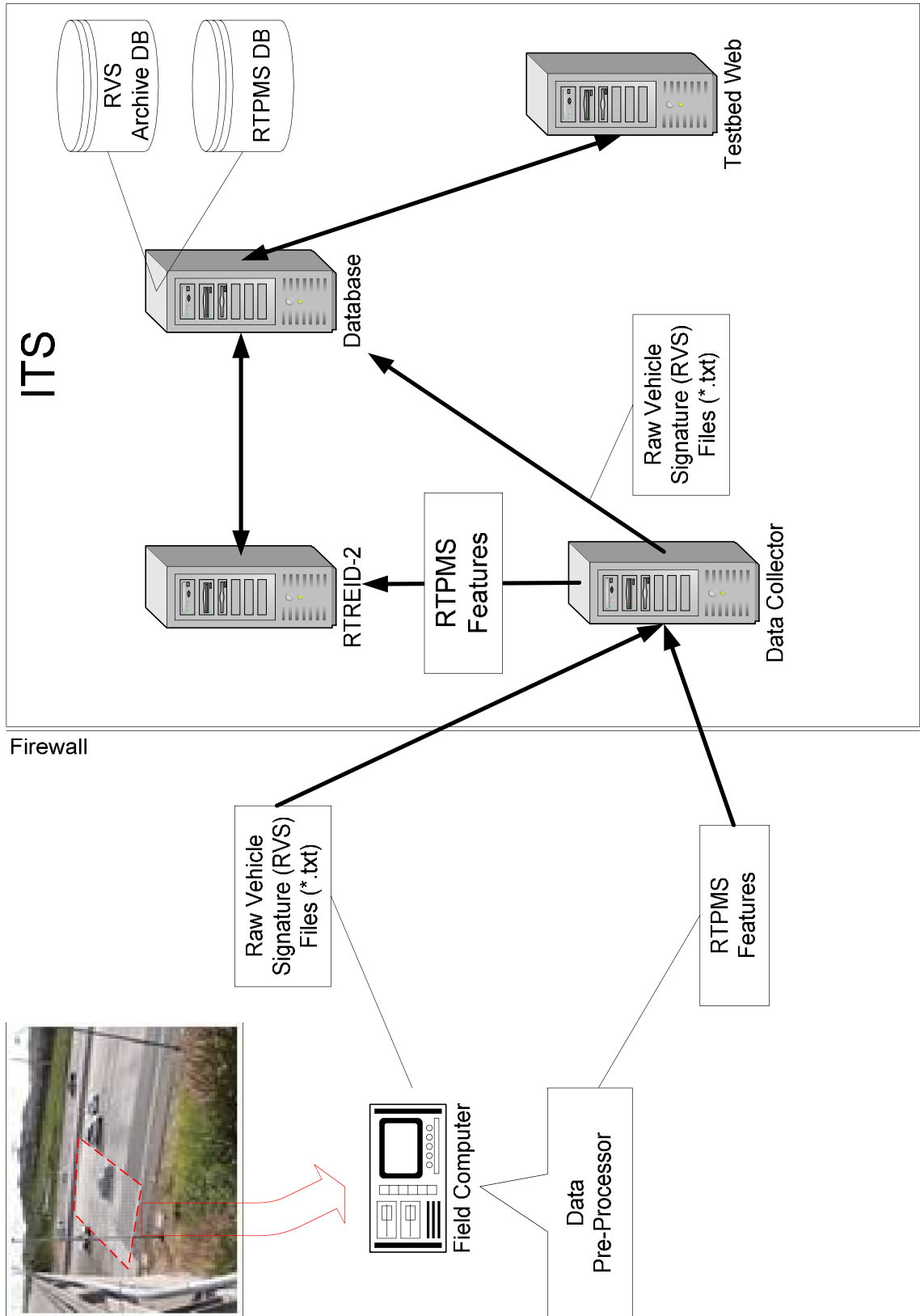
Figure 7-1 RTPMS deployment framework.

As shown in Figure 7-1, in the field data preprocessing system a module named, "Data Pre-Processor" will generate two types of data: raw vehicle signatures and RTPMS features. The raw vehicle signatures are unprocessed vehicle signatures obtained from advanced detector cards. The RTPMS features includes PSR values and speed estimation results. For the performance measurement system, there will be four servers including RTREID-2, Data Collector, Testbed Web, and Database. The Data Collector will communicate with the field computers through an interface, which will be programmed in CORBA, and collect the preprocessed RTPMS features.

The vehicle reidentification and vehicle classification tasks will be managed on the RTREID-2 server. The raw vehicle signature data obtained from the field as well as the outputs of the RTREID-2 server will be sent to the Database server for storage. Moreover, the Testbed Web server will obtain necessary information from the Database server, execute performance evaluation, and display the results.

7.2 DATABASE DESIGN

The Database server consists of two databases: Raw Vehicle Signature (RVS) Archive database and RTPMS database. The raw vehicle signature files obtained from the field are stored as text format. Those files will be sent back to RVS Archive database. The RTPMS database will be built using Oracle. There are 10 reference tables: Cabinet Table, Card Table, Station Table, Perf_Stns Table, Vehicle reidentification (REID)

Performance Table, Upstream Table, Signature Table, Sample Table, REID Input Table, and REID Output Table. The contents of each table are shown in Figure 7-2.
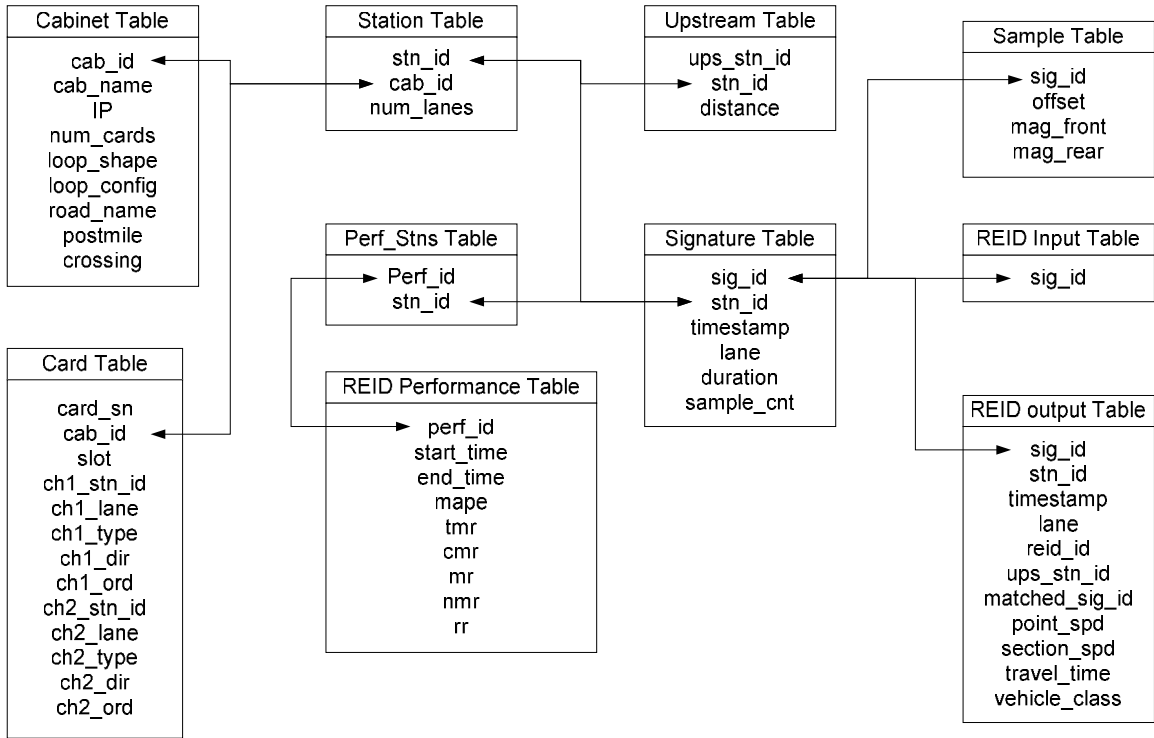
Figure 7-2 Reference tables for RTPMS database.

Moreover, the reference tables can be grouped into two types: static table and dynamic table as tabulated in Table 7-1. The static tables hold station and detector card configuration, while the dynamic tables hold signature data and results. The functions of the reference tables, and the definition of each variable and its attributes are listed from Table 7-2 to Table 7-11. Moreover, the performance indices and estimates obtained from the RTREID-2 server such as vehicle tracking information, vehicle class, speed, etc., will be stored at the RTPMS database.

Table 7-1 Static Tables and Dynamic Tables

Static Table	Dynamic Table	
Cabinet Table	Signature Table	REID Output Table
Card Table	Sample Table	REID Performance Table
Station Table	REID Input Table	Perf_Stns Table
Upstream Table		

Table 7-2 Static Tables: Cabinet Table

Cabinet Table: holds physical location information		
cab_id	int	cabinet id; 3 digits
cab_name	varchar[20]	cabinet name; e.g. Laguna Canyon
IP	varchar[15]	DNS name or IP of field pc
num_cards	int	number of cards in field pc
loop_shape	varchar[10]	square, round, blade, etc
loop_config	varchar[10]	single, double
road_name	varchar[20]	e.g. I-405, Alton Parkway
postmile	float	post mile information
crossing	varchar[20]	name of nearest crossing arterial

Table 7-3 Static Tables: Card Table

Card Table: holds physical card configuration		
card_sn	int	IST card serial number
cab_id	int	maps to cab_id in cabinet table
slot	int	location in PC
ch1_stn_id	int	station channel 1 belongs to
ch1_lane	int	lane channel 1 goes to
ch1_type	varchar[10]	HOV, ML (mainline), etc
ch1_dir	varchar[1]	channel 1 lane direction (N, S, E, W)
ch1_ord	varchar[1]	front or rear if double loop (F, R)
ch2_stn_id	int	station channel 2 belongs to
ch2_lane	int	lane channel 2 goes to
ch2_type	varchar[10]	HOV, ML, etc
ch2_dir	varchar[1]	channel 2 lane direction (N, S, E, W)
ch2_ord	varchar[1]	front or rear if double loop (F, R)

Table 7-4 Static Tables: Station Table

Station Table: holds virtual station information		
stn_id	int	station id; 3 digits
cab_id	int	maps to cab_id in cabinet table
num_lanes	int	number of lanes in station

Table 7-5 Static Tables: Upstream Table

Upstream Table: holds mapping for multiple upstream stations		
ups_stn_id	int	upstream station id; maps to stn_id in station table
stn_id	int	maps to stn_id in station table
distance	float	

Table 7-6 Dynamic Tables: Signature Table

Signature Table: holds vehicle signature information		
sig_id	long	signature id; first 3 digits are stn_id
stn_id	int	maps to stn_id in station table
timestamp	float	signature timestamp; convert to local time (second)
Lane	int	lane number; count from leftmost lane (including HOV lanes)
duration	float	duration of time the detector is on; same as last offset
sample_cnt	int	number of samples

Table 7-7 Dynamic Tables: Sample Table

Sample Table: holds magnitudes		
sig_id	long	maps to sig_id in signature table
offset	float	7 digit precision
mag_front	int	magnitude of front loop
mag_rear	int	magnitude of rear loop

Table 7-8 Dynamic Tables: REID Input Table

REID Input Table: holds mapping for REID input data		
sig_id	long	maps to sig_id in signature table

Table 7-9 Dynamic Tables: REID Output Table

REID Output Table: holds REID results		
sig_id	long	maps to sig_id in signature table
stn_id	int	maps to stn_id in station table
timestamp	float	signature timestamp
lane	int	lane number
reid_id	int	id of reidentified signature
ups_stn_id	int	maps to ups_stn_id in upstream table
matched_sig_id	int	id of matched signature
point_spd	float	point speed; output from speed-trap or speed estimation module
section_spd	float	section speed (travel speed)
travel_time	float	travel time
vehicle_class	varchar[10]	classification of vehicle types; output from vehicle classification module

Table 7-10 Dynamic Tables: REID Performance Table

REID Performance Table: holds ground-truthed results		
perf_id	int	id of ground-truthed dataset
start_time	float	start-time of ground-truthed dataset
end_time	float	end-time of ground-truthed dataset
mape	float	mean absolute percentage error for travel time estimation
tmr	float	total match rate
cmr	float	correct match rate
mr	float	mismatch rate
nmr	float	no match rate
rr	float	reliability rate

Table 7-11 Dynamic Tables: Perf_Stns Table

Perf_Stns Table: contains mapping of performance info to multiple stations		
perf_id	int	maps to perf_id in REID performance table
stn_id	int	maps to stn_id in station table

The inputs and outputs of the RTPMS database include configuration data, input data for REID and Output data from REID:

- Configuration: describes configuration of detection station, such as detection station ID, detector type, road index, etc. (see Table 7-12)

- Input data for REID: hold raw vehicle signature data obtained from detection station (see Table 7-13)

- Output data from REID

  □ Individual vehicle level: provide vehicle tracking information for each individual vehicle (see Table 7-14)

  □ Section level: provide performance measurements for each single section (see Table 7-15)

  □ Lane-related: provide performance measurements for each lane (see Table 7-16)

  □ Path-related: provide path-related information such as path travel time (see Table 7-17)

  □ REID performance: provide vehicle reidentification performances whenever ground-truthed data is available (see Table 7-18)

Examples of the above-mentioned tables are detailed and demonstrated in APPENDIX A.

Table 7-12 Configurations: Design Scheme

Name	Type	Description	Note
Road Index	• Freeway • Urban	Freeway or Road/Intersection name	Pre-defined
Detection Station ID (DS ID)	-	A unique ID for each detector	Pre-defined
Detector Type	• Round Loop • Square Loop • Blade • Video	Detector type specification	Pre-defined
Detector Configuration	• Single • Double • Other	Configuration of the detectors	Pre-defined

Upstream Detection Station ID (UDS ID)	• Freeway
	  o Mainline
	  o Ramp
	• Urban
	  o Through
	  o Left turn
	  o Right turn
		The adjacent upstream detection station(s)	Pre-defined

Distance	-	Distance to the each adjacent upstream detection station(s)	Pre-defined

Table 7-13 Input Data for REID: Design Scheme

Name	Type	Description	Note
UCI Record ID (UCI ID)	Header	An ID assigned to each vehicle signature	Detector specific data
DS ID	Header	A unique ID for each detector	Pre-defined
Date	Header	Signature timestamp	Detector specific data
Time	Header	Signature timestamp	Detector specific data
Lane	Header	Lane number	Detector specific data
Duration (sec)	Header	Duration of time the detector is on	Detector specific data
Num samples	Header	Number of samples in the vehicle signature	Detector specific data
Interval	Data	Time interval from the beginning of the vehicle signature	Detector specific data
Magnitude-front	Data	Magnitude of the front loop for double loops or magnitude of the signal loop	Detector specific data
Magnitude-rear	Data	Magnitude of the rear loop	Detector specific data

Table 7-14 Output Data from REID: Individual Vehicle Level Design Scheme

Name	Type	Description	Note
UCI ID	-	An ID assigned to each vehicle signature	Detector specific data
Road Index	• Freeway • Urban	Freeway or Road/Intersection name	Pre-defined (Configurations)
DS ID	-	A unique ID for each detector	Pre-defined (Configurations)
Detector Type	• Round Loop • Square Loop • Blade • Video	Detector type specification	Pre-defined (Configurations)
Detector Configuration	• Single • Double • Other	Configuration of the detectors	Pre-defined (Configurations)
Date	-	Signature timestamp	Detector specific data
Time	-	Signature timestamp	Detector specific data
Lane	-	Lane number	Detector specific data
REID ID	-	An ID assigned to the reidentified vehicle	REID result: Individual vehicle

UDS ID	• Freeway
	  o Mainline
	  o Ramp
	• Urban
	  o Through
	  o Left turn
	  o Right turn
		The adjacent upstream detection station(s)	Pre-defined (Configurations)

Distance (mile)	-	Distance to the each adjacent upstream detection station(s)	Pre-defined (Configurations)
Point speed (mph)	-	Output from speed-trap or speed estimation module	REID result: Individual vehicle
Section speed (mph)	-	Travel speed for individual vehicle	REID result: Individual vehicle
Travel time (sec)	-	Travel time for individual vehicle	REID result: Individual vehicle
Vehicle class	• FHWA • RTPMS	Classification of vehicle types based on FHWA/RTPMS standard	Output from vehicle classification module

Table 7-15 Output Data from REID: Section Level Design Scheme

Name	Type	Description	Note
DS ID	-	A unique ID for each detector	Pre-defined (Configurations)
UDS ID	• Freeway o Mainline o Ramp • Urban o Through o Left turn o Right turn	The nearest upstream detection station	Pre-defined (Configurations)
Section travel time (Sec. TT)	• Max • Min • Average (Avg) • Std	Statistics of section travel time for each single section	REID result: Single section
Section volume (Sec. Vol)	• Max • Min • Avg • Std	Statistics of section volume for each signal section	REID result: Single section
Section speed (Sec. Speed)	• Max • Min • Avg • Std	Statistics of section speed for each single section	REID result: Single section
Section occupancy % (Sec. Occ)	• Max • Min • Avg • Std	Statistics of section occupancy for each single section	REID result: Single section
Section density (Sec. Density)	• Max • Min • Avg • Std	Statistics of section density for each single section	REID result: Single section
Section Vehicle composition (Sec. Veh Comp)	• FHWA • UCI	Output from vehicle classification module	REID result: Single section

Table 7-16 Output Data from REID: Lane-Related Design Scheme

Name	Type	Description	Note
DS ID	-	A unique ID for each detector	Pre-defined (Configurations)

UDS ID	• Freeway
	  o Mainline
	  o Ramp
	• Urban
	  o Through
	  o Left turn
	  o Right turn
		The nearest upstream detection station	Pre-defined (Configurations)

Lane	-	Lane number	Detector specific data
Lane travel time (Lane TT)	• Max • Min • Avg • Std	Statistics of travel time for each lane	REID result: Lane related
Lane volume (Lane Vol)	• Max • Min • Avg • Std	Statistics of volume for each lane	REID result: Lane related
Lane speed	• Max • Min • Avg • Std	Statistics of section speed for each lane	REID result: Lane related
Lane occupancy (Lane Occ)	• Max • Min • Avg • Std	Statistics of occupancy for each lane	REID result: Lane related
Lane density	• Max • Min • Avg • Std	Statistics of density for each lane	REID result: Lane related
Lane Vehicle composition (Lane Veh Comp)	• FHWA • UCI	Output from vehicle classification module	REID result: Lane related

Table 7-17 Output Data from REID: Path-Related Level Design Scheme

Name	Type	Description	Note
Origin-Destination	-	O-D table	REID result: Path related
Total travel distance (Tot. TDist)	-	Total travel distance for a specific path	REID result: Path related
Path travel time in minute (Path TT)	• Max • Min • Avg • Std	Statistics of path travel time for a specific path	REID result: Path related
Path speed (mph)	• Max • Min • Avg • Std	Statistics of path speed for a specific path	REID result: Path related
Path info	-	Path info for individual vehicle (table)	REID result: Path related

Table 7-18 Output Data from REID: REID Performance Design Scheme

Name	Description	Note
MAPE	Mean absolute percentage error for travel time estimation (ground-truthed)	REID performance
TMR	Total match rate (ground-truthed)	REID performance
CMR	Correct match rate (ground-truthed)	REID performance
MR	Mismatch rate (ground-truthed)	REID performance
NMR	No match rate (ground-truthed)	REID performance
RR	Reliability rate (ground-truthed)	REID performance

7.3 MODULE DESCRIPTION

There are six modules in RTPMS, as illustrated in Figure 7-3. In the field data preprocessing system, the raw vehicle signature data is first processed via the Signature Examination Module to detect bad and abnormal vehicle signatures. The RTREID-2 PSR Generation Module is then performed to extract PSR values for each vehicle signature. Moreover, the single loop speed estimation is implemented via the Speed Estimation Module.
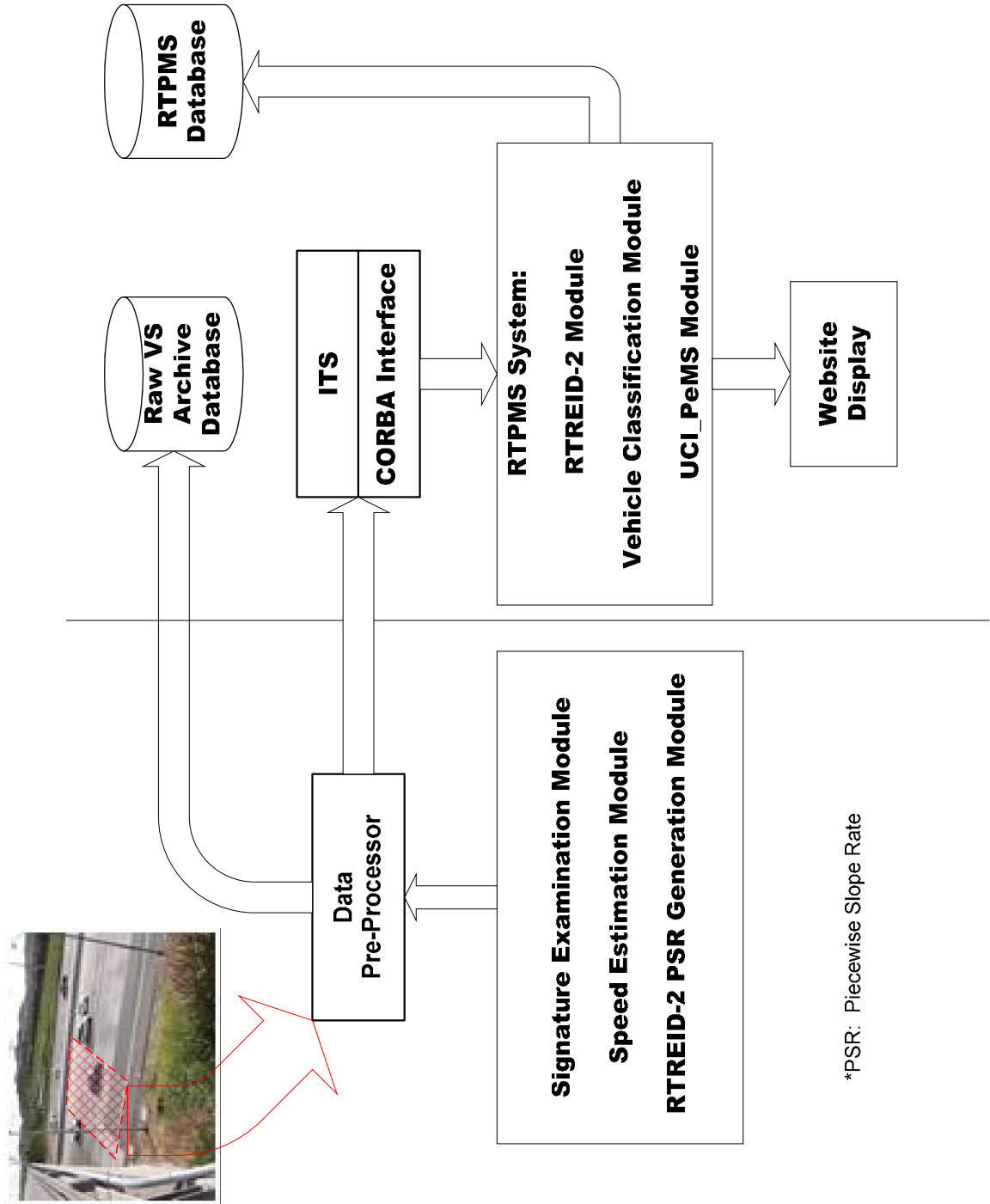
Figure 7-3 RTPMS modules descriptions.

The PSR values together with the estimated speeds from each field unit will be sent back to RTREID-2 server through CORBA interface. RTREID-2 and Vehicle Classification modules are then performed to obtain vehicle class and vehicle tracking information for each individual vehicle. Finally, the UCI_PeMS Module will query the RTPMS database to access necessary information, and hence, generate performance indices and estimates.

7.4 RTPMS SIMULATION

Because key data communication links were not ready within the research time frame, the implementation of RTPMS was conducted off-line in this research. A simulation of RTPMS was conducted to evaluate its feasibility. The framework is illustrated in Figure 7-4. After the RTREID-2 server was set, Data collector (i.e., CORBA interface), Database and Testbed Web servers were built by UCI research team according to the proposed RTPMS framework. The tasks of Data Collector were to receive raw vehicle signature data and RTPMS features (named, CORBA Supplier) and to feed RTPMS server with RTPMS features (named, CORBA Consumer).
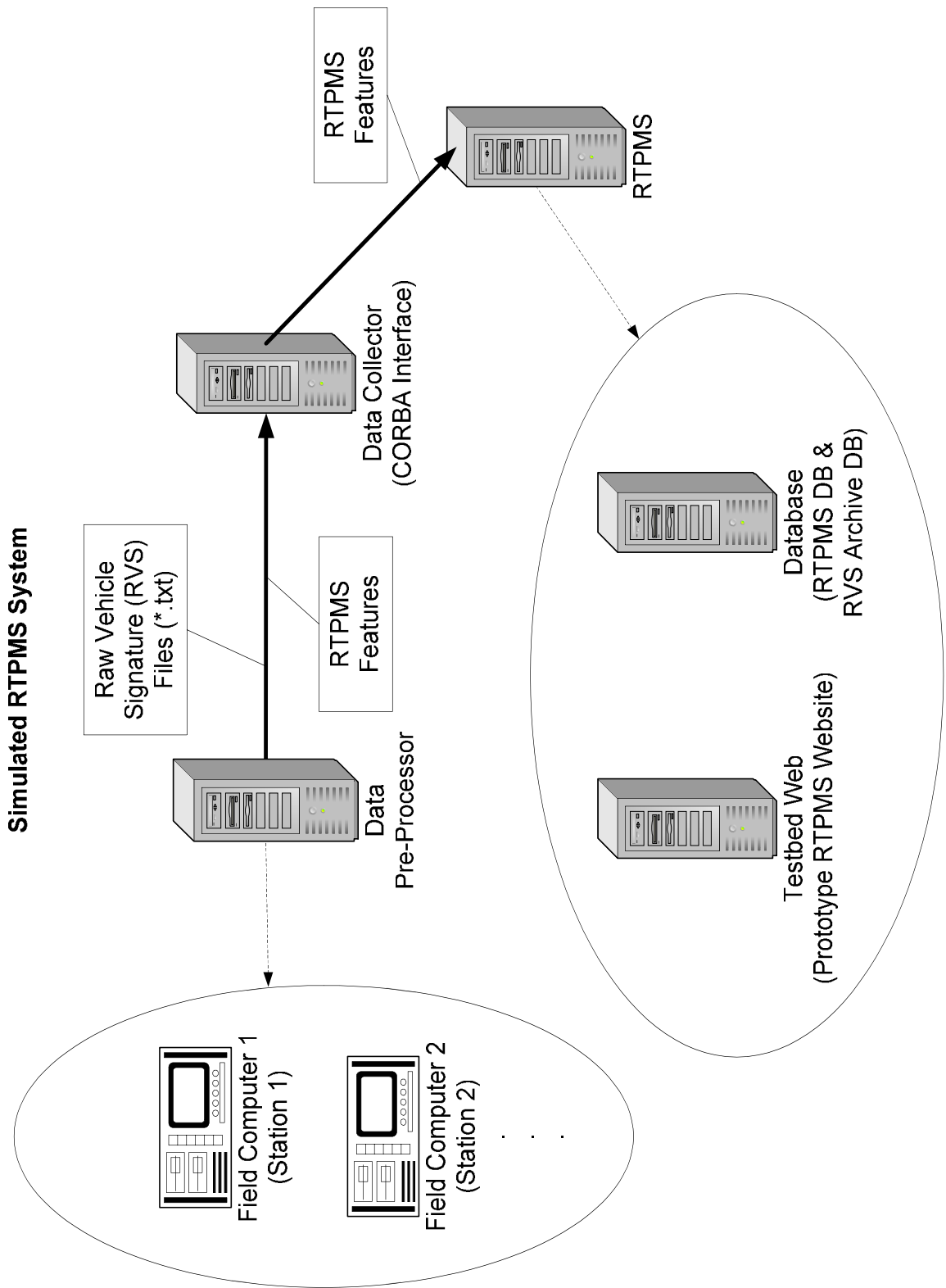
Figure 7-4 RTPMS simulation.

152

The Data Pre-Processor was to emulate field computers. The functions of Data Pre-Processor included simulating real-time scenario of generating raw vehicle signature data, detecting and eliminating irregular and tailgating vehicle signatures data, and extracting PSR values. The task of the RTPMS server in this simulation was to emulate RTREID-2 server, Database server and Testbed Web server. RTREID-2 Module and Vehicle Classification Module were performed once RTPMS features were received from CORBA Consumer, and the results were sent to database (i.e. the simulate Database server).

It was found that amendment was needed for the minimum AMD searching approach described in Step 5 of RTREID-2 procedure when implementing RTREID-2 Module in a real-time setting. This searching approach firstly defines an upstream candidate vehicle set for a downstream vehicle within a time window, and a reverse time window is applied to each upstream candidate vehicle to find its corresponding candidate vehicle set at its downstream (details can be found in Chapter 3).

For a given upstream candidate vehicle, however, it is not possible to properly include all candidate vehicles at downstream since the upper bound of the reverse time window may exceed the current timestamp. Accordingly, adjustment was made to hold those vehicles and to postpone the vehicle reidentification task until all candidate vehicles could be properly included. It must be noted that since some delays may occur due to this change, the "current" travel time information will be an estimate obtained from the vehicles that can be reidentified in the current time interval.

For the UCI_PeMS Module, which was embedded in the simulated Testbed Web server, it queried the database to get necessary information so that performance measurements could be generated. All of the modules were programmed in C/C++ except the UCI_PeMS module, which has been programmed in Java by UCI research team. For displaying the results of the real-time performance measurements, it can be shown graphically or in text format.

It is worth noting that the RTPMS simulation results have proven the feasibility of the proposed RTPMS framework. The snapshots of the developed website are demonstrated in Figure 7-5, Figure 7-6, and Figure 7-7. As illustrated in Figure 7-5, the gray shadow along the freeway corridor depicts capacity. The widths of the colored area indicate traffic volumes. The color itself shown along the freeway corridor represents travel speed information. In addition, vehicle classification results are illustrated by a pie chart shown next to each detection station.
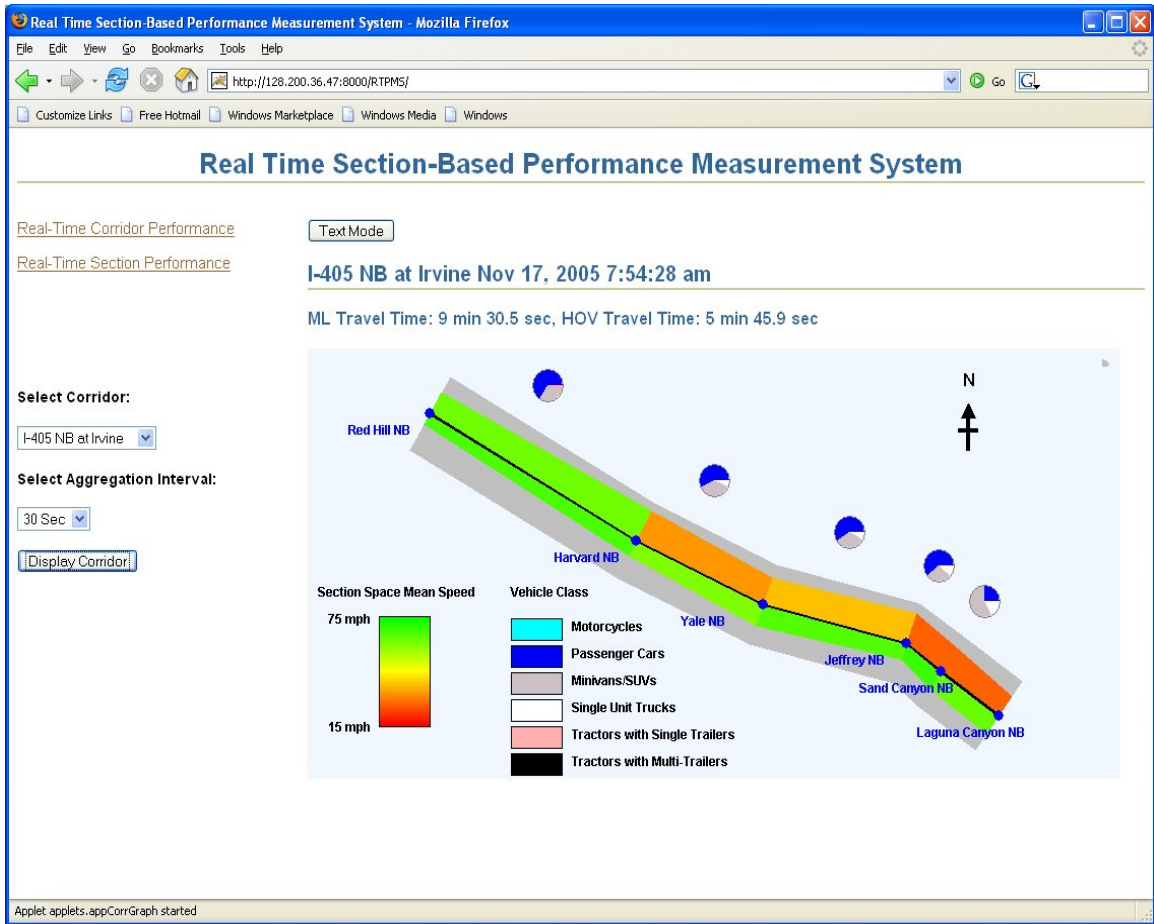
Figure 7-5 Real-time corridor performance: Graphical display.

Figure 7-6 and Figure 7-7 demonstrate the RTPMS results in text format. In Figure 7-6, each section within the freeway corridor is stated by its post mile, traffic flow, travel time, and speed information. All the traffic measurements are furthered detailed according to the usage of lane, i.e., high occupancy vehicle (HOV) lane and mainline (ML).
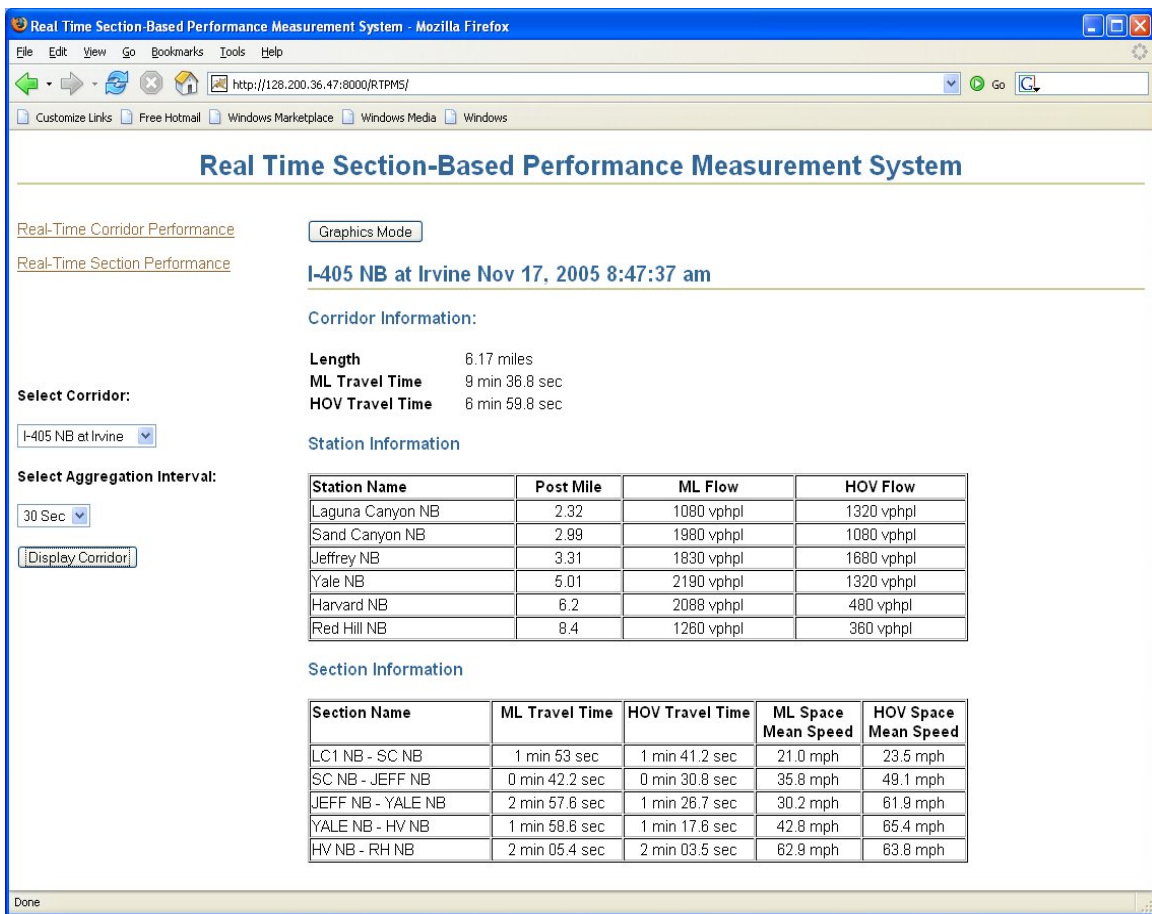
Figure 7-6 Real-time corridor performance: Text display for Corridor information.

Figure 7-7 presents vehicle classification information for a selected freeway section. The first table shows mainline section performance by vehicle class, while the second depicts HOV section performance by vehicle class. In addition to the vehicle class proportion, travel times and speeds are also provided for each vehicle class.
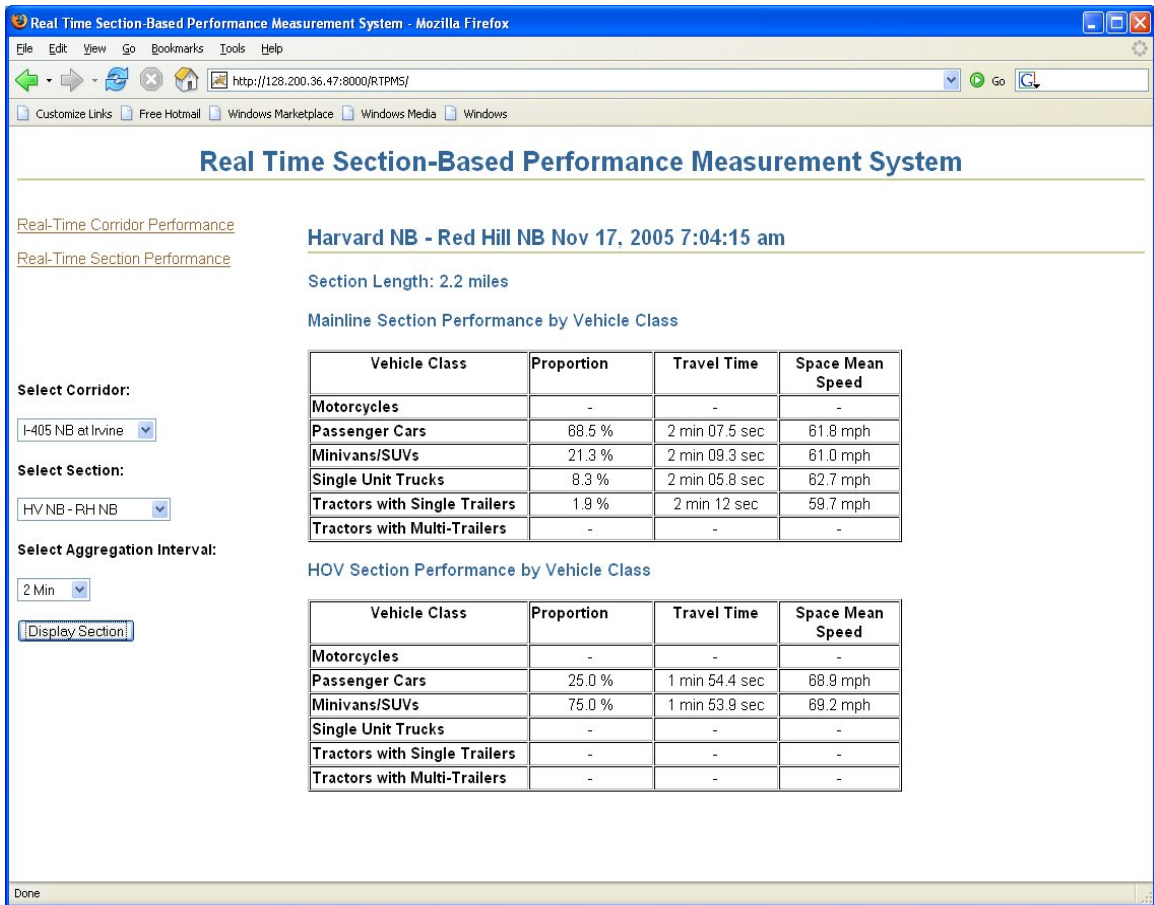
Figure 7-7 Real-time corridor performance: Text display for section information.

CHAPTER 8 CONCLUSIONS

Vehicle reidentification has emerged due to its substantial potential for effective implementation of ATMIS (Advanced Transportation Management and Information Systems). Several technologies have been studied for vehicle reidentification in the last three decades including intrusive detection systems and non-intrusive detection systems. As opposites of intrusive detection systems, non-intrusive detection systems are free from privacy concerns and, usually, market penetration problems. Among the non-intrusive detection systems, although ILDs (Inductive Loop Detector) are not without limitations as a traffic sensor, they are widely used for historical reasons and the sunken investment in the large installed base makes their use in this dissertation highly cost-effective.

Moreover, the ILD-based system has shown its capability of anonymous vehicle tracking in previous studies, and could be potentially applied to reidentify individual vehicles across multiple detection stations. Therefore, this dissertation developed a new vehicle reidentification algorithm (i.e., RTREID-2) for real-time implementation by employing PSR (Piecewise Slope Rate) approach that extracts features from raw vehicle signature data. The results of cases studies indicated that RTREIS-2 is capable of providing individual vehicle tracking information and performance such as travel time along a freeway corridor.

The potential contributions of RTREID-2 are application to square and round single loop vehicle reidentification and straightforward implementation, while avoiding issues associated with re-estimation or transferability of the speed models used in the previously developed approach. In addition, the results of sensitivity analyses, vehicle reidentification performance, and the accuracy of section travel time, are very promising and suggest that with this approach, the reduction in both computational effort and computer memory needed to store signatures information could potentially benefit real-time implementation.

Furthermore, RTREID-2 was applied along a 6.2-mile freeway corridor under congested morning peak-period conditions. The applicability and transferability of RTREID-2 to homogenous loop detection systems (square loops or round loops systems) and heterogeneous loop detection systems (mixed square and round loops system) was also investigated in this freeway corridor. Excellent results are obtained compared with GPS measurements from control vehicles and suggest that RTREID-2 has the potential to be implemented successfully in a congested freeway corridor, utilizing either or both round or square inductive loop detectors.

A real-time vehicle classification model, which is part of RTREID-2, is also introduced. The proposed vehicle classification model can not only categorize vehicle types based on the FHWA scheme, but also can group vehicles into more detailed classes. The results are very encouraging since the proposed model can successfully classify vehicles using single loop detector data without any axle information, and reliable model

created using
BCL easyPDF
Printer Driver
Click here to purchase a license to remove this image

transferability is also demonstrated. The advantages of the proposed method are its simplicity and employing the current detection infrastructure.

Moreover, to understand the real-time freeway performance measurement system in a real-world setting, the design of RTPMS (Real-time Traffic Performance Measurement System) is presented in this dissertation. A simulation of RTPMS is conducted to evaluate its feasibility. The simulation results demonstrate the potential of implementing the proposed RTPMS framework in the real world.

For future study, it is proposed that RTPMS be implemented in a real world setting. In addition, the investigations can be taken to address the issues arising from this dissertation research, including improvement of vehicle signature data quality, improvement of system reliability for heterogeneous detection systems, refinement of the proposed vehicle classification model, and corridor O-D estimation. Further research can also extend RTPMS to arterials, or for network-wide implementation.

REFERENCES

Abdulhai, B., Tabib, S. M., 2002. Towards anonymous vehicle tracking via inductance-pattern recognition. In: Proceedings of Transportation Research Board 81st Annual Meeting, January 13-17. Washington, DC.

Asakura, Y., Hato, E., Kashiwadani, M., 2000. Origin-destination matrices estimation model using automatic vehicle identification data and its application to the Han-Shin Expressway network. Transportation, 27, 419-438.

Böhnke, p., Pfannerstill, E., 1986. A system for the automatic surveillance of traffic situations. ITE Journal, 56, 41-45.

Bullock, D., 1996. Vehicle tracking using radial basis function neural networks. In: Proceedings of Supercomputer Applications in the Transportation Industries, 211-218. 29th International Symposium on Automotive Technology & Automation. Florence, Italy.

Cayford, R., Johnson, T., 2003. Operational parameters affecting the use of anonymous cell phone tracking for generating traffic information. In: Proceedings of Transportation Research Board 82nd Annual Meeting, January 12-16. Washington, DC.

Cheung, S. Y., Coleri, S., Dundar, B., Ganesh, S., Tan, C.-W., Varaiya, P., 2006. Traffic measurement and vehicle classification with a single magnetic sensor. Journal of Transportation Research Record, 1917, 173-181.

Coifman, B., Beymer, D., McLauchlan, P., Malik, J., 1998. A real-time computer vision system for vehicle tracking and traffic surveillance. Transportation Research, 6C (4), 271-288.

Davies, P., 1986. Vehicle detection and classification. Information Technology Applications in Transport, VNU Science Press, Haarlem, The Netherlands, 11-40.

Dixon, M., Rilett, L.R., 2000. Real-time origin-destination estimation using automatic vehicle identification data. In: Proceedings of Transportation Research Board 79th Annual Meeting, January 9-13. Washington, DC.

Garrott, W.R., Howe, G.J., Forkenbrock, G., 1999. An experimental examination of selected maneuvers that may induce on-road untripped, light vehicle rollover. National Highway Traffic Safety Administration, Washington, D.C.

Gerald, C. F., and Wheatley, P. O., 1989. Applied Numerical Analysis. Addison-Wesley Publishing Company, Reading, MA.

Gupte, S., Masoud, O., Martin, R., Papanikolopoulos, N.P., 2002. Detection and classification of vehicles. IEEE Transportation on Intelligent Transportation Systems, 3(1), 37-47.

Hossfeld, B., 1991. GPS for vehicle tracking. GPS world, 2 (9), 44-46.

ITE, 1990. Traffic Detector Handbook (Second Edition). Institute of Transportation Engineers. Washington, DC.

Jeng, S.-T., Ritchie, S. G., 2005. A new inductive signature method for vehicle reidentification. In: Proceedings of Transportation Research Board 84th Annual Meeting, January 9-13. Washington, DC.

Jet Propulsion Laboratory, 1997. Traffic surveillance and detection technology development, sensor development final report. Federal Highway Administration, U.S. Department of Transportation, Washington, DC.

Kim, J., Oh, J., 2000. A land vehicle tracking algorithm using stand-alone GPS. Control Engineering Practice, 8, 1189-1196.

Knee, H. E., Smith, Cy, Black, G., Petrolino, Joe, 2004. Demonstration of alternative traffic information collection and management technologies. In: Proceedings of SPIE: Industrial and Highway Sensors Technology, 5272, 286-293.

Kühne, R. D., Immes, S., 1993. Freeway control systems for using section-related traffic variable detection. In: Pacific Rim. Trans. Tech. Conference, July 25-28. Seattle, Washington.

Kühne. R. D., Palen, J., Gardner, C., Ritchie, S. G., 1997. Section-related measure of traffic system performance. In: Proceedings of Transportation Research Board 76th Annual Meeting, January 12-16. Washington, DC.

Kwon, T. M., Parsekar, A., 2005. Exploring the relationship between freeway speed variance, land changing, and vehicle heterogeneity. In: Proceedings of Transportation Research Board 84th Annual Meeting, January 9-13. Washington, DC.

Leuck, H., Nagel, H. H., 1999. Automatic differentiation facilitates OF-integration into steering-angle-based road vehicle tracking. In: Proceedings of IEEE Computer Society Conference on Computer Vision and Pattern Recognition, 2, 360-365.

Leuven, J. van, Leeuwen, M.B. van, Groen, F.C.A., 2001. Real-time vehicle tracking in image sequences. In: Proceedings of IEEE Instrumentation and Measurement Technology Conference, 3, 2049-2054.

Looney, C. G., 1997. Pattern Recognition Using Neural Networks: Theory and Algorithm for Engineers and Scientists. Oxford University Press, Inc., New York, NY.

Lu, Y., Hsu, Y., Maldague, X., 1992. Vehicle classification using infrared image analysis. Journal of Transportation Engineering, 188(2), 223-240.

MacCarley, C.A., 2001. Video-based vehicle signature analysis and tracking system phase 2: algorithm development and preliminary testing. MOU 350 Final Report to California PATH, California Polytechnic State University, San Luis Obispo.

Malik, J., Russell, S., 1997. Traffic surveillance and detection technology development: new traffic sensor technology final report. UCB-ITS-PRR-97-6, California PATH Research Report.

Mimbela, L. E. Y., Klein, L. A., Kent, p., Hamrick, J. L., Luces, K. M., Herrera, S., 2000. A summary of vehicle detection and surveillance technologies used in intelligent transportation systems. Funded by the Federal Highway Administration's Intelligent Transportation Systems Joint Program Office.

Nooralahiyan, A.Y., Dougherty, M., McKeown, D., Kirby, H.R., 1997. A field trial of acoustic signature analysis for vehicle classification. Transportation Research 5C (3/4), 165-177.

Oh, C., 2003. Anonymous vehicle tracking for real-time performance measures. Ph.D. Dissertation, University of California, Irvine.

Oh, C., Ritchie, S. G., 2002. Real-time inductive-signature-based level of service for signalized intersections. Transportation Research Record, 1802, 97-104.

Oh, C., Ritchie, S. G., 2003. Anonymous vehicle tracking for real-time traffic surveillance and performance on signalized arterials. In: Proceedings of Transportation Research Board 82nd Annual Meeting, January 12-16. Washington, DC.

Oh, C., Ritchie, S. G., Jeng, S.-T., 2004. Anonymous vehicle reidentification with heterogeneous detection systems. In: Proceedings of Transportation Research Board 83rd Annual Meeting, January 11-15. Washington, DC.

Oh, C., Ritchie, S. G., Park, S., 2002. Development of a real-time probabilistic vehicle reidentification algorithm for signalized intersections. ITS Working Paper, Institute of Transportation Studies, University of California, Irvine.

Oh, C., Tok, A., Ritchie, S. G., 2004. Real-time freeway level of service based on anonymous vehicle re-identification. In: Proceedings of Transportation Research Board 83rd Annual Meeting, January 11-15. Washington, DC.

Oh, S., Ritchie, S. G., Oh, C., 2002. Real-time traffic measurement from single loop inductive signatures. Transportation Research Record, 1804, 98-106.

Park, S., Ritchie, S. G., 2004. Exploring the relationship between freeway speed variance, land changing, and vehicle heterogeneity. In: Proceedings of Transportation Research Board 83rd Annual Meeting, January 11-15. Washington, DC.

Pfannerstill, E., 1989. Automatic monitoring of traffic conditions by reidentification of vehicles. In: Proceedings of IEEE Conference on Road Traffic Monitoring, 299, 172-175.

Pursula, M., Pikkarainen, P., 1994. A neural network approach to vehicle classification with double induction loops. In: Proceedings of the 17th ARRB Conference, Part 4, 29-44.

Recktenwald, G. W., 2000. Numerical Methods with MATLAB Implementation and Application. Prentice-Hall, Upper Saddle River, NJ.

Ritchie, S. G., Park, S., Oh, C., Jeng S.-T., Tok, A., 2005. Anonymous vehicle tracking for real-time freeway and arterial street performance measurement. UCB-ITS-PRR-2005-9, California PATH Research Report.

Ritchie, S. G., Park, S., Oh, C., Sun, C., 2001. Field investigation of advanced vehicle reidentification techniques and detector technologies. MOU 3008 Draft Final Report to California PATH, Institute of Transportation Studies, University of California, Irvine.

Ritchie, S. G., Sun, C., 1998. Section related measures of traffic system performance: final report. UCB-ITS-PRR-98-33, California PATH Research Report.

Smith, B. L., Zhang, H., Fontaine, M., Green, M., 2003. Cell Phone Probes as an ATMS tool. Research Report No. UVACTS-15-5-79, Center for Transportation Studies, University of Virginia.

Sun, C., 1998. Use of vehicle signature analysis and lexicographic optimization for vehicle reidentification on freeways. Ph.D. Dissertation, University of California, Irvine.

Sun, C., Ritchie, S. G., 1999. Individual vehicle speed estimation using single loop inductive waveforms. Journal of Transportation Engineering, 125 (6), 531-538.

Sun, C., Ritchie, S. G., Oh, S., 2003. Inductive classifying artificial network for vehicle type categorization. Computer-Aided Civil and Infrastructure Engineering, 18 (3), 161-172.

Sun, C., Ritchie, S. G., Tsai, K., Jayakrishnan, R., 1999. Use of vehicle signature analysis and lexicographic optimization for vehicle reidentification on freeways. Transportation Research, 7C (4), 167-185.

Tabib, S. M., 2001. Vehicle re-identification based on inductance signature matching. Master Thesis, University of Toronto.

Tawfik, A. Y., Abdulhai, B., Peng, A., Tabib S. M., 2004. Improving the accuracy of vehicle signature reidentification using decision trees. In: Proceedings of Transportation Research Board 83rd Annual Meeting, January 11-15. Washington, DC.

Tawfik, A. Y., Peng, A., Tabib, S. M. and Abdulhai, B., 2002. Learning spatio-temporal context for vehicle reidentification. In: Proceedings of 2nd IEEE International Symposium on Signal Processing and Information Technology. Marrakesh, Morocco.

Taylor, S., Green, J., Richardson, A., 1998. Applying vehicle tracking and palmtop technology to urban freight. ITS-WP-98-23. Working Paper, Institute of Transportation Studies, Australia.

USDOT, 2007. FHWA Vehicle Classification Scheme F Report. Referred Website: http://www.dot.state.oh.us/techservsite/availpro/Traffic_Survey/SchemeF/FHWA _Scheme_F_Report.PDF.

Vlcek, C., McLain, P., Murphy, M., 1993. GPS/dead reckoning for vehicle tracking in the "urban canyon" environment. In: Proceedings of IEEE-IEE Vehicle Navigation and Information Systems Conference, 461 and A34-A41.

Yim, Y.B.Y., Cayford, R., 2001. Investigation of vehicles as probes using global positioning system and cellular phone tracking: field operational test. UCB-ITS-PWP-2001-9, California PATH Research Report.

Yuan, X., Lu, Y.-J., Sarraf, S., 1994. Computer vision system for automatic vehicle classification. ASCE Journal of Transportation Engineering, 120(6), 861-876.

APPENDIX A RTPMS DATABASE DESIGN

Configurations: Design Scheme

Name	Type	Description	Note
Road Index	• Freeway • Urban	Freeway or Road/Intersection name	Pre-defined
Detection Station ID (DS ID)	-	A unique ID for each detector	Pre-defined
Detector Type	• Round Loop • Square Loop • Blade • Video	Detector type specification	Pre-defined
Detector Configuration	• Single • Double • Other	Configuration of the detectors	Pre-defined

Upstream Detection Station ID (UDS ID)	• Freeway
	  o Mainline
	  o Ramp
	• Urban
	  o Through
	  o Left turn
	  o Right turn
		The adjacent upstream detection station(s)	Pre-defined

Distance	-	Distance to the each adjacent upstream detection station(s)	Pre-defined

Configurations: Example

Road Index	DS ID	Detector Type	Detector Configuration	UDS ID	Distance
I-405 NB	LC	Square Loop	Double	-1	-1
I-405 NB	SCONR	Round Loop	Double	-1	-1
I-405 NB	SC	Square Loop	Double	LC	0.63
				SCONR	0.50
I-405 NB	YL	Round Loop	Single	SC	2
…	…	…	…	…	…
Alton-ICD	AltonICD-1	Square Loop	Double	-1	-1
Alton-ICD	AltonICD-2	Square Loop	Double	-1	-1
…	…	…	…	…	…

Input Data for REID: Design Scheme

Name	Type	Description	Note
UCI Record ID (UCI ID)	Header	An ID assigned to each vehicle signature	Detector specific data
DS ID	Header	A unique ID for each detector	Pre-defined
Date	Header	Signature timestamp	Detector specific data
Time	Header	Signature timestamp	Detector specific data
Lane	Header	Lane number	Detector specific data
Duration (sec)	Header	Duration of time the detector is on	Detector specific data
Num samples	Header	Number of samples in the vehicle signature	Detector specific data
Interval	Data	Time interval from the beginning of the vehicle signature	Detector specific data
Magnitude-front	Data	Magnitude of the front loop for double loops or magnitude of the signal loop	Detector specific data
Magnitude-rear	Data	Magnitude of the rear loop	Detector specific data

Input Data for REID: Example

UCI ID	DS ID	Lane	Date	Time	Duration	Num samples
12345	SC	2	2004-11-02	09:00:0.26800	0.524000	630
0.000000	-329.000000	0.000000				
0.000833	-358.000000	0.000000				
0.001667	-396.000000	0.000000				
…	…	…				

Output Data from REID: Individual Vehicle Level Design Scheme

Name	Type	Description	Note
UCI ID	-	An ID assigned to each vehicle signature	Detector specific data
Road Index	• Freeway • Urban	Freeway or Road/Intersection name	Pre-defined (Configurations)
DS ID	-	A unique ID for each detector	Pre-defined (Configurations)
Detector Type	• Round Loop • Square Loop • Blade • Video	Detector type specification	Pre-defined (Configurations)
Detector Configuration	• Single • Double • Other	Configuration of the detectors	Pre-defined (Configurations)
Date	-	Signature timestamp	Detector specific data
Time	-	Signature timestamp	Detector specific data
Lane	-	Lane number	Detector specific data
REID ID	-	An ID assigned to the reidentified vehicle	REID result: Individual vehicle

UDS ID	• Freeway
	  o Mainline
	  o Ramp
	• Urban
	  o Through
	  o Left turn
	  o Right turn
		The adjacent upstream detection station(s)	Pre-defined (Configurations)

Distance (mile)	-	Distance to the each adjacent upstream detection station(s)	Pre-defined (Configurations)
Point speed (mph)	-	Output from speed-trap or speed estimation module	REID result: Individual vehicle
Section speed (mph)	-	Travel speed for individual vehicle	REID result: Individual vehicle
Travel time (sec)	-	Travel time for individual vehicle	REID result: Individual vehicle
Vehicle class	• FHWA • RTPMS	Classification of vehicle types based on FHWA/RTPMS standard	Output from vehicle classification module

Output Data from REID: Example of Individual Vehicle Level

UCI ID	Road Index	US ID	Detector Type	Detector Configuration	Date	Time	Lane
12345	I-405 NB	SC	Square Loop	Double	2004-11-02	09:00:0.26800	2
REID ID	**UDS ID**	**Distance**	**Point speed**	**Section speed**	**Travel time**	**Vehicle class**	
444	LC	0.63	70	64.98	34.9	**2**	

Output Data from REID: Section Level Design Scheme

Name	Type	Description	Note
DS ID	-	A unique ID for each detector	Pre-defined (Configurations)
UDS ID	• Freeway o Mainline o Ramp • Urban o Through o Left turn o Right turn	The nearest upstream detection station	Pre-defined (Configurations)
Section travel time (Sec. TT)	• Max • Min • Average (Avg) • Std	Statistics of section travel time for each single section	REID result: Single section
Section volume (Sec. Vol)	• Max • Min • Avg • Std	Statistics of section volume for each signal section	REID result: Single section
Section speed (Sec. Speed)	• Max • Min • Avg • Std	Statistics of section speed for each single section	REID result: Single section
Section occupancy % (Sec. Occ)	• Max • Min • Avg • Std	Statistics of section occupancy for each single section	REID result: Single section
Section density (Sec. Density)	• Max • Min • Avg • Std	Statistics of section density for each single section	REID result: Single section
Section Vehicle composition (Sec. Veh Comp)	• FHWA • UCI	Output from vehicle classification module	REID result: Single section

Output Data from REID: Example of Section Level

DS ID	UDS ID	Sec. TT Max	Sec. TT Min	Sec. TT Avg	Sec. TT Std
SC	LC	38	28	33	10.65
Sec. Vol Max	**Sec. Vol Min**	**Sec. Vol Avg**	**Sec. Vol Std**	**Sec. Speed Max**	**Sec. Speed Min**
110	72	90	5.86	82	58
Sec. Speed Avg	**Sec. Speed Std**	**Sec. Occ Max**	**Sec. Occ Min**	**Sec. Occ Avg**	**Sec. Occ Std**
72	8.70	45.00%	38.97%	41.2%	2.33
Sec. Density Max	**Sec. Density Min**	**Sec. Density Avg**	**Sec. Density Std**	**Sec. Veh Comp (FHWA)**	**Sec. Veh Comp (UCI)**
521	487	500	4.44	2	2

Output Data from REID: Lane-Related Design Scheme

Name	Type	Description	Note
DS ID	-	A unique ID for each detector	Pre-defined (Configurations)

UDS ID	• Freeway
	  o Mainline
	  o Ramp
	• Urban
	  o Through
	  o Left turn
	  o Right turn
		The nearest upstream detection station	Pre-defined (Configurations)

Lane	-	Lane number	Detector specific data
Lane travel time (Lane TT)	• Max • Min • Avg • Std	Statistics of travel time for each lane	REID result: Lane related
Lane volume (Lane Vol)	• Max • Min • Avg • Std	Statistics of volume for each lane	REID result: Lane related
Lane speed	• Max • Min • Avg • Std	Statistics of section speed for each lane	REID result: Lane related
Lane occupancy (Lane Occ)	• Max • Min • Avg • Std	Statistics of occupancy for each lane	REID result: Lane related
Lane density	• Max • Min • Avg • Std	Statistics of density for each lane	REID result: Lane related
Lane Vehicle composition (Lane Veh Comp)	• FHWA • UCI	Output from vehicle classification module	REID result: Lane related

Output Data from REID: Example of Lane-Related

DS ID	UDS ID	Lane	Lane TT Max	Lane TT Min	Lane TT Avg	Lane TT Std	Lane Vol Max	Lane Vol Min
SC	LC	4	38	28	33	10.65	110	72
Lane Vol Avg	**Lane Vol Std**	**Lane Speed Max**	**Lane Speed Min**	**Lane Speed Avg**	**Lane Speed Std**	**Lane Occ Max**	**Lane Occ Min**	**Lane Occ Avg**
90	5.86	82	58	72	8.70	45.00%	38.97%	41.2%
Lane Occ Std	**Lane Density Max**	**Lane Density Min**	**Lane Density Avg**	**Lane Density Std**	**Lane Veh Comp (FHWA)**		**Lane Veh Comp (UCI)**	
2.33	521	487	500	4.44	2		2	

Output Data from REID: Path-Related Level Design Scheme

Name	Type	Description	Note
Origin-Destination	-	O-D table	REID result: Path related
Total travel distance (Tot. TDist)	-	Total travel distance for a specific path	REID result: Path related
Path travel time in minute (Path TT)	• Max • Min • Avg • Std	Statistics of path travel time for a specific path	REID result: Path related
Path speed (mph)	• Max • Min • Avg • Std	Statistics of path speed for a specific path	REID result: Path related
Path info	-	Path info for individual vehicle (table)	REID result: Path related

Output Data from REID: Example of Path-Related

Path	Tot. TDist	Path TT Max	Path TT Min	Path TT Avg	Path TT Std	Path Speed Max	Path Speed Min	Path Speed Avg	Path Speed Std
LC to YLOFFR	4.5	5.2	4.8	5.0	2.2	81	65	77	4.44
SCONR to YL	4	5.0	4.5	4.7	3.4	77	62	70	3.33
…	…	…	…	…	…	…	…	…	…

Output Data from REID: Example of O-D Table

Destination \ Origin	1	2	3	…
1	12	4	38	…
2	1,003	42	77	…
3	112	520	58	…
…	…	…	…	…

Output Data from REID: Example of Path Info

REID ID	Date	Start Time	Origin	Destination	Path TT	Vehicle Type
444	2004-11-04	09:00:0.26800	LC	YL	12	2
Road Index	DS ID	Lane	Time	Section Speed		
I-405 NB	LC	2	09:00:0.26800	-		
I-405 NB	SC	3	09:00:35.16800	64.98		
…	…	…	…	…		

Output Data from REID: REID Performance Design Scheme

Name	Description	Note
MAPE	Mean absolute percentage error for travel time estimation (ground-truthed)	REID performance
TMR	Total match rate (ground-truthed)	REID performance
CMR	Correct match rate (ground-truthed)	REID performance
MR	Mismatch rate (ground-truthed)	REID performance
NMR	No match rate (ground-truthed)	REID performance
RR	Reliability rate (ground-truthed)	REID performance

Output Data from REID: Example of REID Performance

Study Site	Date	Start Time	End Time	Detector Type	REID Algorithm
LC SC	2004-11-04	09:00:0.26800	09:30:00	Square Loop	RTREID-2
MAPE	**TMR**	**CMR**	**MR**	**NMR**	**RR**
1.05%	92.00%	80.00%	12.00%	8.00%	86.96%

Output Data from REID: RTPMS Design Scheme

Name	Description	Note
SMR	System match rate for each section	RTPMS
Section travel time	Aggregated travel time for each section	RTPMS
Section volume	Traffic count for each section	RTPMS
Section speed	Statistics of average section speed for each section	RTPMS
Section occupancy	Statistics of average section occupancy for each section	RTPMS
Section density	Statistics of average section density for each section	RTPMS
VMT	Vehicle miles traveled for each section	RTPMS
VHT	Vehicle hours traveled for each section	RTPMS
Vehicle composition	The proportion of each vehicle class for each section	RTPMS

Output Data from REID: Example of RTPMS

From (DS ID)	To (DS ID)	SMR	Section Travel Time	Section Volume	Section Speed
LC	SC	92%	33	110	82
Section Occupancy	**Section Density**	**VMT**	**VHT**	**Vehicle Composition**	
41.2%	500	1000	10	**Table	